Activity modulation of Ubiquitin-Specific Proteases

Alexis Caspar Faesen

Activity modulation of Ubiquitin-Specific Proteases

Activiteits modulatie van Ubiquitine-Specifieke Proteases

Proefschrift

ter verkrijging van de graad van doctor aan de
Erasmus Universiteit Rotterdam
op gezag van de
rector magnificus

Prof. dr. H. G. Schmidt

en volgens besluit van het College voor Promoties.
De openbare verdediging zal plaats vinden op

woensdag 9 november 2011, om 11.30 uur

door

Alexis Caspar Faesen

geboren te Amsterdam.

ERASMUS UNIVERSITEIT ROTTERDAM

Promotie commissie

Promotor:
Prof. dr. T.K. Sixma

Overige leden:
Prof. dr. J. Neefjes
Prof. dr. R. Kanaar
Prof. dr. C.P. Verrijzer

Table of contents

$\rightarrow$

Chapter 1

General introduction

Parts adapted from:

Alex C Faesen[1], Titia K Sixma[1] and Roger D Everett[2]

"Ubiquitin Specific Protease 7"

Chapter in Handbook of Proteolytic Enzymes
Edited by Neil Rawlings and Guy Salvesen, volume 3 (2011)

[1] Division of Biochemistry and Center for Biomedical Genetics, The Netherlands Cancer Institute, Amsterdam, The Netherlands. [2] MRC-University of Glasgow Centre for Virus Research, Glasgow, Scotland, U.K.

Cell biological processes require intense and continuous regulation. This often involves complex systems that, when disturbed, fail to generate the desired outcome and finally result in diseases. Defects in these systems can have different origins. For example, the translation of the genes can be misregulated, leading to altered protein expression levels. Alternatively, genes can encode for mutated, truncated or chimeric fusion proteins, altering the function and activity of that protein. On the other hand, the defects can also originate from the regulation of the activity of otherwise correctly functional proteins. These regulation systems often rely on chemical modifications of the proteins, and these are also frequently perturbed in diseases. The focus of this thesis will be on one such important modification: ubiquitination.

Ubiquitination

Once DNA is translated and proteins have been properly folded, most proteins are subject to a diverse range of post-translational processes. These processes allow for drastically changing both function and fate of the target proteins. It is usually a very fast and specific process and it effectively expands the functional outcomes of a single gene. The modification arsenal is large and proteins are differentially hydroxylated, methylated, acetylated, phosphorylated or conjugated to ubiquitin and ubiquitin-like polypeptides.

Ubiquitin (originally called "ubiquitous immunopoietic polypeptide") was first identified in 1975 as an 8.5-kDa protein of unknown function that exists in all eukaryotic cells. The importance of ubiquitin is nicely illustrated by the evolutionary conservation of its 76 amino acids, which between mammals, yeast, and plants only differs at three positions. It is an abundant modification and up to 20% of yeast proteins are conjugated to ubiquitin under standard culture conditions[1]. The basic functions of ubiquitin and the components of the ubiquitination pathway were elucidated in the early 1980s. These fundamental discoveries describing how cells regulate the breakdown of intracellular proteins using protein ubiquitination were awarded the Nobel Prize in Chemistry in 2004[2].

Ubiquitination is more versatile and flexible than small molecule modifications such as phosphorylation and acetylation. Traditionally, ubiquitin conjugation has been believed to invariably serve as the final station in the destiny of a protein, serving to target its substrates for degradation by the proteasome[3]. Nowadays it has been recognized that ubiquitination is not only a signal for destruction, but represents a more general modification influencing a broad repertoire of cellular processes[4,5]. Protein ubiquitination is a critical post-translational modification that can have profound effects on protein stability, localization or interactions. Importantly, in order to enable a dynamic regulation of signalling events, ubiquitination is a reversible process that is specifically counteracted by the deubiquitinating (DUB) family of proteases.

Degradation by the proteasome

The most studied and best understood role of ubiquitin involves the targeted destruction of proteins by the proteasome. The proteasome can be viewed as the cellular garbage disposal machine that literally grinds up proteins into small peptides, whilst recycling intact ubiquitin molecules[6].

In contrast to protein synthesis, ubiquitination and degradation are fast processes that take place within minutes. Therefore, if steady-state levels of proteins must undergo fast and dramatic changes, they are often regulated by active protein degradation. One example is the regulation of p53 levels. This tumour suppressor is continuously expressed and degraded, resulting in low protein levels. However, upon stress, the ubiquitination and the corresponding degradation of p53 are suddenly stopped, resulting in a fast increase of p53 protein levels. This allows a cell to respond quickly to changes in the environment and adjust to meet the new requirements.

The signal for destruction by the proteasome

however is not a single ubiquitin molecule. As discussed later in more detail, mono-ubiquitination is only one of the many possible ubiquitination states of proteins. Rather, the covalent attachment of at least four ubiquitin moieties in a poly-ubiquitin chain serves as the tag to send the protein for destruction by the proteasome. These ubiquitin chains are linked through the lysine at position 48 (K48) on ubiquitin itself. This was the first ubiquitin signal to be identified, however since then also K11- and K29-linked poly ubiquitin have been identified as degradation markers[7-9].

The importance of this system is underlined by the critical role of the proteasome that has been described in cancer. Changes in the profiles of protein degradation are linked to defects in apoptosis, the cell division cycle, DNA damage signalling and to gene transcription[10-12]. Furthermore, many cancer cells are more susceptible to proteasome inhibition than normal cells. These discoveries lead to intensive research into the application of proteasome inhibitors as a cancer drugs. Bortezomib (Velcade®) is a first-in-class proteasome inhibitor and binds the catalytic site of the proteasome with high affinity and specificity[13] and is approved for treatment of multiple myeloma and mantle cell lymphoma, while many clinical trials in other malignancies are ongoing[14]. Unfortunately, the mechanism(s) responsible for the increased sensitivity of cancer cells to proteasome inhibitors remain poorly understood.

The mechanism of ubiquitin conjugation

The biochemical processes underlying ubiquitination of proteins have been studied in great detail. It requires an enzymatic cascade to activate and conjugate the ubiquitin molecule to a target protein or ubiquitin itself[15]. This results in a covalent isopeptide bond between ubiquitin and the target lysine (Figure 1A).

In this ubiquitin conjugation process, the first step is the activation of ubiquitin by the E1 ubiquitin-activating enzyme in an
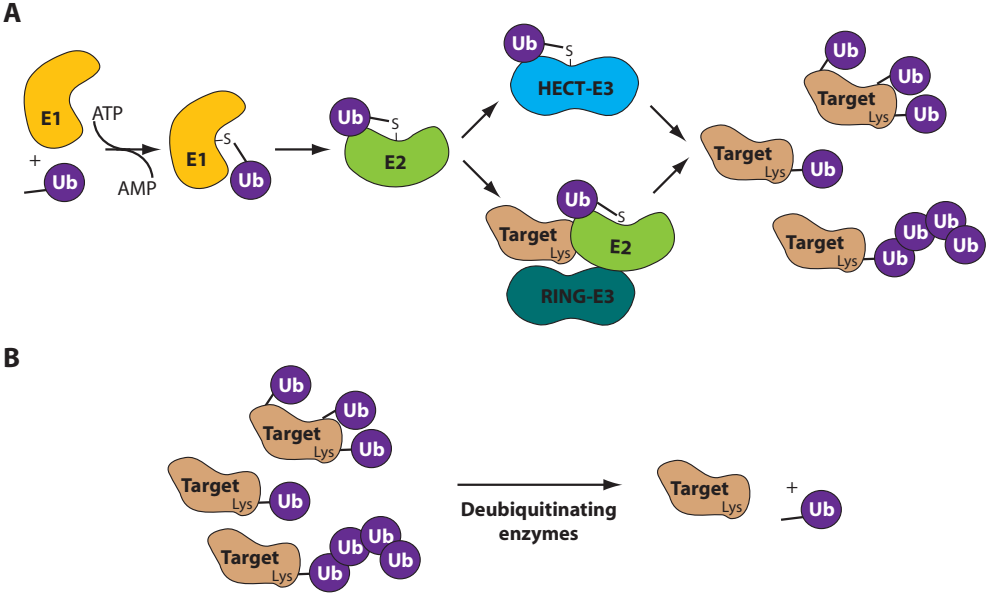
Figure 1. Schematic view of the (de-)ubiquitination system. A. Ubiquitination is a multi-step process, where the conjugation of ubiquitin is mediated by the E1 activating enzyme, the E2 conjugating enzyme and an E3 ubiquitin ligase, either a HECT or RING type. This process can yield a multitude of ubiquitin signals on the target protein and a variety of cellular outcomes. **B.** In contrast to the ubiquitination, the removal of ubiquitin from the target is not mediated by an enzyme cascade but rather by a single deubiquitinating enzyme.

ATP dependent manner. After production of a ubiquitin-adenylate intermediate, the ubiquitin is transferred to the E1 active site cysteine residue, with the release of AMP. This step results in a thioester linkage between the C-terminal carboxyl group of G76 of ubiquitin and the E1 cysteine. In the second step, the ubiquitin is transferred from the E1 to the active site cysteine of a ubiquitin-conjugating enzyme E2. In the third and final step, the isopeptide bond is created between the lysine of the target protein and ubiquitin. This transfer can occur in two ways, either directly from the E2, catalyzed by RING/UBox domain containing E3's that act as chaperones by bringing the E2 and target in close proximity, or via a covalent E3-ubiquitin intermediate, catalyzed by the HECT domain-type E3's.

An interesting feature is the hierarchy within this cascade. Until now, only two E1's have been indentified. However, these can bind with dozens of E2s, which in their turn cooperate with hundreds of E3s, allowing for ubiquitination of specific proteins. This hierarchical organization is conserved, as ubiquitin-like proteins are also conjugated via a dedicated but similar E1–E2–E3 cascade.

This enzyme cascade has successfully been targeted by drugs in the treatment of cancer. One of the most recent successes is the MLN4924 compound, which is an specific inhibitor of the E1 in the ubiquitin-like Nedd8 pathway[16,17]. Inhibiting E2 and E3 enzymes with drugs is considered difficult, due to the absence of a classic active site. However, a recent study reports the first inhibitor of the human E2 CDC34[18]. It describes an allosteric inhibitor (CC0651) that does not directly contact the active cysteine of the enzyme. Instead, it binds the helix bearing the catalytic cysteine yielding a displacement by 2.0 Å. By doing so, it specifically disturbed the ability of CDC34 to promote ubiquitin transfer and chain formation on substrates, turning its conjugating activity on itself and free ubiquitin. This compound is remarkably selective for CDC34, and these results imply that it might be possible to selectively target other E2s in the future.

However, a problem with targeting E2's, is that one might affect a wide range of downstream targets. To gain more target specificity, E3's can be inhibited instead. For example, the Nutlin compounds (cis-imidazoline analogs) inhibit the interaction between the E3 ligase HDM2 and its substrate, tumour suppressor p53[19]. Inhibiting this interaction stabilizes p53 and is thought to selectively induce a growth-inhibiting state called senescence in cancer cells[20].

Ubiquitination in many flavours
As mentioned before, ubiquitination comes in many more flavours than the K48 poly-ubiquitination. These additional ubiquitin signals can equally serve more functions than the signal for protein degradation. Mono-ubiquitination can alter the activity and localization of a protein, and is found to regulate endocytosis, lysosomal targeting, meiosis and chromatin remodelling[21-23].

Ubiquitin itself can be ubiquitinated forming poly-ubiquitin chains. There are seven available lysines in ubiquitin (K6, K11, K27, K29, K33, K48 and K63; Figure 2). Besides that, they can also be linked through their N- and C-termini resulting in linear ubiquitin chains. The precursor of ubiquitin is expressed in these head-to-tail ubiquitin-chains, which is subsequently processed by DUBs into mono-ubiquitin and then used for conjugation[24]. However, linear poly-ubiquitin chains can also be assembled from mono-ubiquitin by a dedicated E3 ligase complex, the Linear Ubiquitin Chain Assembly Complex (LUBAC)[25]. Overall, since poly-ubiquitin chains can contain mixtures of linkages, there is a seemingly endless variability in composition and thus downstream signalling. At present, it is not clear just how complex the ubiquitination system is.

All the different linkages between ubiquitin moieties (ubiquitin topoisomers) have been found in cells[26], and mass spectrometry analysis revealed relative abundances of most ubiquitin topoisomers[27]. K48 linked ubiquitin is the most abundant ubiquitin chain type (~30%), and the K63 linkages accounted for another ~20% of all linkages. K11-linked ubiquitin was found to be almost as abundant as K48 linkages.
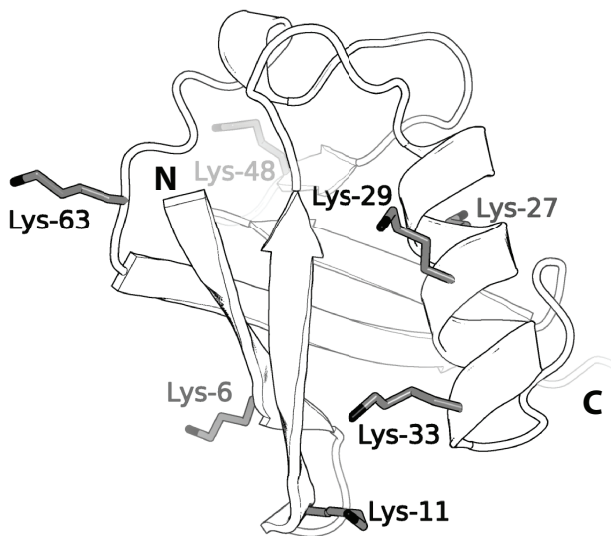
Figure 2. Ubiquitin itself contains 7 lysines that can be used to produce poly-ubiquitin chains. Ubiquitin can also be linked through their N- and C-termini, resulting in linear ubiquitin chains.

In contrast to K48-linked poly-ubiquitin, K63-linked ubiquitination has non-degradative roles, and is involved in endocytosis, in DNA-damage responses and in cell signalling[21]. K11-linked chains still represent a relatively unstudied linkage but seem to also serve as a potent proteasomal degradation signal[8,9]. It is involved in many different pathways, including the cell cycle[9,28]. However, due to the lack of tools to study and to make most ubiquitin chains[29,30], both the functions and the conjugation mechanisms of most linkages are less well understood.

Ubiquitin binding domains

In comparison to the small molecule modifiers, the conjugation of a ubiquitin moiety provides a larger and chemically more diverse surface. This resulted in the co-evolution of a multitude of specialized Ubiquitin Binding Domains (UBDs) to translate the many ubiquitination states into specific signals. The UBDs bind non-covalently to ubiquitin or specific ubiquitin chains and mediate different outputs depending on the protein they are part of. The various classes of UBDs and their biological properties are relatively well studied and characterized, and

several crystal structures provide structural insights[31-35].

UBDs can bind, and often distinguish, different types of ubiquitin modifications. The number of identified UBDs is increasing, with more than twenty different families[36]. They diverge both in structure and in the type of ubiquitin recognition that they use, but most of them use an α-helical structure to bind the β-sheet of ubiquitin. Especially the residues L8, I44 and V70 in this region on ubiquitin often play an important role in the binding.

Usually the affinity for ubiquitin is weak and dynamic and the dissociation constants (Kd's) are typically in the (high) micro molar range. The majority of UBDs do not have an intrinsic specificity towards any type of poly-ubiquitin linkage[37]. Instead, the specificity is induced by surrounding domains within the protein of complex. Therefore, combinations of UBDs are needed to bind poly-ubiquitin or discriminate different linkages.

Interpretation of the ubiquitin chains is achieved in several ways and sometimes this

is accompanied by a preference for ubiquitin chains of a specific linkage, like in RAP80 for K63-linked ubiquitin[38] and NEMO for linear ubiquitin[39]. For example, the C-terminal Ubiquitin-Associated (UBA) domain of Rad23A binds K48-linked chains 70-fold tighter compared to mono-ubiquitin, but additionally displays a 4-fold preference over K63-linked ones[37]. The crystal structure nicely explains how this is achieved[38]. It shows that the UBA domain is sandwiched between the two ubiquitin moieties of the K48-linked di-ubiquitin. There it binds to both ubiquitin moieties, using a significantly larger binding surface than it could form with a single ubiquitin. Since it also binds the di-ubiquitin linker region, this binding mode induces a linkage preference.

Ubiquitin and disease
Since the ubiquitin pathway is involved in many key cellular processes, it is no surprise that aberrant ubiquitination or ubiquitin signalling has been implicated in various diseases, ranging from cancer, viral infection, neurodegenerative disorders, muscle wasting, diabetes to inflammation. Several published reviews adress the role of ubiquitin in specific diseases; here we will briefly discuss two[40-44].

Cancer
The development of cancer is a multistep process, and originates from the accumulation of mutations in the cellular pathways regulating proliferation and survival under adverse conditions[45]. Deregulation of components of the ubiquitination system is common in the development of cancers[46-49]. Many direct substrates of E3 ligases and DUBs play key roles in the cell cycle[45], DNA repair[50], NF-κB signaling[51], RTK signaling[52] and angiogenesis[53] and their levels or activity are precisely regulated by ubiquitination. Furthermore, as discussed before, the clinical success of Bortezomib illustrates the importance of the ubiquitin-mediated signalling in cancer.

Mutations or overexpression of numerous E3 ligases render them potent oncogenes[54,55], examples are the SCF ligases that regulate cell-cycle progression, and HDM2, which is a negative regulator of the tumour-suppressor protein p53[56,57]. Besides the degradative role of ubiquitination, is the non-degradative type also important in tumour suppressor biology. For example, the mono-ubiquitination of tumour suppressors p53 and PTEN (Phosphatase and Tensin Homologue) is involved in cancer development, as discussed later in more detail[58-60].

Also many DUBs are involved in tumour progression, and several deubiquitinating enzymes are found overexpressed in tumours and stabilize oncogenes. Recent examples are USP9X[61] and DUB3[62]. USP9X is overexpressed in haematological malignancies, where it deubiquitinates and stabilizes the pro-survival BCL-2 family member MCL1. DUB3 stabilizes cell cycle-regulating phosphatase CDC25A, which has been linked to breast cancer initiation and progression.

Neurodegenerative disease
Neurodegenerative diseases such as Parkinson's, Alzheimer's and Huntington's, originate from protein aggregates that contain ubiquitin[63]. For example, expansion of the polyglutamine repeat in the mutant Huntington protein promotes the formation of protein aggregates that are resistant to degradation by the proteasome, but also impair proteasome function[64]. Similarly in Alzheimer's disease, proteasome function is impaired by the formation of plaques associated with amyloid-β protein aggregation and ubiquitinated TAU[65]. In Parkinson's disease, mutations in the E3 ligase PARKIN impair its activity *in vitro*, suggesting that accumulation of its substrates could contribute to disease development[66]. Additionally, down-regulation, extensive modifications and truncations of the DUB UCH-L1 have been observed in both Alzheimer's as well as in Parkinson's disease patients[67]. UCH-L1 is a multifunctional protein, since it displays both deubiquitinating[68] and ubiquitin conjugation activity[69]. It is exclusively localized in the brain[70], and its precise role in neurodegeneration is still unresolved.

De-Ubiquitination

Like other post-translational modifications, ubiquitination is a dynamic and therefore reversible process. The removal of ubiquitin is carried out by more than 90 DUBs[24,71]. In contrast to ubiquitination, de-ubiquitination is performed by single enzymes rather than an enzyme cascade. The importance of the deubiquitination is illustrated by the involvement of several DUBs in various diseases[72-75]. Also, DUBs are overexpressed or activated in tumour cells and contribute to the transformed phenotype[76,77]. As a consequence, they are acknowledged as promising therapeutic targets[78,24], and therefore actively pursued as potential drug targets, both by academia and industry. This led for example to a remarkably selective small-molecule inhibitor for USP14. This inhibitor enhanced the degradation of several proteasome substrates that have been implicated in neurodegenerative disease[79]. Also, the partly selective inhibitor WP1130 (USP9x, USP5, USP14, and UCH37) was found. Applying this inhibitor results in the downregulation of anti-apoptotic and upregulation of pro-apoptotic proteins, such as MCL-1 and p53[80].
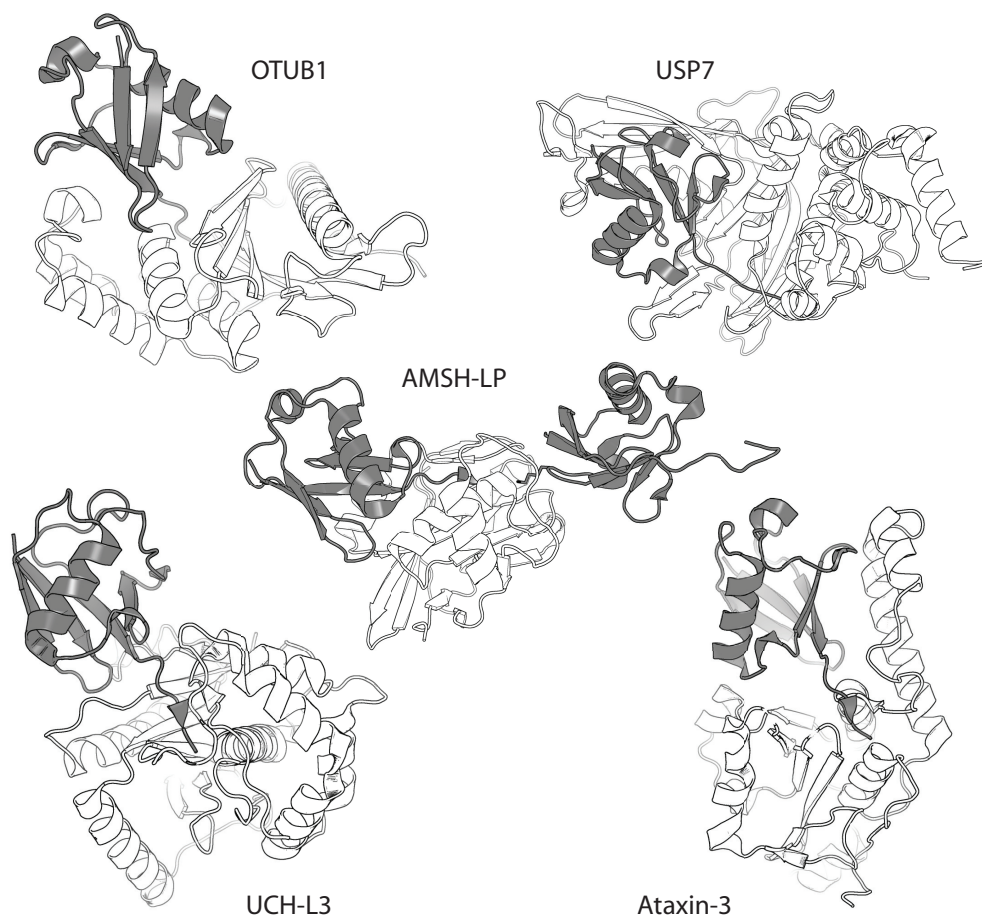

Figure 3. A cartoon representation of the structures of representative members of each DUB family. Ubiquitin is coloured grey. PDB codes USP7:1NBF, OTUB1:3BY4, AMSH-LP:2ZNV, UCH-L3:1XD3 and Ataxin-3:1JRI (NMR).

The DUBs are categorized in five structurally unrelated families: Ovarian Tumour proteases (OTUs), the Ubiquitin C-terminal hydrolyses (UCH), the Machado-Josephin disease protease (MJD), JAMM (JAB1/MPN/MOV34) proteases and the Ubiquitin-Specific proteases (USPs), (Figure 3)[71].

Proteolysis by DUBs
Cysteine-protease DUBs
The DUBs from the USP, OTU, UCH and MJD families are cysteine dependent proteases. They use a papain-like mechanism to hydrolyze the isopeptide bond between the carboxyl terminus of ubiquitin and the ε-amine of the target lysine. The mechanism to break the isopeptide bond involves the lowering of the pKa of the catalytic cysteine by a histidine, resulting in the deprotonation of the cysteine. This is facilitated by an aspartate or asparagine, by orienting the imidazole ring of histidine to allow the deprotonation to take place[81]. The cysteine then performs a nucleophilic attack on the carbonyl carbon of the isopeptide bond. This frees the ε-amine of the target lysine, and forms a covalent acyl-enzyme intermediate with ubiquitin. The enzyme is then deacylated by a water molecule, thereby releasing free ubiquitin.

Metallo-protease DUBs
The JAMM metallo-protease DUBs contain zinc ions in their active site, coordinated by histidine, aspartate and serine residues[82]. The zinc ion activates a water molecule, and the resulting hydroxide performs a nucleophilic attack on the carboxyl carbon of the isopeptide bond, releasing the ε-amine of the target lysine.

Ovarian Tumour Proteases (OTUs)
There are fifteen family members, that can be phylogenetically subdivided in three subclasses, the Otubains, the OTUs and the A20-like OTUs[24]. So far, the family members mainly function in cell signalling processes, where they regulate NF-κB signalling[83,84], Wnt signalling[85], IRF3 signalling[86] and DNA damage responses[87]. They vary in size (230 - 1200 residues) and often contain additional domains with links to the ubiquitin system, like Ubiquitin Interacting Motifs (UIMs), UBA domains and Ubiquitin-Like (UBL) folds[24].

Several structures of OTU catalytic domains have been solved. The catalytic core domain comprises 150 to 200 residues, and the A20-like OTU subtype (A20, Cezanne1/2, TRABID and VCIP135) contain an N-terminal extension. In OTUB1, the ubiquitin binding site is remodelled upon ubiquitin binding, and the active site is in an unproductive configuration, requiring conformational changes to become an active enzyme[88]. This requirement for remodelling is shared with members of the UCH, MJD and USP families[81,89-92].

The OTU family displays remarkable ubiquitin-linkage specificity. Most OTUs do not cleave linear chains efficiently, and therefore are strict isopeptidases[93]. TRABID[93] and DUBA[86] cleave K63 ubiquitin chains, while OTUB1[88] is K48-specific. Interestingly, A20 hydrolyzes K48-linked ubiquitin *in vitro*, yet its substrates are modified with K63-linked chains[94,95]. There is also cross reactivity with other ubiquitin-like modifiers; OTUB1 was suggested to cleave both ubiquitin and Nedd8 conjugates[88]. In order to evade the host immune response, viral OTUs have evolved cross-reactivity and are active against both ubiquitin and the ubiquitin-like ISG15. Due to recent structures of the viral OTUs in complex with ubiquitin and ISG15, this cross reactivity is now understood at the molecular level[96,97].

Remarkably, OTUB1 inhibits the DNA double strand break (DSB) response independently of its catalytic activity[87]. It does so by suppressing the poly-ubiquitination by the E3 ligase RNF168, by binding to and inhibiting the E2 enzyme UBC13. Non-catalytic roles for DUBs are not unique. For example, Ubp6 regulates proteasome-dependent degradation in a non-catalytic manner[98]. Also DUBs such as USP39 and USP52 to USP54 lack the necessary active residues for peptidase activity[71,99], suggesting non-canonical functions.

Ubiquitin C-terminal Hydrolases (UCHs)
The UCH family contains only four members, two of which consist of only the minimal catalytic domain (UCH-L1 and UCH-L3)[24,71]. These

both have functions in the brain[67,100,101] and UCH-L1, has been associated with Parkinson's disease[66]. A third member, UCH-L5, binds to the proteasome, where it is responsible for recycling ubiquitin from proteasome substrates[102]. The fourth human UCH enzyme, BRCA1 associated protein-1 (BAP1) is a tumour suppressor and interacts with the BRCA1 E3 ubiquitin ligase which is involved in DNA repair[103]. Additionally, it is involved in chromatin repression by deubiquitinating histone 2A (H2A) as part of the Polycomb repressive DUB (PR-DUB) complex[104]. Structural and biochemical studies have indicated that UCHs preferentially cleave small protein substrates (up to 20-30 amino acids) from ubiquitin[105].

The crystal structure of UCH-L1 shows that both the catalytic residues and several loops need remodelling upon ubiquitin binding[89]. Interestingly, in UCH-L3 the ubiquitin C-terminus is covered by an active site cross-over loop, which forms upon ubiquitin binding[106,107]. This does not allow binding of folded ubiquitinated proteins or ubiquitin chains, which would be too big to enter through the cross-over loop. This feature nicely explains the lack of activity against larger substrates[108]. Possibly, UCHs are mainly targeting ubiquitination sites in unfolded regions of proteins or residual ubiquitin-peptide conjugates after proteasomal degradation. Possibly, this cross-over loop can be remodelled, like in the case of UCH-L5, where binding to the proteasome allows cleavage of poly-ubiquitin[109].

Machado-Josephin Disease proteases (MJDs)
The MJD family also contains only four members[110,111]. Like the UCH family, two members consist of only the minimal catalytic domain (Josephin-1 and Josephin-2), while the two others (Axatin-3 and Ataxin-3-like) have additional UIMs. The most prominent member of the family is Ataxin-3, which is mutated in Machado-Joseph disease, the most common form of spinocerebellar ataxia[112]. NMR studies on Ataxin-3 showed a misaligned catalytic triad, but upon ubiquitin binding the active conformation is stabilized[90-92,113]. The key feature of MJD domains is a large helical lever that restricts access to the active site in absence of

ubiquitin[90,92]. Ataxin-3 itself is ubiquitinated by which it is activated, possibly by stabilization of the helical lever in an open conformation[114]. The substrates of Ataxin-3 and the roles of the remaining MJDs are currently unclear.

JAMM motif proteases (JAMMs)
There are eight JAMM containing ubiquitin proteases[24], of which PRPF8 is predicted to be inactive based on structural analysis[115]. The JAMM domain is a general protease domain, and is also found in prokaryotes (that do not have a ubiquitin conjugation system). The JAMMs are metallo-proteases and are active as part of multi-subunit protein complexes. For example, POH1 binds the proteasome and contributes to recycling ubiquitin chains[102], while AMSH and AMSH-LP regulate membrane trafficking within to the ESCRT machinery[116]. The JAMM/MPN+ DUBs seem to prefer K63 ubiquitin chains, and some show remarkable specifity[117,118]. The specificity of AMSH-LP is explained by the crystal structure with K63-linked di-ubqiuitin[119]. This shows that it binds to both the linker region as well as the of K63 sequence context.

Ubiquitin Specific proteases (USPs)
This thesis is focussed on the USP family. It is the largest and most diverse family of DUBs with more than 60 members[24,71]. As the number of ubiquitin E3 ligases increased during evolution, so did the number of USPs, suggesting an intimate antagonistic relationship[120]. Knowledge about the USPs is increasing, however for a large number both the physiological function and specific substrates still remain elusive.

USPs are regulated by interacting proteins and about 800 DUB interacting proteins have been identified to date[121]. These interactions can be categorised into distinct classes that have particular functional consequences. The first functional interaction is between DUBs and E3 ubiquitin ligases, which protects E3s from auto-ubiquitination and thereby increases their stability[122-127]. Examples of this regulatory feedback include USP9 that prevents auto-ubiquitination of E3 Itch126, MARCH7 auto-ubiquitination is prevented by

USP7 and USP9X[125], and USP15 prevents auto-ubiquitination of RBX1[124]. A second class of interaction is a simpler version of the above, in which the USP interacts with a target of an E3, thereby stabilising the target protein directly. A third type of interaction includes proteins whose mono-ubiquitination status is regulated by USPs without affecting their stability, but instead influencing their biological functions. A fourth category of interaction partner modulates the activity of the USP. For example, USP1, USP12 and USP46 interact with the WD40 protein UAF1 (USP1 associated factor, also known as WDR48), which subsequently results in an enhanced activity of the USP1[128,129]. And finally, the fifth commonly observed interaction exists between DUBs, as for example the interaction between USP7 and USP11 which plays a role in stabilizing the Polycomb Repressive Complex 1 (PRC1)[130]. Most interactions have not been characterized and therefore their biological function is still unknown.

Concerning the biochemistry of the USPs there are still questions to be addressed. For example, studies for chain preference of the USPs have so far mainly focussed on the canonical K48- and K63-linked ubiquitin. Most of the analyzed USPs are nonspecific and will cleave any chain type, however they do show distinct preferences[93]. Examples are USP14, that preferentially cleaves K48 linked ubiquitin chains[131], and CYLD, that specifically hydrolyzes K63 linked and linear chains[93,132]. In chapter 2 we now for the first time include the remaining ubiquitin linkages and characterization the differential activity of twelve USPs towards all seven lysine-linked di-ubiquitin.

USP structure
Usually USPs are large proteins with a minimal core catalytic domain of about 350 amino acids[71]. Outside of their catalytic domain, USPs contain large unrelated sequences that harbour additional domains used for protein-protein interaction. Some are dedicated for substrate binding, while others are more general interaction domains. These include UBDs, such as the zinc finger ubiquitin specific protease domains (ZnF-UBP), UIMs and UBAs. Some domains facilitate the subcellular localization of their USPs, like the transmembrane regions in USP19 (endoplasmatic reticulum), USP30 (mitochondria) and USP48.

Structures of the USP catalytic domains show a conserved fold. It consists of three sub domains, Palm, Thumb and Fingers, resembling a right hand (Figure 3 and 8B)[81]. The catalytic centre lies at the interface between Palm and Thumb, while the Fingers domain grasps the distal ubiquitin. Some USPs display dramatic conformational changes upon ubiquitin binding For instance, in USP7 the active site is remodelled to an active conformation upon ubiquitin binding[81]. In contrast, the catalytic residues of USP14 and USP8 are properly aligned for catalysis in absence of ubiquitin, but in these USPs the ubiquitin binding site is blocked by surface loops[131,133]. Furthermore, in USP8, which has only been crystallized without ubiquitin, the Fingers domain is tightened inward, additionally blocking the ubiquitin binding site.

About half the USPs have insertions in their catalytic domain, and some of these insertions are larger than the catalytic domain itself. Detailed analysis revealed that the USP catalytic core domain can be subdivided into six conserved sequence boxes[134]. The five boundaries between the subdomains are integration sites of the insertions. Some inserted sequences contain additional independently folded domains, including protein interaction domains (e.g. a B box in CYLD[132], the MYND domain in USP19[135], UBA domains in USP5[136], and a UIM in USP37[134]).

UBL domains in USPs and their functions
USPs have large regions that have been annotated for neither fold nor function. Fold recognition methods revealed an unexpectedly high number of (multiple) UBLs in at least 17 USPs (Figure 4)[137,138]. This makes the UBL domain the most abundant accessory domain in the USP family. The intruiging presence of these domains might suggest an auto-regulatory function. Though to date, most UBL domains remain unstudied.

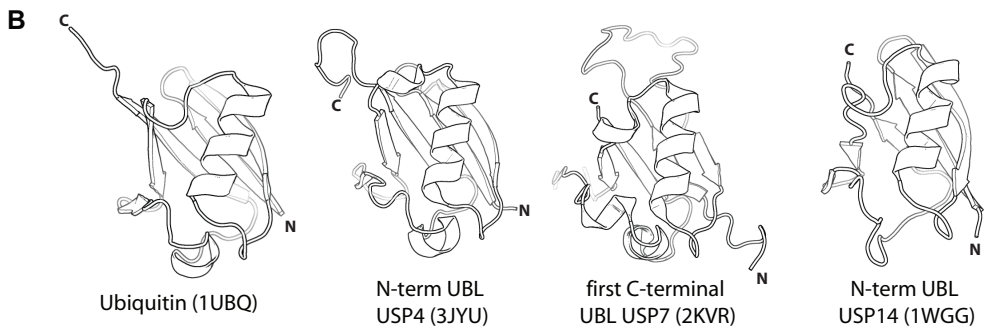The UBL domains are located in different

A

B

| Ubiquitin (1UBQ) | N-term UBL USP4 (3JYU) | first C-terminal UBL USP7 (2KVR) | N-term UBL USP14 (1WGG) |
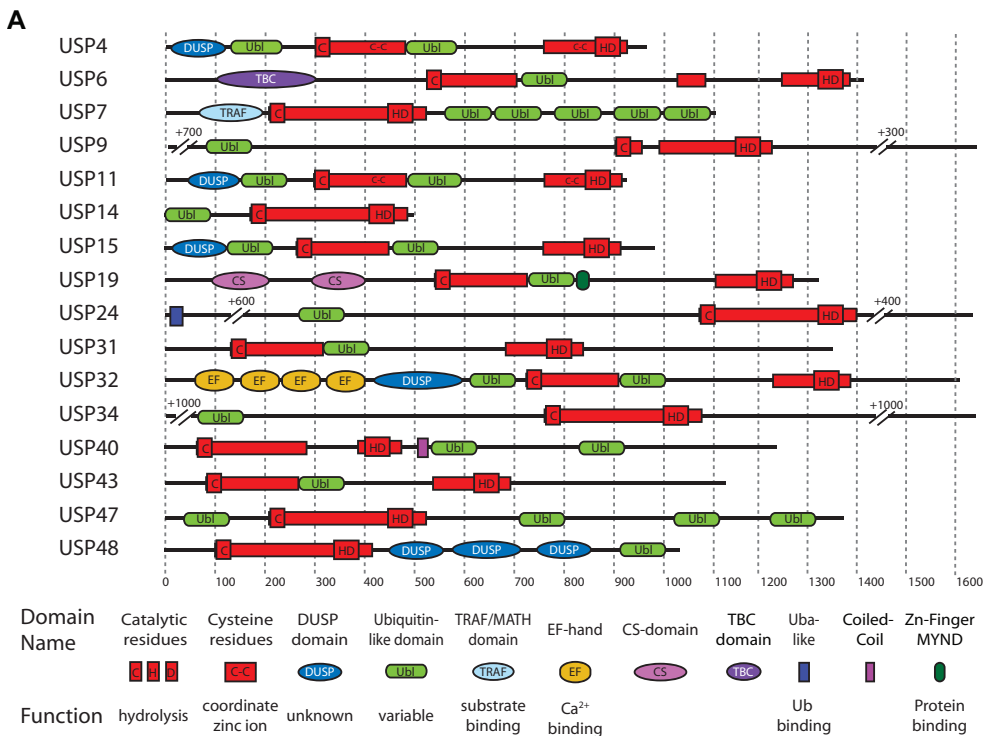
Figure 4. UBL domains in USPs A. Domain architecture of the USPs with predicted UBL domains. The UBL domains can be inserted in a conserved site between two subdomains of the catalytic domains, but they are also found in the flanking regions. **B.** Structures of individual UBL domains from USPs show the conserved β-grasp ubiquitin-like fold.

positions in the enzymes, and they can be found both N- and C-terminally of the catalytic domain. Interestingly, eight USPs have a UBL domain inserted in a conserved position between two subdomains in the catalytic domain (USP4, 6, 11, 15, 19, 31, 32, and 43). The remainder of the inserted sequences mostly lack predicted secondary structure elements and therefore are most likely unstructured regions. USP19 is the

only exception, where the UBL is immediately followed by an MYND Zn-finger domain, while the rest of the insert has no obvious fold.

UBL domains have a ubiquitin-like fold, which is characterized by a five stranded β-sheet with a single α-helix on top, but they lack the C-terminal residues required for conjugation to a target. This β-grasp fold is often found as

part of larger multi-domain protein. Among the studied UBL domains, distinct subclasses can be identified with different functions[139]. In the USPs the sequence homology of the UBL domains is low (below 20%), but in many other proteins they strongly resemble ubiquitin in primary sequence as well as in fold. These homologies are for example found in proteasomal shuttle factors RAD23 and Ubiquilin[140-143], where the UBL is responsible for the association to the proteasome. UBL domains are also involved in signal transduction and enzymatic activity. For example, the UBL domains in IKKβ[144,145] and IKKε[146] are essential for their kinase activity. Some have multiple functions, like in the E3 ligase PARKIN where the UBL domain regulates the proteasomal localization, the cellular levels of PARKIN, and also inhibits its auto-ubiquitination[147-149].

Another example of an integrated UBL domain is the Ubiquitin-regulatory X (UBX) domain. Like the UBL domains in the USPs they have only a limited sequence similarity with ubiquitin, but still have the β-grasp fold[150]. UBX domains are found in FAF1, p47, Y33K, and Rep8 proteins[150], and are needed for targeting ubiquitinated proteins to the proteasome or ERAD pathway (recruitment to p97)[150-152]. UBL domains are often important integrated elements of proteins, and are present in a large variety of proteins families; however only a few of these have been studied functionally[153,154].

Within the USP family, the function of the UBL domain in USP14 was the first to be elucidated. It is needed for the association of USP14 to the proteasome[155] and this binding activates USP14 activity[156]. Specifically, USP14 resides on the 19S regulatory particle of the proteasome where it removes ubiquitin from the substrate before degradation. In this thesis we present the function and mechanism of the UBL domains in USP4 (chapter three) and USP7 (chapter four).

USP4

USP4 was previously known as a ubiquitous nuclear protein (UNP)[157] that is able to bind to the tumour suppressor retinoblastoma (RB) protein, suggesting a role in cancer development[158]. Later USP4 was identified as a proto-oncogene and shows a consistently elevated gene expression level in small cell tumours and lung adenocarcinomas[159]. Several functions and targets of USP4 have since been identified. First, genetic screens identified an interaction between USP4 and two WNT signalling components. It binds to the NEMO like kinase (NLK), which subsequently leads to the recruitment of USP4 to its target, transcription factor T-cell factor 4 (TCF4)[160]. Secondly, USP4 is involved in the endoplasmic reticulum (ER) quality control by binding to the A2A receptor, a prototypical G-coupled receptor[161]. Its de-ubiquitination by USP4 enhances the cell surface expression of the A2A receptor. In the third case, USP4 is linked to cell cycle control. It interacts with SART3, which is a component of the spliceosome complex[162]. This is a dynamic complex of proteins and RNAs that catalyzes the excision of intron sequences from nascent mRNAs. SART3 recruits the U4 component PRP3, which is subsequently deubiquitinated by USP4. This deubiquitination probably facilitates the ejection of Prp3 from the spliceosome[162]. The loss of USP4 interferes with the accumulation of correctly spliced mRNAs and impairs cell cycle progression. Finally, a recent study revealed a fourth function, where USP4 regulates p53 protein levels by antagonizing the p53 E3 ligase ARF-BP1[163,164].

Interestingly, USP4 has two paralogs: USP11 and USP15 and they share 60-80% sequence similarity (Figure 5A). Despite the striking resemblance, the USP4 paralogs seem to have different functions. USP11 has been shown to interact with a diverse array of cellular proteins. For example, it negatively regulates TNFα-induced NF-κB activation by targeting on IκBα[165,166]. It is also involved in the double strand DNA repair by interacting with BRCA2[167], and regulating RAD51 and 53BP1 localization after the initial γH2AX signal[168]. As discussed later in more detail, together with USP7 it is also responsible for stabilizing the PRC1 complex[130]. On the other hand, USP15 seems to be involved in the COP9-signalosome, a conserved multi-protein complex that regulates the Cullin-RING ligase (CRL) superfamily of ubiquitin E3 ligases[124,169]. It is proposed that in this complex,
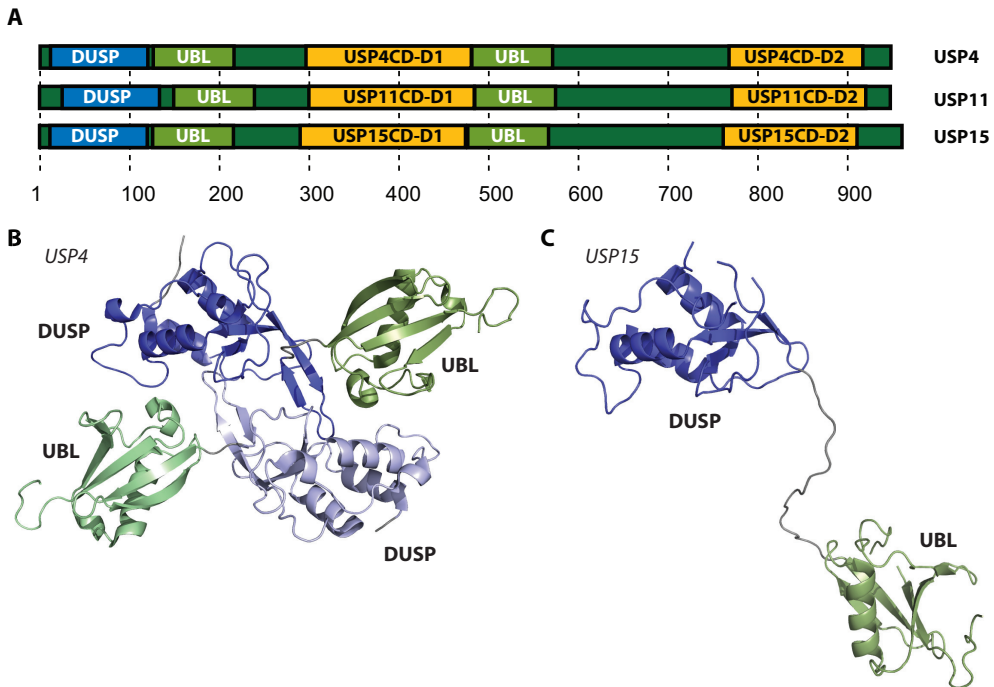
Figure 5. Overview of structural information USP4. A. Schematic domain architecture showing the DUSP (blue), two UBL (green) and a split catalytic domain (D1 and D2; orange). This architecture is shared with the paralogs USP11 and USP15. **B.** The crystal structure of the DUSP-UBL domain of USP4 (3JYU) shows a possible dimerization. The second molecule is coloured in a lighter shade. C. The crystal structure of the DUSP-UBL domain of USP15 (3PPA) shows a flexible relative orientation of the DUSP and UBL domain. No dimerization was observed in the crystal.

USP15 protects against auto-ubiquitination and degradation of CRL components, in particular the substrate-specific adaptors[170], or directly oppose CRL E3 ligase activity by deubiquitinating specific substrates[171-173].

USP4 itself is a 963 amino acid (109 kDa) large protein (Figure 5A). It has at the N-terminus a single DUSP (domain in USPs) domain, which is characterized by a tripod-like fold with a conserved hydrophobic surface patch that is predicted to participate in protein-protein interaction (Figure 5B)[174,175]. This domain is followed by a UBL of unknown function. After the DUSP-UBL domain comes a split catalytic domain, with a second UBL as part of a larger insert. In chapters two and three we show that this UBL insertion influences the activity through a competitive inhibition mechanism.

USP7 / HAUSP

USP7 also contains UBL domains, and in chapter two we describe that these that are involved in the activity[176,177]. In USP7 it is not a single UBL as in USP4, but in chapter four we show that there are five consecutive UBL domains at the C-terminal of the protein (Figure 4A). Also in contrast to USP4, the UBL domains in USP7 are responsible for an intriguing increase of the activity, rather than an inhibition[178].

USP7 represents one of the most studied DUBs. It was originally named HAUSP (herpes virus associated ubiquitin specific protease), and in practice both names are in use in current literature. USP7 is widely expressed in many different tissues and it is predominantly a nuclear protein. In the nucleus it has a diffuse localization, but with discrete accumulations associated with nuclear substructures

known as ND10 or promyelocytic leukaemia nuclear bodies (PML-NBs)[179]. Difficulties in the maintenance of cell lines lacking USP7 indicates that it is required for long term cell survival[127], a conclusion supported by the observation that knock out of the gene in mice causes death in early embryo development[180]. This lethality could be related to widespread proteome changes in cells depleted of USP7, which link the enzyme to the regulation of transcription, DNA replication and apoptosis[181]. USP7 is upregulated in prostate cancer and has been linked to an important role in non small cell lung carcinogenesis, and an aberrant USP7 function is involved in oncogenesis and viral infection[182,183].

Functional interactions

Since USP7 was first identified[179], the number of reported interaction partners and substrate proteins has increased significantly. USP7 is a direct regulator of activities of numerous proteins broadly characterized as tumour suppressors, DNA repair proteins, immune responders, viral proteins and epigenetic modulators. Given the complexity and number of all these interactions, it is not surprising that USP7 plays a very important role in the cell such that in its absence cells exhibit many defects. Given the important and the multifaceted role of USP7, and also the fact that at least one of the interactors (GMPS) can influence the activity of USP7, we will now briefly describe the most prominent interaction partners of USP7 (Figure 6).
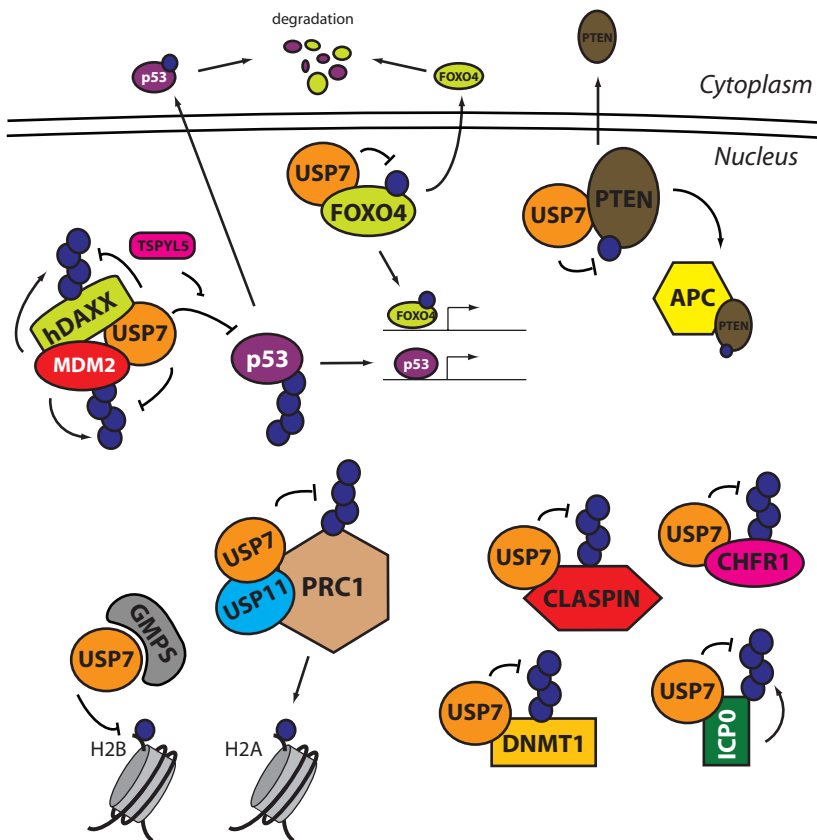

Figure 6. The most prominent interaction partners and targets of USP7. Ubiquitin is colored purple.

ICP0

USP7 was first identified as a strong interaction partner of herpes simplex virus type 1 (HSV-1) immediate-early regulatory protein Infected Cell Protein 0 (ICP0; previously also known as Vmw110)[179]. It is a component of the inner viral matrix that it is released into the cytoplasm shortly after infection. To date, the precise function of ICP0 is unknown. However ICP0-deficient viruses are avirulent due to their sensitivity to interferon α/β and have an aberrant viral gene expression at a pre-immediate-early step in infection[184,185]. ICP0 is required for productive low-multiplicity infection, and therefore controls the balance between the viral latency and lytic states[186,187]. As HSV-1 infection prevents induction of apoptosis in an ICP0-dependent manner, it is possible that ICP0 inhibits the initiation of apoptotic responses by p53[188].

ICP0 contains an N-terminal RING domain, needed for its ubiquitin ligase activity, a nuclear localization signal, and an oligomerization domain in the C-terminus[189]. It mediates the degradation of several cellular proteins by inducing ubiquitin conjugation[179,190,191] and sequesters proteasomes in the nucleus[192]. The C-terminal region is critical for both the HSV-1 virulence and the interaction with USP7[193]. An intriguing consequence of this interaction with USP7 is the occurrence of reciprocal activities such that USP7 stabilises ICP0, while ICP0 ubiquitinates and destabilises USP7[122]. Possibly, the virus recruits USP7 to facilitate its survival in the host.

Interestingly, a recent study showed that ICP0 expression resulted in export of USP7 from nucleus to cytoplasm where USP7 binds and deubiquitinates TRAF6 and IKKγ, thereby inhibiting the NF-κB mediated innate immune response[194]. This suggests that USP7 regulates Toll-like Receptor (TLR) signalling and that ICP0 exploits this physiologic process to hamper innate response to HSV-1.

HDM2/HDMx, DAXX and p53

The p53 tumour suppressor is essential for the cell-cycle arrest and apoptosis after genotoxic stress[195,196]. It is also required for the induction of senescence after oncogene activation, which is considered to be a mechanism to prevent tumourigenesis[196]. One of the major roles of p53 is to activate transcription of a wide range of target genes to exert its role the stress response[197]. Its importance as a tumour suppressor is nicely demonstrated by the fact that it is mutated, inactivated or misregulated in almost all human cancers[195].

p53 is tightly regulated, mainly at the level of protein stability, to allow rapid protein accumulation and activation after DNA damage. Hence under normal condition, the p53 protein levels are kept low, due to continuous ubiquitin-dependent degradation by the proteasome[198]. This ubiquitination is carried out by the E3 ligase Human Double Minute 2 (HDM2). It is essential in regulating p53 levels, since the embryonic lethality observed in HDM2 knockout mice is rescued in a p53-/- background[199,200].

Interestingly, USP7 interacts and stabilises p53 by removing the ubiquitin[201]. However, the regulation of p53 protein levels less straightforward. For example, when USP7 expression is lost, it results in a counterintuitive upregulation of p53 with associated cell cycle arrest[127,202-204]. This shows that the p53 regulation is dynamic and much more complex, and that many factors contribute to the control and activation of p53[195,196].

Structural studies revealed that both HDM2 and p53 are able to bind to USP7, and therefore are both valid targets of USP7[205-208]. However, since USP7 has a higher affinity for HDM2, it is now believed that under normal conditions USP7 deubiquitinates and therefore stabilizes auto-ubiquitinated HDM2 (Figure 7; left panel). Death domain-associated protein (DAXX) simultaneously binds to HDM2 and USP7, and it mediates the stabilizing effect of USP7 on HDM2[209]. In addition, DAXX enhances the intrinsic E3 activity of HDM2 towards p53. DAXX itself is also a target of both HDM2 and USP7[210]. The net effect of this complex is the ubiquitination and subsequently destabilization of p53, which explains the upregulation of p53 after the loss of USP7.
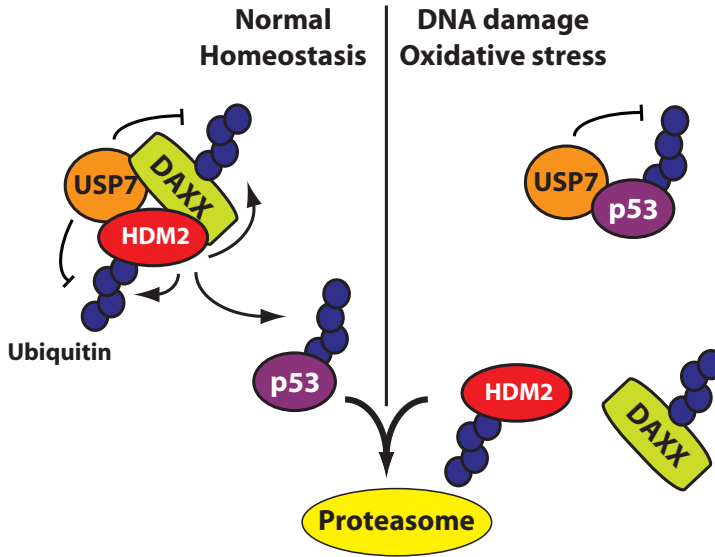
Figure 7. USP7 regulates both HDM2 and p53 protein levels. In normal homeostasis, USP7 interacts with DAXX and HDM2, antagonizing their (auto-) ubiquitination. This results in ubiquitinated p53, which is subsequently targeted for degradation by the proteasome. However, upon stress, HDM2 is phosphorylated by the ATM/ATR pathway. As a result USP7 now switches targets and interacts with p53. This prevents its ubiquitination and both HDM2 and DAXX are degraded by the proteasome, since their (auto-) ubiquitination is no longer antagonized by USP7[127,202,203]. Ubiquitin is colored purple.

However, following stress like DNA damage, HDM2 is phosphorylated by Ataxia Telangiectasia Mutated (ATM)/Ataxia Telangiectasia and Rad3-related protein (ATR). This results in first the dissociation of the USP7/HDM2/DAXX complex, and subsequently the proteasomal degradation of HDM2 and DAXX (Figure 7; right panel). Now USP7 can target and ultimately upregulate p53[203].

Taken together, if USP7 would be targeted by drugs as part of cancer therapy, this would inactivate HDM2 and activate p53. This would result in tumour cell arrest and apoptosis in cells retaining a functional p53 pathway.

TSPYL5 and EBNA-1
The regulation of USP7 mediated p53 homeostasis has two more players. The first is TSPYL5, which is among the genes in a prognostic expression signature (MammaPrint®) that predicts clinical outcome of breast cancer[211]. It has a causal role in breast oncogenesis, but the function of this protein is still unknown. TSPYL5 overexpression results in the decrease of p53

levels and its target genes[212].

The second protein involved in USP7 mediated p53 homeostasis is Epstein-Barr Nuclear Antigen-1 (EBNA-1), which is essential in replicating and maintaining Epstein-Barr virus genomes. After infection it alters the host cellular processes, including the disruption of PML-NBs through the degradation of PML proteins[213]. This degradation affects apoptosis, DNA repair and antiviral responses. Finally, it can counteract the stabilization of host p53 by inhibiting host USP7, thereby decreasing apoptosis and increasing host cell survival which may contribute to malignant transformation[214].

Both TSPYL5[212] and EBNA-1[215] bind to the TRAF domain of USP7 (Figure 8). This interaction does not influence the stability of either protein, but rather this competitive binding negatively regulates USP7 activity towards p53. This explains the oncogenic-like activity of both TSPYL5 and EBNA-1.

PTEN

Phosphatese and Tensin Homolog (PTEN) is among the most frequently lost or mutated tumour suppressors, with a 30 to 80% mutation frequency in endometrial carcinoma, glioblastoma, and prostate cancer and breast, colon, and lung tumours[216-221]. Complete loss of PTEN is observed at highest frequencies in endometrial cancer and glioblastoma and is generally associated with metastatic cancers[222,223].

PTEN protein acts as a phosphatase to dephosphorylate phosphoinositide-3,4,5-triphosphate (PIP3), which is a potent activator of AKT[224]. Therefore, loss of PTEN function stimulates cell growth, survival and proliferation[225]. However, since phosphatase-inactive PTEN still retains tumour suppressive activity, it is believed PTEN also has AKT-independent functions[226]. This is carried out by the nuclear fraction of PTEN[58]. This nuclear compartmentalization is regulated by the ubiquitination state of PTEN[59]. Specifically, PTEN is mono-ubiquitinated by NEDD4-1[58], which is the signal for translocation to the nucleus from the cytoplasm. In the nucleus, PTEN interacts with the E3 ligase Anaphase Promoting Complex (APC)[227]. The APC is a large E3 ligase complex that marks target cell cycle proteins for degradation and is therefore one of the main players in regulating mitotic events. CDH1 is one of the co-activator proteins of APC by providing substrate specificity to the E3-ligase in a cell-cycle regulated manner[228]. Binding of PTEN allosterically promotes the interaction between the APC and CDH1, and thereby enhancing the tumour-suppressive activity of the APC-CDH1 complex.

The mono-ubiquitination of PTEN is antagonized by USP7. Therefore USP7 promotes the nuclear exclusion of PTEN. Since this relocalization results in a lowered apoptotic potential in prostate cancer cells, inhibiting USP7 would be beneficial for targeting the PTEN pathway in cancer cells[182].

FOXO4

The Forkhead box O (FOXO) family of proteins are transcription factors that are involved in several cellular responses regulating longevity and tumour suppression, including cell cycle inhibition, oxidative-stress resistance, apoptosis and metabolism[229]. Analogous to PTEN, the localization and activity of FOXO4 is regulated through mono-ubiquitination, which in turn is antagonized by direct binding[230] and hydrolysis by USP7[231].

In normal homeostasis, FOXO4 is phosphorylated by the protein kinase AKT in response to cellular stimulation by insulin and growth factors[232]. This relocalizes FOXO4 from the nucleus to the cytoplasm, where it is subjected to ubiquitin-mediated proteasomal degradation. This ensures low FOXO4 protein levels and therefore low transcription of its target genes.

However upon metabolic stress, like a lack of insulin, low glucose or increased cellular oxidative stress, FOXO4 is mono-ubiquitinated by HDM2[233] and possibly other E3's[234]. This mono-ubiquitination is possibly preceded by deacetylation by SIRT1[231]. After this mono-ubiquitination, nuclear FOXO4 protein levels increase and subsequently cause the increase of translation of FOXO4 target genes. This translates metabolic stress in a FOXO4-mediated arrest in G1–G0, increased gluconeogenesis and protection against cellular oxidative stress. Overall, this mechanism allows mammalian cells to quickly respond and survive periods of nutrient shortage.

In addition, the prolyl isomerase PIN1, frequently found to be overexpressed in cancer, is a critical regulator of the Cyclin dependent kinase inhibitor p27 through FOXO4 inhibition[235]. After specific phosphorylation events on FOXO4, PIN1 is able to negatively regulate FOXO transcriptional activity. Interestingly, PIN1 enhances the activity of USP7, thereby preventing nuclear accumulation of FOXO4. However, the mechanism is still unclear.

REST

Repressor Elelement 1-Silencing Transcription Factor (REST) is a transcriptional repressor of the Kruppel-type zinc finger transcription factor family. It binds to neuron-restrictive

silencer element (NRSE) and therefore represses neuronal genes in non-neuronal tissues and undifferentiated neuronal progenitor cells. It associates with two co-repressors, mSin3 and CoREST, which in turn recruit the BHC complex, which deacetylates and demethylates specific histones, thereby acting as a chromatin modifier[236]. Overall, REST is believed to be a master negative regulator of neurogenesis[237].

To relieve this repression, REST is ubiquitinated during neuronal differentiation by the E3 ubiquitin ligase complex SCF–β-TrCP which targets REST for proteasomal degradation[238,239]. Not surprisingly, aberrant REST function is associated with neurodegenerative diseases like Huntington's disease[240], but also to tumourigenesis[241,242]. A recent study showed that USP7 positively regulates REST protein levels, by direct interactions and subsequent deubiquitination and therefore promotes the maintenance of neuronal progenitor cells[243].

PRC1
Two tandem protein complexes modify histones to yield transcriptionally silent chromatin. First the Polycomb Repression Complex 2 (PRC2) complex is recruited to the PRC Response Elements (PREs) on the chromatin. This complex has histone methyltransferase activity and primarily trimethylates histone H3 on K27[244]. This silencing is further stabilized by subsequent mono-ubiquitination of K119 of Histone 2A (H2A) by the second complex: PRC1. These complexes are required for long term epigenetic silencing of chromatin after cellular differentiation and have an important role in stem cell differentiation and early embryonic development.

Two ubiquitin-specific proteases, USP7 and USP11, are associated with the PCR1 complex by direct binding to BMI1 and MEL18[130]. This results in the stabilization of the PRC1 components. Ablation of either USP7 or USP11 expression results in de-repression of the p16/INK4a tumour suppressor accompanied by loss of PRC1 binding at the locus and a senescence-like proliferative arrest. USP7 and USP11 show no obvious similarities in their primary sequence apart from the catalytic domains[71], and there

are few overlaps among the interacting proteins[121]. The function and mechanisms of these interactions remain unclear.

H2B and GMPS
In contrast to ubiquitinated H2A, which functions as a repressive chromatin mark, ubiquitinated Histone 2B (H2B) is associated with active translation. Interestingly, genetic and biochemical experiments revealed that USP7 interacts with Guanosine Monophosphate Synthetase (GMPS). This interaction enhances USP7 activity towards ubiquitinated p53 and is essential for H2B deubiquitination, but not H2A[245-247]. This mechanism is independent of the enzymatic activity of GMPS. This complex acts as a gene-selective transcriptional corepressor that associates with Polycomb response elements (PREs), ecdysteroid regulated genes and the Epstein–Barr virus latent origin of replication[245-247]. Furthermore, this complex might be involved in tumorigenesis, since GMPS was found upregulated in tumorigenic cells[248,249], and knockdown of USP7 in carcinoma cells increased the levels of ubiquitinated H2B[247].

In chapter four we study this unexpected complex, and explain the general allosteric mechanism of USP7 hyper-activation by GMPS. However, the GMPS activation most likely also involves target specific effects, since it is required for the activity on H2B.

CLASPIN
CLASPIN is an adaptor protein that is required for checkpoint mediated cell cycle arrest after DNA damage. It binds to BRCA1 and CHK1, thereby facilitating their ATM/ATR-mediated phosphorylation. To terminate the signalling invoked by BRCA1 and CHK1, CLASPIN is ubiquitinated by both the APC complex and SCF-βTrCP, leading to its degradation by the proteasome. USP7 in vivo interacts with CLASPIN and thereby prevents this ubiquitination and therefore increases its stability and subsequent CHK1 phosphorylation[250]. Interestingly, USP7 specifically prevents the SCF-βTrCP- but not APC-mediated degradation of CLASPIN.

CHFR

Checkpoint Protein with FHA and RING Finger Domains (CHFR) is an E3 ligase that functions in early prophase before chromosome condensation, by actively delaying passage into metaphase in response to mitotic stress. It plays an important role in cell cycle progression and tumour suppression as a stress checkpoint, and ensures chromosomal stability by controlling the expression levels of key mitotic proteins such as PLK1 and AURORA A[251,252]. CHFR binds to USP7 and their interaction greatly increase the stability of CHFR, by preventing its auto-ubiquitination both *in vivo* and *in vitro*[253].

DNMT1

DNA (cytosine-5)-methyltransferase 1 (DNMT1) is the major DNA methyltransferase responsible for maintaining genomic methylation patterns through DNA replication cycles. It is localised at DNA replication foci during the S phase, which agrees well with its role as a maintenance methyltransferase[254]. It is responsible for the preservation of the methylation patterns during cell divisions by methylation of hemimethylated CG dinucleotides[254]. UHFR1 is an E3 ligase and a crucial co-factor of DNMT1. Both proteins form a ternary complex with USP7, in which UHFR1 and USP7 balance the stability of DNMT1[255].

And beyond, towards a molecular understanding of USP7

Overall, USP7 is able to directly regulate key players in many crucial cellular processes. Since a large high confidence proteomics effort has identified many more (uncharacterized) interactors, more studies are required to fully grasp the biological role of USP7 and the effect of these interactions on USP7 activity[121]. However, the potential of USP7 as a drug target is clear, which is also appreciated by several major pharmaceutical companies. This has resulted in some initial successes. For example, a cyano-indenopyrazine derivative (HBX 41,108; Hybrigenics) reversibly inhibits USP7 in the sub-micromolar range, resulting in stabilization and activation of p53[256]. However, to aid future drug design it is crucial that we gain more insights in the activity mechanisms of USP7.

USP7 structural information

USP7 is a single chain enzyme of 128 kDa (1102 amino acids) and contains broadly three domains; an N-terminal TRAF/MATH domain, a catalytic USP domain and a 64 kDa C-terminal region (Figure 8). The N-terminal TRAF/MATH domain comprises an eight-stranded anti-parallel β-sandwich and is responsible for recruitment of substrates such as p53 and HDM2, and TSPYL5[257,201,212]. It also binds to the viral protein EBNA-1[257]. These proteins bind to the TRAF domain through direct interactions with its binding groove (Figure 8D)[205-207]. There are virtually no structural changes in the TRAF domain upon binding to peptides from these interaction partners, with only a slight shift of the side chain of W165. The peptide ligands bind the same shallow groove on the surface of the TRAF domain. The main difference between the HDM2 and p53 peptide interactions with that of the EBNA-1 peptide is with respect to the total buried surface areas (500 and 700 Å2 compared to 1000 Å2). All three peptides bind to the same surface of USP7, explaining the competitive nature of the interactions. The structures and mutagenesis studies showed a preference for a P/AxxS-motif in the peptide. Contacts by the serine are identical and crucial for all peptides, and W165 in the peptide binding pocket of USP7 is also crucial. The affinities for the peptides range from 10 μM and 8 μM for p53 and HDM2, respectively, to 1 μM for EBNA-1. However, since the catalytic domain provides additional interactions with ubiquitin on the target, and at least p53 and HDM2 also bind to the C-terminal region[177], the affinity for the ubiquitinated substrate will be higher.

Structural studies revealed that the catalytic domain of USP7 has the conserved fold of the USP family (Figure 8B)[81,132,205]. They show a papain-like architecture plus an extended, fingers-like domain that forms the ubiquitin binding pocket[258]. In contrast to many USPs, the finger region in USP7 does not contain zinc. Several crystal structures show that the catalytic domain is maintained in a non-functional state, in which the active site residues are in a non-reactive conformation (Figure 8C). The active conformation involves rearrangements of the catalytic domain that allow ubiquitin binding

and organization of the catalytic triad, as was shown in the structure of a complex with the suicide substrate ubiquitin aldehyde[81]. Kinetic data suggest that the affinity for ubiquitin is in the low micro-molar range.

The C-terminal region of USP7 is essential for effective catalytic activity against a minimal synthetic substrate, ubiquitin with a C-terminal fluorescent group, 7-amido-4-methylcoumarin (Ub-AMC)[176,177]. Also, it harbors additional HDM2 and p53 binding sites, and is essential

to promote sequence specific DNA binding of p53[177,259]. As described in chapter four, this C-terminal domain contains five consecutive UBL domains.

Despite our extensive understanding of USP7, there are still many questions to be addressed. The first question concerns the role of the UBL domains in the activity of USP7. They seem to activate the catalytic domain, where an (competitive) inhibition is expected. Morever, do we need all UBL domains or would a smaller
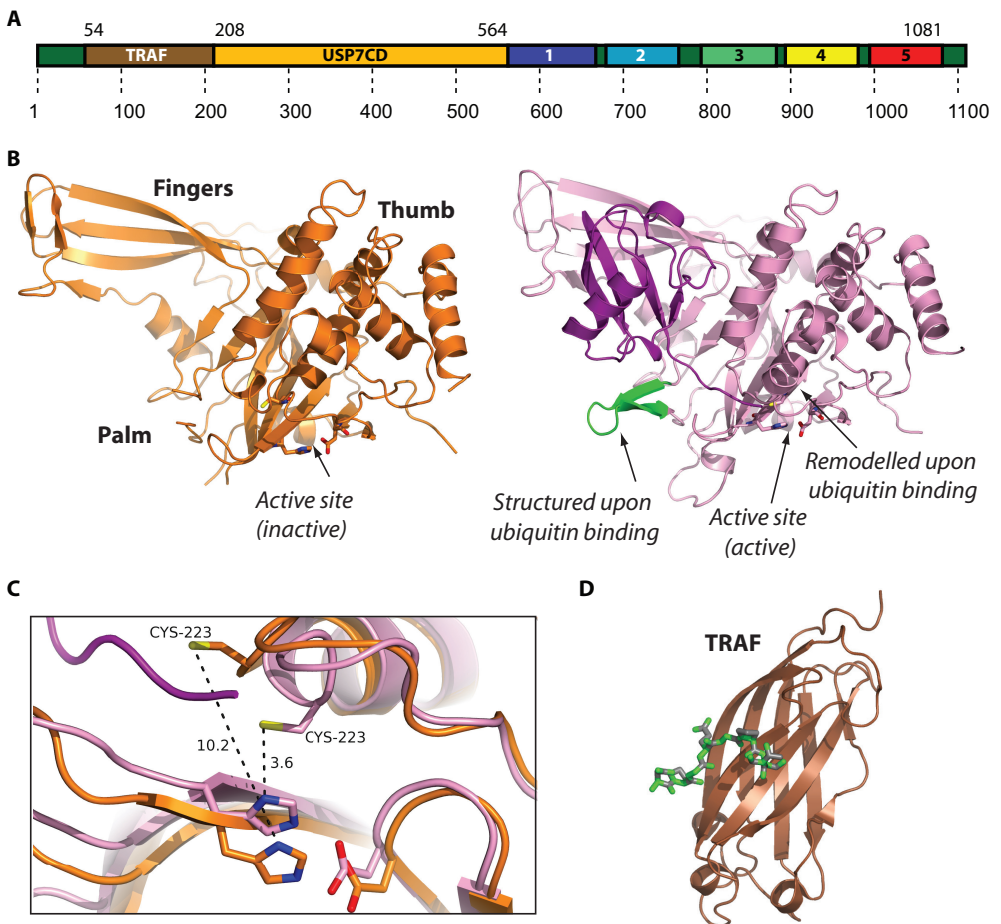
Figure 8. Overview of structural information USP7. A. Schematic domain architecture showing the TRAF substrate binding domain (brown), the catalytic domain (orange) and the predicted UBL domains (rainbow coloured). B. The crystal structures of the catalytic domain without ubiquitin co-crystallized (orange; 1NBF) and with ubiquitin (pink; 1NB8). Ubiquitin is purple and the β-hairpin remodelled upon ubiquitin binding is green. C. The active is remodelled upon ubiquitin binding. D. Crystal structure of the TRAF substrate binding domain (brown) with an EBNA peptide (green) (1YY6).

part already suffice for this activation. Another issue arises with GMPS, of which we know it binds and activates USP7, but we do not where it binds USP7 and how this (hyper-)activates USP7. These and other questions, will be discussed and adressed in chapter 4.

Outline of this thesis

A thourough understanding of the activity and biological role of the DUBs is important for drug development. To that end, this thesis focuses on gaining mechanistic insight in USPs though structural and biochemical characterization. In **chapter two**, we characterized the biochemical properties of twelve members of the USP family. This revealed that despite their homologous catalytic domain, they have very different kinetic properties. Subsequent analysis of their di-ubiquitin topoisomer preference, revealed modest but surprising differences. The characterization also describes activity modulation by both inter- and intra-molecular domains and proteins. In the next two chapters, we will focus on two distinct cases of intra-molecular activity modulation and present their mechanisms; USP4 in **chapter three** and USP7 in **chapter four**. The activities of both USPs are modulated by internal UBL domains. However, the UBL domains have different functions. In USP4 the UBL domain is inserted in the catalytic domain, where it inhibits USP4 activity by competing for ubiquitin binding.

Others USPs can also bind to the UBL insert, which in turn relieves USP4 from its inhibition. However in USP7, the multiple UBL domains just outside the catalytic domain are essential for activity and ubiquitin binding, and therefore play an activating role. We present the crystal structure of this domain and characterized the activation, which revealed a mechanism where binding of part of this domain remodels the catalytic domain, resulting in the activation. This activation is dynamic and the metabolic enzyme GMP synthetase (GMPS) can allosterically hyper-activate USP7 by binding to the remainder of the domain, enhancing the interaction to the catalytic domain. Finally, in **chapter five** we present a general discussion of results described in chapter two to four.

Domain	Residues	PDB code	Comments
TRAF	54 - 205	1YZE[206]	
		1YY6[206]	with EBNA1-peptide
		2FOJ[207]	with p53 peptide 364-367
		2FOO[207]	with p53 peptide 359-362
		2FOP[207]	with HDM2 peptide 147-150
	54 - 206	2F1W, 2F1X[205]	with p53 peptide
	53 - 198	2F1Y[205]	with HDM2 peptide
	54 - 205	3MQR[208]	with HDMx peptide
	54 - 205	3MQS[208]	with HDM2 peptide
TRAF and CD	43 - 560	2F1Z[205]	
CD	208 - 560	1NB8[81]	
	208 - 560	1NBF[81]	in complex with ubiquitin aldehyde
C-terminal domain	537 - 664	2KVR	first UBL, NMR

Table 1. Overview of available structural information of USP7.

References

1.   Peng, J. et al. A proteomics approach to understanding protein ubiquitination. Nat Biotechnol 21, 921-6 (2003).
2.   URL: nobelprize.org/nobel_prizes/chemistry/laureates/2004/.
3.   Hershko, A. The ATP-ubiquitin proteolytic pathway. Prog Clin Biol Res 180, 11-6 (1985).
4.   Hershko, A. & Ciechanover, A. The ubiquitin system. Annu Rev Biochem 67, 425-79 (1998).
5.   Kirkin, V. & Dikic, I. Role of ubiquitin- and Ubl-binding proteins in cell signaling. Curr Opin Cell Biol 19, 199-205 (2007).
6.   Pickart, C.M. & Cohen, R.E. Proteasomes and their kin: proteases in the machine age. Nat Rev Mol Cell Biol 5, 177-87 (2004).
7.   Chastagner, P., Israel, A. & Brou, C. Itch/AIP4 mediates Deltex degradation through the formation of K29-linked polyubiquitin chains. EMBO Rep 7, 1147-53 (2006).
8.   Baboshina, O.V. & Haas, A.L. Novel multiubiquitin chain linkages catalyzed by the conjugating enzymes E2EPF and RAD6 are recognized by 26 S proteasome subunit 5. J Biol Chem 271, 2823-31 (1996).
9.   Jin, L., Williamson, A., Banerjee, S., Philipp, I. & Rape, M. Mechanism of ubiquitin-chain formation by the human anaphase-promoting complex. Cell 133, 653-65 (2008).
10.   Ciechanover, A., Orian, A. & Schwartz, A.L. Ubiquitin-mediated proteolysis: biological regulation via destruction. Bioessays 22, 442-51 (2000).
11.   Conaway, R.C., Brower, C.S. & Conaway, J.W. Emerging roles of ubiquitin in transcription regulation. Science 296, 1254-8 (2002).
12.   Mayer, R.J. The meteoric rise of regulated intracellular proteolysis. Nat Rev Mol Cell Biol 1, 145-8 (2000).
13.   Bonvini, P., Zorzi, E., Basso, G. & Rosolen, A. Bortezomib-mediated 26S proteasome inhibition causes cell-cycle arrest and induces apoptosis in CD-30+ anaplastic large cell lymphoma. Leukemia 21, 838-42 (2007).
14.   Crawford, L.J., Walker, B. & Irvine, A.E. Proteasome inhibitors in cancer therapy. J Cell Commun Signal 5, 101-10.
15.   Scheffner, M., Nuber, U. & Huibregtse, J.M. Protein ubiquitination involving an E1-E2-E3 enzyme ubiquitin thioester cascade. Nature 373, 81-3 (1995).
16.   Brownell, J.E. et al. Substrate-assisted inhibition of ubiquitin-like protein-activating enzymes: the NEDD8 E1 inhibitor MLN4924 forms a NEDD8-AMP mimetic in situ. Mol Cell 37, 102-11.
17.   Soucy, T.A. et al. An inhibitor of NEDD8-activating enzyme as a new approach to treat cancer. Nature 458, 732-6 (2009).
18.   Ceccarelli, D.F. et al. An allosteric inhibitor of the human cdc34 ubiquitin-conjugating enzyme. Cell 145, 1075-87 (2011).
19.   Vassilev, L.T. et al. In vivo activation of the p53 pathway by small-molecule antagonists of MDM2. Science 303, 844-8 (2004).
20.   Shangary, S. & Wang, S. Small-molecule inhibitors of the MDM2-p53 protein-protein interaction to reactivate p53 function: a novel approach for cancer therapy. Annu Rev Pharmacol Toxicol 49, 223-41 (2009).
21.   Chen, Z.J. & Sun, L.J. Nonproteolytic functions of ubiquitin in cell signaling. Mol Cell 33, 275-86 (2009).
22.   Haglund, K. & Dikic, I. Ubiquitylation and cell signaling. Embo J 24, 3353-9 (2005).
23.   Mukhopadhyay, D. & Riezman, H. Proteasome-independent functions of ubiquitin in endocytosis and signaling. Science 315, 201-5 (2007).
24.   Komander, D., Clague, M.J. & Urbe, S. Breaking the chains: structure and function of the deubiquitinases. Nat Rev Mol Cell Biol 10, 550-63 (2009).
25.   Kirisako, T. et al. A ubiquitin ligase complex assembles linear polyubiquitin chains. Embo J

25, 4877-87 (2006).

26.   Komander, D. The emerging complexity of protein ubiquitination. Biochem Soc Trans 37, 937-53 (2009).

27.   Xu, P. et al. Quantitative proteomics reveals the function of unconventional ubiquitin chains in proteasomal degradation. Cell 137, 133-45 (2009).

28.   Mo, M., Fleming, S.B. & Mercer, A.A. Cell cycle deregulation by a poxvirus partial mimic of anaphase-promoting complex subunit 11. Proc Natl Acad Sci U S A 106, 19527-32 (2009).

29.   El Oualid, F. et al. Chemical synthesis of ubiquitin, ubiquitin-based probes, and diubiquitin. Angew Chem Int Ed Engl 49, 10149-53 (2010).

30.   Virdee, S., Ye, Y., Nguyen, D.P., Komander, D. & Chin, J.W. Engineered diubiquitin synthesis reveals Lys29-isopeptide specificity of an OTU deubiquitinase. Nat Chem Biol 6, 750-7 (2010).

31.   Di Fiore, P.P., Polo, S. & Hofmann, K. When ubiquitin meets ubiquitin receptors: a signalling connection. Nat Rev Mol Cell Biol 4, 491-7 (2003).

32.   Harper, J.W. & Schulman, B.A. Structural complexity in ubiquitin recognition. Cell 124, 1133-6 (2006).

33.   Hicke, L., Schubert, H.L. & Hill, C.P. Ubiquitin-binding domains. Nat Rev Mol Cell Biol 6, 610-21 (2005).

34.   Hofmann, K. Ubiquitin-binding domains and their role in the DNA damage response. DNA Repair (Amst) 8, 544-56 (2009).

35.   Hurley, J.H., Lee, S. & Prag, G. Ubiquitin-binding domains. Biochem J 399, 361-72 (2006).

36.   Dikic, I., Wakatsuki, S. & Walters, K.J. Ubiquitin-binding domains - from structures to functions. Nat Rev Mol Cell Biol 10, 659-71 (2009).

37.   Raasi, S., Varadan, R., Fushman, D. & Pickart, C.M. Diverse polyubiquitin interaction properties of ubiquitin-associated domains. Nat Struct Mol Biol 12, 708-14 (2005).

38.   Varadan, R., Assfalg, M., Raasi, S., Pickart, C. & Fushman, D. Structural determinants for selective recognition of a Lys48-linked polyubiquitin chain by a UBA domain. Mol Cell 18, 687-98 (2005).

39.   Rahighi, S. et al. Specific recognition of linear ubiquitin chains by NEMO is important for NF-kappaB activation. Cell 136, 1098-109 (2009).

40.   Riederer, B.M., Leuba, G., Vernay, A. & Riederer, I.M. The role of the ubiquitin proteasome system in Alzheimer's disease. Exp Biol Med (Maywood) 236, 268-76 (2011).

41.   Petroski, M.D. The ubiquitin system, disease, and drug discovery. BMC Biochem 9 Suppl 1, S7 (2008).

42.   Isaacson, M.K. & Ploegh, H.L. Ubiquitination, ubiquitin-like modifiers, and deubiquitination in viral infection. Cell Host Microbe 5, 559-70 (2009).

43.   Wing, S.S. The UPS in diabetes and obesity. BMC Biochem 9 Suppl 1, S6 (2008).

44.   Duwel, M., Hadian, K. & Krappmann, D. Ubiquitin Conjugation and Deconjugation in NF-kappaB Signaling. Subcell Biochem 54, 88-99 (2010).

45.   Hanahan, D. & Weinberg, R.A. Hallmarks of cancer: the next generation. Cell 144, 646-74 (2011).

46.   Fang, S., Lorick, K.L., Jensen, J.P. & Weissman, A.M. RING finger ubiquitin protein ligases: implications for tumorigenesis, metastasis and for molecular targets in cancer. Semin Cancer Biol 13, 5-14 (2003).

47.   Hoeller, D., Hecker, C.M. & Dikic, I. Ubiquitin and ubiquitin-like proteins in cancer pathogenesis. Nat Rev Cancer 6, 776-88 (2006).

48.   Jiang, Y.H. & Beaudet, A.L. Human disorders of ubiquitination and proteasomal degradation. Curr Opin Pediatr 16, 419-26 (2004).

49.   Nakayama, K.I. & Nakayama, K. Ubiquitin ligases: cell-cycle control and cancer. Nat Rev Cancer 6, 369-81 (2006).

50.   Bennett, E.J. & Harper, J.W. DNA damage: ubiquitin marks the spot. Nat Struct Mol Biol 15,

1

20-2 (2008).

51.   Karin, M. Nuclear factor-kappaB in cancer development and progression. Nature 441, 431-6 (2006).

52.   Bache, K.G., Slagsvold, T. & Stenmark, H. Defective downregulation of receptor tyrosine kinases in cancer. Embo J 23, 2707-12 (2004).

53.   Kaelin, W.G., Jr. Molecular basis of the VHL hereditary cancer syndrome. Nat Rev Cancer 2, 673-82 (2002).

54.   Hoeller, D. & Dikic, I. Targeting the ubiquitin system in cancer therapy. Nature 458, 438-44 (2009).

55.   Haglund, K.D., I. Ubiquitin Signaling and Cancer Pathogenesis. Protein Degradation, Vol. 4: The Ubiquitin-Proteasome System and Disease. (2008).

56.   Bond, G.L., Hu, W. & Levine, A.J. MDM2 is a central node in the p53 pathway: 12 years and counting. Curr Cancer Drug Targets 5, 3-8 (2005).

57.   Vousden, K.H. & Prives, C. P53 and prognosis: new insights and further complexity. Cell 120, 7-10 (2005).

58.   Fridberg, M. et al. Protein expression and cellular localization in two prognostic subgroups of diffuse large B-cell lymphoma: higher expression of ZAP70 and PKC-beta II in the non-germinal center group and poor survival in patients deficient in nuclear PTEN. Leuk Lymphoma 48, 2221-32 (2007).

59.   Trotman, L.C. et al. Ubiquitination regulates PTEN nuclear import and tumor suppression. Cell 128, 141-56 (2007).

60.   Zhang, Y. & Xiong, Y. Control of p53 ubiquitination and nuclear export by MDM2 and ARF. Cell Growth Differ 12, 175-86 (2001).

61.   Schwickart, M. et al. Deubiquitinase USP9X stabilizes MCL1 and promotes tumour cell survival. Nature 463, 103-7 (2010).

62.   Pereg, Y. et al. Ubiquitin hydrolase Dub3 promotes oncogenic transformation by stabilizing Cdc25A. Nat Cell Biol 12, 400-6 (2010).

63.   Bennett, E.J. et al. Global changes to the ubiquitin system in Huntington's disease. Nature 448, 704-8 (2007).

64.   Davies, J.E., Sarkar, S. & Rubinsztein, D.C. The ubiquitin proteasome system in Huntington's disease and the spinocerebellar ataxias. BMC Biochem 8 Suppl 1, S2 (2007).

65.   Upadhya, S.C. & Hegde, A.N. Role of the ubiquitin proteasome system in Alzheimer's disease. BMC Biochem 8 Suppl 1, S12 (2007).

66.   Leroy, E. et al. The ubiquitin pathway in Parkinson's disease. Nature 395, 451-2 (1998).

67.   Setsuie, R. & Wada, K. The functions of UCH-L1 and its relation to neurodegenerative diseases. Neurochem Int 51, 105-11 (2007).

68.   Wilkinson, K.D. et al. The neuron-specific protein PGP 9.5 is a ubiquitin carboxyl-terminal hydrolase. Science 246, 670-3 (1989).

69.   Liu, Y., Fallon, L., Lashuel, H.A., Liu, Z. & Lansbury, P.T., Jr. The UCH-L1 gene encodes two opposing enzymatic activities that affect alpha-synuclein degradation and Parkinson's disease susceptibility. Cell 111, 209-18 (2002).

70.   Wilson, P.O. et al. The immunolocalization of protein gene product 9.5 using rabbit polyclonal and mouse monoclonal antibodies. Br J Exp Pathol 69, 91-104 (1988).

71.   Nijman, S.M. et al. A genomic and functional inventory of deubiquitinating enzymes. Cell 123, 773-86 (2005).

72.   Nijman, S.M. et al. The deubiquitinating enzyme USP1 regulates the Fanconi anemia pathway. Mol Cell 17, 331-9 (2005).

73.   Singhal, S., Taylor, M.C. & Baker, R.T. Deubiquitylating enzymes and disease. BMC Biochem 9 Suppl 1, S3 (2008).

74.   Brummelkamp, T.R., Nijman, S.M., Dirac, A.M. & Bernards, R. Loss of the cylindromatosis tumour suppressor inhibits apoptosis by activating NF-kappaB. Nature 424, 797-801

1

(2003).

75. Bignell, G.R. et al. Identification of the familial cylindromatosis tumour-suppressor gene. Nat Genet 25, 160-5 (2000).

76. Papa, F.R. & Hochstrasser, M. The yeast DOA4 gene encodes a deubiquitinating enzyme related to a product of the human tre-2 oncogene. Nature 366, 313-9 (1993).

77. Sacco, J.J., Coulson, J.M., Clague, M.J. & Urbe, S. Emerging roles of deubiquitinases in cancer-associated pathways. IUBMB Life 62, 140-57.

78. Colland, F. The therapeutic potential of deubiquitinating enzyme inhibitors. Biochem Soc Trans 38, 137-43 (2010).

79. Lee, B.H. et al. Enhancement of proteasome activity by a small-molecule inhibitor of USP14. Nature 467, 179-84 (2010).

80. Kapuria, V. et al. Deubiquitinase inhibition by small-molecule WP1130 triggers aggresome formation and tumor cell apoptosis. Cancer Res 70, 9265-76.

81. Hu, M. et al. Crystal structure of a UBP-family deubiquitinating enzyme in isolation and in complex with ubiquitin aldehyde. Cell 111, 1041-54 (2002).

82. Maytal-Kivity, V., Reis, N., Hofmann, K. & Glickman, M.H. MPN+, a putative catalytic motif found in a subset of MPN domain proteins from eukaryotes and prokaryotes, is critical for Rpn11 function. BMC Biochem 3, 28 (2002).

83. Enesa, K. et al. NF-kappaB suppression by the deubiquitinating enzyme Cezanne: a novel negative feedback loop in pro-inflammatory signaling. J Biol Chem 283, 7036-45 (2008).

84. Wertz, I.E. et al. De-ubiquitination and ubiquitin ligase domains of A20 downregulate NF-kappaB signalling. Nature 430, 694-9 (2004).

85. Tran, H., Hamada, F., Schwarz-Romond, T. & Bienz, M. Trabid, a new positive regulator of Wnt-induced transcription with preference for binding and cleaving K63-linked ubiquitin chains. Genes Dev 22, 528-42 (2008).

86. Kayagaki, N. et al. DUBA: a deubiquitinase that regulates type I interferon production. Science 318, 1628-32 (2007).

87. Nakada, S. et al. Non-canonical inhibition of DNA damage-dependent ubiquitination by OTUB1. Nature 466, 941-6 (2010).

88. Edelmann, M.J. et al. Structural basis and specificity of human otubain 1-mediated deubiquitination. Biochem J 418, 379-90 (2009).

89. Das, C. et al. Structural basis for conformational plasticity of the Parkinson's disease-associated ubiquitin hydrolase UCH-L1. Proc Natl Acad Sci U S A 103, 4675-80 (2006).

90. Mao, Y. et al. Deubiquitinating function of ataxin-3: insights from the solution structure of the Josephin domain. Proc Natl Acad Sci U S A 102, 12700-5 (2005).

91. Nicastro, G., Habeck, M., Masino, L., Svergun, D.I. & Pastore, A. Structure validation of the Josephin domain of ataxin-3: conclusive evidence for an open conformation. J Biomol NMR 36, 267-77 (2006).

92. Nicastro, G. et al. The solution structure of the Josephin domain of ataxin-3: structural determinants for molecular recognition. Proc Natl Acad Sci U S A 102, 10493-8 (2005).

93. Komander, D. et al. Molecular discrimination of structurally equivalent Lys 63-linked and linear polyubiquitin chains. EMBO Rep 10, 466-73 (2009).

94. Komander, D. & Barford, D. Structure of the A20 OTU domain and mechanistic insights into deubiquitination. Biochem J 409, 77-85 (2008).

95. Lin, S.C. et al. Molecular basis for the unique deubiquitinating activity of the NF-kappaB inhibitor A20. J Mol Biol 376, 526-40 (2008).

96. Akutsu, M., Ye, Y., Virdee, S., Chin, J.W. & Komander, D. Molecular basis for ubiquitin and ISG15 cross-reactivity in viral ovarian tumor domains. Proc Natl Acad Sci U S A 108, 2228-33 (2011).

97. James, T.W. et al. Structural basis for the removal of ubiquitin and interferon-stimulated gene 15 by a viral ovarian tumor domain-containing protease. Proc Natl Acad Sci U S A

108, 2222-7.

98. Hanna, J. et al. Deubiquitinating enzyme Ubp6 functions noncatalytically to delay proteasomal degradation. Cell 127, 99-111 (2006).

99. Quesada, V. et al. Cloning and enzymatic analysis of 22 novel human ubiquitin-specific proteases. Biochem Biophys Res Commun 314, 54-62 (2004).

100. Semenova, E., Wang, X., Jablonski, M.M., Levorse, J. & Tilghman, S.M. An engineered 800 kilobase deletion of Uchl3 and Lmo7 on mouse chromosome 14 causes defects in viability, postnatal growth and degeneration of muscle and retina. Hum Mol Genet 12, 1301-12 (2003).

101. Wood, M.A., Kaplan, M.P., Brensinger, C.M., Guo, W. & Abel, T. Ubiquitin C-terminal hydrolase L3 (Uchl3) is involved in working memory. Hippocampus 15, 610-21 (2005).

102. Finley, D. Recognition and processing of ubiquitin-protein conjugates by the proteasome. Annu Rev Biochem 78, 477-513 (2009).

103. Jensen, D.E. et al. BAP1: a novel ubiquitin hydrolase which binds to the BRCA1 RING finger and enhances BRCA1-mediated cell growth suppression. Oncogene 16, 1097-112 (1998).

104. Scheuermann, J.C. et al. Histone H2A deubiquitinase activity of the Polycomb repressive complex PR-DUB. Nature 465, 243-7 (2010).

105. Amerik, A.Y. & Hochstrasser, M. Mechanism and function of deubiquitinating enzymes. Biochim Biophys Acta 1695, 189-207 (2004).

106. Johnston, S.C., Larsen, C.N., Cook, W.J., Wilkinson, K.D. & Hill, C.P. Crystal structure of a deubiquitinating enzyme (human UCH-L3) at 1.8 A resolution. Embo J 16, 3787-96 (1997).

107. Misaghi, S. et al. Structure of the ubiquitin hydrolase UCH-L3 complexed with a suicide substrate. J Biol Chem 280, 1512-20 (2005).

108. Popp, M.W., Artavanis-Tsakonas, K. & Ploegh, H.L. Substrate filtering by the active site crossover loop in UCHL3 revealed by sortagging and gain-of-function mutations. J Biol Chem 284, 3593-602 (2009).

109. Lam, Y.A., Xu, W., DeMartino, G.N. & Cohen, R.E. Editing of ubiquitin conjugates by an isopeptidase in the 26S proteasome. Nature 385, 737-40 (1997).

110. Scheel, H., Tomiuk, S. & Hofmann, K. Elucidation of ataxin-3 and ataxin-7 function by integrative bioinformatics. Hum Mol Genet 12, 2845-52 (2003).

111. Burnett, B., Li, F. & Pittman, R.N. The polyglutamine neurodegenerative protein ataxin-3 binds polyubiquitylated proteins and has ubiquitin protease activity. Hum Mol Genet 12, 3195-205 (2003).

112. Riess, O., Rub, U., Pastore, A., Bauer, P. & Schols, L. SCA3: neurological features, pathogenesis and animal models. Cerebellum 7, 125-37 (2008).

113. Nicastro, G. et al. Josephin domain of ataxin-3 contains two distinct ubiquitin-binding sites. Biopolymers 91, 1203-14 (2009).

114. Todi, S.V. et al. Ubiquitination directly enhances activity of the deubiquitinating enzyme ataxin-3. Embo J 28, 372-82 (2009).

115. Pena, V., Liu, S., Bujnicki, J.M., Luhrmann, R. & Wahl, M.C. Structure of a multipartite protein-protein interaction domain in splicing factor prp8 and its link to retinitis pigmentosa. Mol Cell 25, 615-24 (2007).

116. Williams, R.L. & Urbe, S. The emerging shape of the ESCRT machinery. Nat Rev Mol Cell Biol 8, 355-68 (2007).

117. Cooper, E.M. et al. K63-specific deubiquitination by two JAMM/MPN+ complexes: BRISC-associated Brcc36 and proteasomal Poh1. Embo J 28, 621-31 (2009).

118. McCullough, J., Clague, M.J. & Urbe, S. AMSH is an endosome-associated ubiquitin isopeptidase. J Cell Biol 166, 487-92 (2004).

119. Sato, Y. et al. Structural basis for specific cleavage of Lys 63-linked polyubiquitin chains. Nature 455, 358-62 (2008).

120. Semple, C.A. The comparative proteomics of ubiquitination in mouse. Genome Res 13, 1389-94 (2003).
121. Sowa, M.E., Bennett, E.J., Gygi, S.P. & Harper, J.W. Defining the human deubiquitinating enzyme interaction landscape. Cell 138, 389-403 (2009).
122. Boutell, C., Canning, M., Orr, A. & Everett, R.D. Reciprocal activities between herpes simplex virus type 1 regulatory protein ICP0, a ubiquitin E3 ligase, and ubiquitin-specific protease USP7. J Virol 79, 12342-54 (2005).
123. Canning, M., Boutell, C., Parkinson, J. & Everett, R.D. A RING finger ubiquitin ligase is protected from autocatalyzed ubiquitination and degradation by binding to ubiquitin-specific protease USP7. J Biol Chem 279, 38160-8 (2004).
124. Hetfeld, B.K. et al. The zinc finger of the CSN-associated deubiquitinating enzyme USP15 is essential to rescue the E3 ligase Rbx1. Curr Biol 15, 1217-21 (2005).
125. Nathan, J.A. et al. The ubiquitin E3 ligase MARCH7 is differentially regulated by the deubiquitylating enzymes USP7 and USP9X. Traffic 9, 1130-45 (2008).
126. Mouchantaf, R. et al. The ubiquitin ligase itch is auto-ubiquitylated in vivo and in vitro but is protected from degradation by interacting with the deubiquitylating enzyme FAM/USP9X. J Biol Chem 281, 38738-47 (2006).
127. Cummins, J.M. & Vogelstein, B. HAUSP is required for p53 destabilization. Cell Cycle 3, 689-92 (2004).
128. Cohn, M.A., Kee, Y., Haas, W., Gygi, S.P. & D'Andrea, A.D. UAF1 is a subunit of multiple deubiquitinating enzyme complexes. J Biol Chem 284, 5343-51 (2009).
129. Cohn, M.A. et al. A UAF1-containing multisubunit protein complex regulates the Fanconi anemia pathway. Mol Cell 28, 786-97 (2007).
130. Maertens, G.N., El Messaoudi-Aubert, S., Elderkin, S., Hiom, K. & Peters, G. Ubiquitin-specific proteases 7 and 11 modulate Polycomb regulation of the INK4a tumour suppressor. Embo J 29, 2553-65 (2011).
131. Hu, M. et al. Structure and mechanisms of the proteasome-associated deubiquitinating enzyme USP14. Embo J 24, 3747-56 (2005).
132. Komander, D. et al. The structure of the CYLD USP domain explains its specificity for Lys63-linked polyubiquitin and reveals a B box module. Mol Cell 29, 451-64 (2008).
133. Avvakumov, G.V. et al. Amino-terminal dimerization, NRDP1-rhodanese interaction, and inhibited catalytic domain conformation of the ubiquitin-specific protease 8 (USP8). J Biol Chem 281, 38061-70 (2006).
134. Ye, Y., Scheel, H., Hofmann, K. & Komander, D. Dissection of USP catalytic domains reveals five common insertion points. Mol Biosyst 5, 1797-808 (2009).
135. Hassink, G.C. et al. The ER-resident ubiquitin-specific protease 19 participates in the UPR and rescues ERAD substrates. EMBO Rep 10, 755-61 (2009).
136. Reyes-Turcu, F.E., Shanks, J.R., Komander, D. & Wilkinson, K.D. Recognition of polyubiquitin isoforms by the multiple ubiquitin binding modules of isopeptidase T. J Biol Chem 283, 19581-92 (2008).
137. Ginalski, K., Rychlewski, L., Baker, D. & Grishin, N.V. Protein structure prediction for the male-specific region of the human Y chromosome. Proc Natl Acad Sci U S A 101, 2305-10 (2004).
138. Zhu, X., Menard, R. & Sulea, T. High incidence of ubiquitin-like domains in human ubiquitin-specific proteases. Proteins 69, 1-7 (2007).
139. Burroughs, A.M., Balaji, S., Iyer, L.M. & Aravind, L. Small but versatile: the extraordinary functional and structural diversity of the beta-grasp fold. Biol Direct 2, 18 (2007).
140. Elsasser, S. et al. Proteasome subunit Rpn1 binds ubiquitin-like protein domains. Nat Cell Biol 4, 725-30 (2002).
141. Fujiwara, K. et al. Structure of the ubiquitin-interacting motif of S5a bound to the ubiquitin-like domain of HR23B. J Biol Chem 279, 4760-7 (2004).

142.   Schauber, C. et al. Rad23 links DNA repair to the ubiquitin/proteasome pathway. Nature 391, 715-8 (1998).

143.   Su, V. & Lau, A.F. Ubiquitin-like and ubiquitin-associated domain proteins: significance in proteasomal degradation. Cell Mol Life Sci 66, 2819-33 (2009).

144.   Xu, G. et al. Crystal structure of inhibitor of kappaB kinase beta. Nature 472, 325-30 (2011).

145.   May, M.J., Larsen, S.E., Shim, J.H., Madge, L.A. & Ghosh, S. A novel ubiquitin-like domain in IkappaB kinase beta is required for functional activity of the kinase. J Biol Chem 279, 45528-39 (2004).

146.   Ikeda, F. et al. Involvement of the ubiquitin-like domain of TBK1/IKK-i kinases in regulation of IFN-inducible genes. Embo J 26, 3451-62 (2007).

147.   Finney, N. et al. The cellular protein level of parkin is regulated by its ubiquitin-like domain. J Biol Chem 278, 16054-8 (2003).

148.   Sakata, E. et al. Parkin binds the Rpn10 subunit of 26S proteasomes through its ubiquitin-like domain. EMBO Rep 4, 301-6 (2003).

149.   Chaugule, V.K. et al. Autoregulation of Parkin activity through its ubiquitin-like domain. Embo J (2011).

150.   Buchberger, A., Howard, M.J., Proctor, M. & Bycroft, M. The UBX domain: a widespread ubiquitin-like module. J Mol Biol 307, 17-24 (2001).

151.   Alexandru, G. et al. UBXD7 binds multiple ubiquitin ligases and implicates p97 in HIF1alpha turnover. Cell 134, 804-16 (2008).

152.   Schuberth, C. & Buchberger, A. UBX domain proteins: major regulators of the AAA ATPase Cdc48/p97. Cell Mol Life Sci 65, 2360-71 (2008).

153.   Grabbe, C. & Dikic, I. Functional roles of ubiquitin-like domain (ULD) and ubiquitin-binding domain (UBD) containing proteins. Chem Rev 109, 1481-94 (2009).

154.   Madsen, L., Schulze, A., Seeger, M. & Hartmann-Petersen, R. Ubiquitin domain proteins in disease. BMC Biochem 8 Suppl 1, S1 (2007).

155.   Borodovsky, A. et al. A novel active site-directed probe specific for deubiquitylating enzymes reveals proteasome association of USP14. Embo J 20, 5187-96 (2001).

156.   Leggett, D.S. et al. Multiple associated proteins regulate proteasome structure and function. Mol Cell 10, 495-507 (2002).

157.   Gupta, K., Copeland, N.G., Gilbert, D.J., Jenkins, N.A. & Gray, D.A. Unp, a mouse gene related to the tre oncogene. Oncogene 8, 2307-10 (1993).

158.   DeSalle, L.M. et al. The de-ubiquitinating enzyme Unp interacts with the retinoblastoma protein. Oncogene 20, 5538-42 (2001).

159.   Gray, D.A. et al. Elevated expression of Unph, a proto-oncogene at 3p21.3, in human lung tumors. Oncogene 10, 2179-83 (1995).

160.   Zhao, B., Schlesiger, C., Masucci, M.G. & Lindsten, K. The ubiquitin specific protease 4 (USP4) is a new player in the Wnt signalling pathway. J Cell Mol Med 13, 1886-95 (2009).

161.   Milojevic, T. et al. The ubiquitin-specific protease Usp4 regulates the cell surface level of the A2A receptor. Mol Pharmacol 69, 1083-94 (2006).

162.   Song, E.J. et al. The Prp19 complex and the Usp4Sart3 deubiquitinating enzyme control reversible ubiquitination at the spliceosome. Genes Dev 24, 1434-47 (2010).

163.   Adhikary, S. et al. The ubiquitin ligase HectH9 regulates transcriptional activation by Myc and is essential for tumor cell proliferation. Cell 123, 409-21 (2005).

164.   Zhang, X., Berger, F.G., Yang, J. & Lu, X. USP4 inhibits p53 through deubiquitinating and stabilizing ARF-BP1. Embo J 30, 2177-89.

165.   Bouwmeester, T. et al. A physical and functional map of the human TNF-alpha/NF-kappa B signal transduction pathway. Nat Cell Biol 6, 97-105 (2004).

166.   Yamaguchi, T., Kimura, J., Miki, Y. & Yoshida, K. The deubiquitinating enzyme USP11 controls an IkappaB kinase alpha (IKKalpha)-p53 signaling pathway in response to tumor

necrosis factor alpha (TNFalpha). J Biol Chem 282, 33943-8 (2007).

167.   Schoenfeld, A.R., Apgar, S., Dolios, G., Wang, R. & Aaronson, S.A. BRCA2 is ubiquitinated in vivo and interacts with USP11, a deubiquitinating enzyme that exhibits prosurvival function in the cellular response to DNA damage. Mol Cell Biol 24, 7444-55 (2004).

168.   Wiltshire, T.D. et al. Sensitivity to poly(ADP-ribose) polymerase (PARP) inhibition identifies ubiquitin-specific peptidase 11 (USP11) as a regulator of DNA double-strand break repair. J Biol Chem 285, 14565-71 (2010).

169.   Wei, N., Serino, G. & Deng, X.W. The COP9 signalosome: more than a protease. Trends Biochem Sci 33, 592-600 (2008).

170.   Wee, S., Geyer, R.K., Toda, T. & Wolf, D.A. CSN facilitates Cullin-RING ubiquitin ligase function by counteracting autocatalytic adapter instability. Nat Cell Biol 7, 387-91 (2005).

171.   Cayli, S. et al. COP9 signalosome interacts ATP-dependently with p97/valosin-containing protein (VCP) and controls the ubiquitination status of proteins bound to p97/VCP. J Biol Chem 284, 34944-53 (2009).

172.   Peth, A., Berndt, C., Henke, W. & Dubiel, W. Downregulation of COP9 signalosome subunits differentially affects the CSN complex and target protein stability. BMC Biochem 8, 27 (2007).

173.   Schweitzer, K., Bozko, P.M., Dubiel, W. & Naumann, M. CSN controls NF-kappaB by deubiquitinylation of IkappaBalpha. Embo J 26, 1532-41 (2007).

174.   Bacik, J.P., Avvakumov, G., Walker, J.R., Xue, S. & Dhe-Paganon, S. Crystal structure of the N-terminal domains of the ubiquitin specific peptidase 4 (USP4). (To be published).

175.   de Jong, R.N. et al. Solution structure of the human ubiquitin-specific protease 15 DUSP domain. J Biol Chem 281, 5026-31 (2006).

176.   Fernandez-Montalvan, A. et al. Biochemical characterization of USP7 reveals post-translational modification sites and structural requirements for substrate processing and subcellular localization. Febs J 274, 4256-70 (2007).

177.   Ma, J. et al. C-terminal region of USP7/HAUSP is critical for deubiquitination activity and contains a second mdm2/p53 binding site. Arch Biochem Biophys 503, 207-12 (2010).

178.   Luna-Vargas, M.P. et al. Ubiquitin-specific protease 4 is inhibited by its ubiquitin-like domain. EMBO Rep 12, 365-72 (2011).

179.   Everett, R.D. et al. A novel ubiquitin-specific protease is dynamically associated with the PML nuclear domain and binds to a herpesvirus regulatory protein. Embo J 16, 1519-30 (1997).

180.   Kon, N. et al. Inactivation of HAUSP in vivo modulates p53 function. Oncogene 29, 1270-9 (2010).

181.   Kessler, B.M. et al. Proteome changes induced by knock-down of the deubiquitylating enzyme HAUSP/USP7. J Proteome Res 6, 4163-72 (2007).

182.   Song, M.S. et al. The deubiquitinylation and localization of PTEN are regulated by a HAUSP-PML network. Nature 455, 813-7 (2008).

183.   Masuya, D. et al. The HAUSP gene plays an important role in non-small cell lung carcinogenesis through p53-dependent pathways. J Pathol 208, 724-32 (2006).

184.   Leib, D.A. et al. Interferons regulate the phenotype of wild-type and mutant herpes simplex viruses in vivo. J Exp Med 189, 663-72 (1999).

185.   Mossman, K.L., Saffran, H.A. & Smiley, J.R. Herpes simplex virus ICP0 mutants are hypersensitive to interferon. J Virol 74, 2052-6 (2000).

186.   Everett, R.D., Parsy, M.L. & Orr, A. Analysis of the functions of herpes simplex virus type 1 regulatory protein ICP0 that are critical for lytic infection and derepression of quiescent viral genomes. J Virol 83, 4963-77 (2009).

187.   Hagglund, R. & Roizman, B. Role of ICP0 in the strategy of conquest of the host cell by herpes simplex virus 1. J Virol 78, 2169-78 (2004).

188.   Boutell, C. & Everett, R.D. The herpes simplex virus type 1 (HSV-1) regulatory protein ICP0

interacts with and Ubiquitinates p53. J Biol Chem 278, 36596-602 (2003).

189.   Boutell, C., Sadis, S. & Everett, R.D. Herpes simplex virus type 1 immediate-early protein ICP0 and is isolated RING finger domain act as ubiquitin E3 ligases in vitro. J Virol 76, 841-50 (2002).

190.   Kawaguchi, Y., Van Sant, C. & Roizman, B. Herpes simplex virus 1 alpha regulatory protein ICP0 interacts with and stabilizes the cell cycle regulator cyclin D3. J Virol 71, 7328-36 (1997).

191.   Everett, R.D. ICP0 induces the accumulation of colocalizing conjugated ubiquitin. J Virol 74, 9994-10005 (2000).

192.   Lopez, P., Van Sant, C. & Roizman, B. Requirements for the nuclear-cytoplasmic translocation of infected-cell protein 0 of herpes simplex virus 1. J Virol 75, 3832-40 (2001).

193.   Halford, W.P., Puschel, R. & Rakowski, B. Herpes simplex virus 2 ICP0 mutant viruses are avirulent and immunogenic: implications for a genital herpes vaccine. PLoS One 5, e12251 (2010).

194.   Daubeuf, S. et al. HSV ICP0 recruits USP7 to modulate TLR-mediated innate response. Blood 113, 3264-75 (2009).

195.   Vogelstein, B., Lane, D. & Levine, A.J. Surfing the p53 network. Nature 408, 307-10 (2000).

196.   Vousden, K.H. & Lane, D.P. p53 in health and disease. Nat Rev Mol Cell Biol 8, 275-83 (2007).

197.   Riley, T., Sontag, E., Chen, P. & Levine, A. Transcriptional control of human p53-regulated genes. Nat Rev Mol Cell Biol 9, 402-12 (2008).

198.   Brooks, C.L. & Gu, W. p53 ubiquitination: Mdm2 and beyond. Mol Cell 21, 307-15 (2006).

199.   Jones, S.N., Roe, A.E., Donehower, L.A. & Bradley, A. Rescue of embryonic lethality in Mdm2-deficient mice by absence of p53. Nature 378, 206-8 (1995).

200.   Montes de Oca Luna, R., Wagner, D.S. & Lozano, G. Rescue of early embryonic lethality in mdm2-deficient mice by deletion of p53. Nature 378, 203-6 (1995).

201.   Li, M. et al. Deubiquitination of p53 by HAUSP is an important pathway for p53 stabilization. Nature 416, 648-53 (2002).

202.   Cummins, J.M. et al. Tumour suppression: disruption of HAUSP gene stabilizes p53. Nature 428, 1 p following 486 (2004).

203.   Meulmeester, E. et al. Loss of HAUSP-mediated deubiquitination contributes to DNA damage-induced destabilization of Hdmx and Hdm2. Mol Cell 18, 565-76 (2005).

204.   Li, M., Brooks, C.L., Kon, N. & Gu, W. A dynamic role of HAUSP in the p53-Mdm2 pathway. Mol Cell 13, 879-86 (2004).

205.   Hu, M. et al. Structural basis of competitive recognition of p53 and MDM2 by HAUSP/USP7: implications for the regulation of the p53-MDM2 pathway. PLoS Biol 4, e27 (2006).

206.   Saridakis, V. et al. Structure of the p53 binding domain of HAUSP/USP7 bound to Epstein-Barr nuclear antigen 1 implications for EBV-mediated immortalization. Mol Cell 18, 25-36 (2005).

207.   Sheng, Y. et al. Molecular recognition of p53 and MDM2 by USP7/HAUSP. Nat Struct Mol Biol 13, 285-91 (2006).

208.   Sarkari, F. et al. Further insight into substrate recognition by USP7: structural and biochemical analysis of the HdmX and Hdm2 interactions with USP7. J Mol Biol 402, 825-37 (2010).

209.   Tang, J. et al. Critical role for Daxx in regulating Mdm2. Nat Cell Biol 8, 855-62 (2006).

210.   Tang, J., Qu, L., Pang, M. & Yang, X. Daxx is reciprocally regulated by Mdm2 and Hausp. Biochem Biophys Res Commun 393, 542-5 (2010).

211.   van 't Veer, L.J. et al. Gene expression profiling predicts clinical outcome of breast cancer. Nature 415, 530-6 (2002).

212.   Epping, M.T. et al. TSPYL5 suppresses p53 levels and function by physical interaction with

USP7. Nat Cell Biol 13, 102-8 (2011).

213.   Frappier, L. Viral disruption of promyelocytic leukemia (PML) nuclear bodies by hijacking host PML regulators. Virulence 2, 58-62 (2011).

214.   Kieff, E. & Rickinson, A.B. Epstein-Barr virus and its replication. In: D.M. Knipe and P.M. Howley, Editors, Fields Virology, Lippincott Williams and Wilkins, Philadelphia, 2511–2573 (2001).

215.   Sivachandran, N., Sarkari, F. & Frappier, L. Epstein-Barr nuclear antigen 1 contributes to nasopharyngeal carcinoma through disruption of PML nuclear bodies. PLoS Pathog 4, e1000170 (2008).

216.   Cairns, P. et al. Frequent inactivation of PTEN/MMAC1 in primary prostate cancer. Cancer Res 57, 4997-5000 (1997).

217.   Feilotter, H.E., Nagai, M.A., Boag, A.H., Eng, C. & Mulligan, L.M. Analysis of PTEN and the 10q23 region in primary prostate carcinomas. Oncogene 16, 1743-8 (1998).

218.   Gray, I.C. et al. Mutation and expression analysis of the putative prostate tumour-suppressor gene PTEN. Br J Cancer 78, 1296-300 (1998).

219.   Lin, W.M. et al. Loss of heterozygosity and mutational analysis of the PTEN/MMAC1 gene in synchronous endometrial and ovarian carcinomas. Clin Cancer Res 4, 2577-83 (1998).

220.   Steck, P.A. et al. Identification of a candidate tumour suppressor gene, MMAC1, at chromosome 10q23.3 that is mutated in multiple advanced cancers. Nat Genet 15, 356-62 (1997).

221.   Wang, S.I. et al. Somatic mutations of PTEN in glioblastoma multiforme. Cancer Res 57, 4183-6 (1997).

222.   Ali, I.U., Schriml, L.M. & Dean, M. Mutational spectra of PTEN/MMAC1 gene: a tumor suppressor with lipid phosphatase activity. J Natl Cancer Inst 91, 1922-32 (1999).

223.   Salmena, L., Carracedo, A. & Pandolfi, P.P. Tenets of PTEN tumor suppression. Cell 133, 403-14 (2008).

224.   Maehama, T. & Dixon, J.E. The tumor suppressor, PTEN/MMAC1, dephosphorylates the lipid second messenger, phosphatidylinositol 3,4,5-trisphosphate. J Biol Chem 273, 13375-8 (1998).

225.   Stambolic, V. et al. Negative regulation of PKB/Akt-dependent cell survival by the tumor suppressor PTEN. Cell 95, 29-39 (1998).

226.   Blanco-Aparicio, C., Renner, O., Leal, J.F. & Carnero, A. PTEN, more than the AKT pathway. Carcinogenesis 28, 1379-86 (2007).

227.   Song, M.S. et al. Nuclear PTEN regulates the APC-CDH1 tumor-suppressive complex in a phosphatase-independent manner. Cell 144, 187-99 (2011).

228.   Visintin, R., Prinz, S. & Amon, A. CDC20 and CDH1: a family of substrate-specific activators of APC-dependent proteolysis. Science 278, 460-3 (1997).

229.   van der Horst, A. & Burgering, B.M. Stressing the role of FoxO proteins in lifespan and disease. Nat Rev Mol Cell Biol 8, 440-50 (2007).

230.   Colland, F. et al. Functional proteomics mapping of a human signaling pathway. Genome Res 14, 1324-32 (2004).

231.   van der Horst, A. et al. FOXO4 transcriptional activity is regulated by monoubiquitination and USP7/HAUSP. Nat Cell Biol 8, 1064-73 (2006).

232.   Cantley, L.C. The phosphoinositide 3-kinase pathway. Science 296, 1655-7 (2002).

233.   Brenkman, A.B., de Keizer, P.L., van den Broek, N.J., Jochemsen, A.G. & Burgering, B.M. Mdm2 induces mono-ubiquitination of FOXO4. PLoS One 3, e2819 (2008).

234.   Yang, J.Y. et al. ERK promotes tumorigenesis by inhibiting FOXO3a via MDM2-mediated degradation. Nat Cell Biol 10, 138-48 (2008).

235.   Brenkman, A.B. et al. The peptidyl-isomerase Pin1 regulates p27kip1 expression through inhibition of Forkhead box O tumor suppressors. Cancer Res 68, 7597-605 (2008).

236.   Lunyak, V.V. et al. Corepressor-dependent silencing of chromosomal regions encoding

neuronal genes. Science 298, 1747-52 (2002).

237. Ballas, N., Grunseich, C., Lu, D.D., Speh, J.C. & Mandel, G. REST and its corepressors mediate plasticity of neuronal gene chromatin throughout neurogenesis. Cell 121, 645-57 (2005).

238. Guardavaccaro, D. et al. Control of chromosome stability by the beta-TrCP-REST-Mad2 axis. Nature 452, 365-9 (2008).

239. Westbrook, T.F. et al. SCFbeta-TRCP controls oncogenic transformation and neural differentiation through REST degradation. Nature 452, 370-4 (2008).

240. Zuccato, C. et al. Huntingtin interacts with REST/NRSF to modulate the transcription of NRSE-controlled neuronal genes. Nat Genet 35, 76-83 (2003).

241. Fuller, G.N. et al. Many human medulloblastoma tumors overexpress repressor element-1 silencing transcription (REST)/neuron-restrictive silencer factor, which can be functionally countered by REST-VP16. Mol Cancer Ther 4, 343-9 (2005).

242. Lawinger, P. et al. The neuronal repressor REST/NRSF is an essential regulator in medulloblastoma cells. Nat Med 6, 826-31 (2000).

243. Huang, Z. et al. Deubiquitylase HAUSP stabilizes REST and promotes maintenance of neural progenitor cells. Nat Cell Biol 13, 142-52 (2011).

244. Cao, R. et al. Role of histone H3 lysine 27 methylation in Polycomb-group silencing. Science 298, 1039-43 (2002).

245. van der Knaap, J.A., Kozhevnikova, E., Langenberg, K., Moshkin, Y.M. & Verrijzer, C.P. Biosynthetic enzyme GMP synthetase cooperates with ubiquitin-specific protease 7 in transcriptional regulation of ecdysteroid target genes. Mol Cell Biol 30, 736-44 (2010).

246. van der Knaap, J.A. et al. GMP synthetase stimulates histone H2B deubiquitylation by the epigenetic silencer USP7. Mol Cell 17, 695-707 (2005).

247. Sarkari, F. et al. EBNA1-mediated recruitment of a histone H2B deubiquitylating complex to the Epstein-Barr virus latent origin of DNA replication. PLoS Pathog 5, e1000624 (2009).

248. Boritzki, T.J., Jackson, R.C., Morris, H.P. & Weber, G. Guanosine-5'-phosphate synthetase and guanosine-5'-phosphate kinase in rat hepatomas and kidney tumors. Biochim Biophys Acta 658, 102-10 (1981).

249. Weber, G. et al. Purine and pyrimidine enzymic programs and nucleotide pattern in sarcoma. Cancer Res 43, 1019-23 (1983).

250. Faustrup, H., Bekker-Jensen, S., Bartek, J., Lukas, J. & Mailand, N. USP7 counteracts SCFbetaTrCP- but not APCCdh1-mediated proteolysis of Claspin. J Cell Biol 184, 13-9 (2009).

251. Kang, D., Chen, J., Wong, J. & Fang, G. The checkpoint protein Chfr is a ligase that ubiquitinates Plk1 and inhibits Cdc2 at the G2 to M transition. J Cell Biol 156, 249-59 (2002).

252. Yu, X. et al. Chfr is required for tumor suppression and Aurora A regulation. Nat Genet 37, 401-6 (2005).

253. Oh, Y.M., Yoo, S.J. & Seol, J.H. Deubiquitination of Chfr, a checkpoint protein, by USP7/HAUSP regulates its stability and activity. Biochem Biophys Res Commun 357, 615-9 (2007).

254. Leonhardt, H., Page, A.W., Weier, H.U. & Bestor, T.H. A targeting sequence directs DNA methyltransferase to sites of DNA replication in mammalian nuclei. Cell 71, 865-73 (1992).

255. Du, Z. et al. DNMT1 stability is regulated by proteins coordinating deubiquitination and acetylation-driven ubiquitination. Sci Signal 3, ra80 (2010).

256. Colland, F. et al. Small-molecule inhibitor of USP7/HAUSP ubiquitin protease stabilizes and activates p53 in cells. Mol Cancer Ther 8, 2286-95 (2009).

257. Holowaty, M.N., Sheng, Y., Nguyen, T., Arrowsmith, C. & Frappier, L. Protein interaction domains of the ubiquitin-specific protease, USP7/HAUSP. J Biol Chem 278, 47753-61

(2003).

258.   Reyes-Turcu, F.E., Ventii, K.H. & Wilkinson, K.D. Regulation and cellular roles of ubiquitin-specific deubiquitinating enzymes. Annu Rev Biochem 78, 363-97 (2009).

259.   Sarkari, F., Sheng, Y. & Frappier, L. USP7/HAUSP promotes the sequence-specific DNA binding activity of p53. PLoS One 5, e13040 (2010).

1

$\leftrightarrow$

Chapter 2

The differential modulation of USP activity by internal regulatory domains, interactors and seven Ub-chain types

Alex C. Faesen[1,#], Mark P.A. Luna-Vargas[1,#], Paul P. Geurink[2], Marcello Clerici[1], Remco Merkx[2], Willem J. van Dijk[1], Dharjath S. Hameed[2], Farid El Oualid[2], Huib Ovaa[2], and Titia K. Sixma[1,*]

Manuscript submitted

[1]Division of Biochemistry and Center for Biomedical Genetics, [2]Division of Cell Biology, the Netherlands Cancer Institute, Plesmanlaan 121, 1066 CX Amsterdam, the Netherlands.

[#] These authors contributed equally to this study.

Abstract

Ubiquitin-specific proteases (USPs) are papain-like isopeptidases with variable inter- and intra-molecular regulatory domains. To understand the effect of these domains on USP activity, we have analyzed enzyme kinetics of a set of twelve USPs in presence and absence of modulators using synthetic reagents. We synthesized all seven wild-type lysine-linked di-ubiquitins and provide the first comprehensive analysis comparing ubiquitin (Ub) chain preference. Our data reveal large variations in both the catalytic turnover and Ub binding between USPs and modest preferences for di-Ub topoisomers. Interestingly, our data show that the preference of USP7 for di-Ub topoisomers can be attributed to the binding affinity (K_M) for the substrate, while the intermolecular activators UAF1 and GMPS mainly increase the catalytic turnover (k_{cat}). Together, this comprehensive kinetic analysis highlights the variability within the USP family.

Introduction

Since the 1980s, the post-translational modification of proteins by Ub has been the focus of many studies due to their important roles in many cellular processes[1,2]. However, the processing and removal of Ub and thus reversal of the modification of target proteins is equally important and is carried out by De-ubiquitinating enzymes (DUBs).

The human genome encodes nearly 100 putative DUBs, belonging to at least five subfamilies of isopeptidases[3]. The Ubiquitin-Specific proteases (USP) family is the largest class of DUBs, with more than sixty members[3,4]. USPs are cysteine proteases that use a papain-like mechanism to hydrolyze the isopeptide bond between the carboxy terminus of Ub and the ε-amine of the target lysine.

USPs are variable both in size and their modular domain architecture, which can include substrate binding domains, ubiquitin-like (UBL) domains and other protein-protein interaction domains[3,5] (Figure 1A). They share a common papain-like fold, but the catalytic domains can have large insertions[6], possibly directly affecting activity, Ub binding or localization as seen in USP4[7], USP5[8], USP14[9] and CYLD[10]. Additionally, some USPs need structural rearrangements to bind their substrate and catalyze hydrolysis[11-15].

USPs are often found in large protein complexes and many interaction partners of USPs have been identified[16]. Although the function of most interaction partners is still unclear, some play a role in the modulation of USP activity. For example, GMP synthetase (GMPS) interacts and activates USP7[17-19], whereas the WD40-repeat containing UAF1 activates USP1, USP12 and USP46[20,21].

With its diversity of domain architectures, internal insertions within the catalytic domain and external modulators, the USP family apparently requires different levels of regulation. This poses a number of unanswered questions. For instance, what is the variability of the activity between the catalytic domains and the full-length proteins? Are there preferences for Ub-chain types and does this change in the presence of external modulators?

To address these questions, we have developed and produced[22] chemical tools, and used these to characterize a set of twelve USPs. This revealed variations of several orders of magnitude in catalytic turnover and Ub binding, and allowed characterizing intra- and inter-molecular activity modulation. Using synthetic di-Ub, we determined the chain preferences of all USPs against all seven lysine-linked topoisomers. This showed a modest chain specificity that was variable between USPs, but did not change in the presence of the modulators. Kinetic analysis of the hydrolysis by USP7 showed that there is no additional Ub binding site, suggesting that the chain preferences are achieved by steric hindrance.

Results

Protein cloning, expression and purification

After protein expression trials[23], we identified constructs suitable for large-scale protein expression of twelve different USPs in either *E.coli* or in *Sf9* insect cells (Figure 1A). In this study we could therefore include sixteen constructs containing either the (almost) full-length constructs (USP1ΔN, USP7FL, USP11FL, USP12FL, USP16FL, USP25FL and USP46ΔN, with ΔN and ΔC denoting N- and C-terminal truncations respectively), or the catalytic domain (USP4CD, USP7CD, USP8CD, USP16CD, USP21CD, USP30CD and USP39CD) (Figure 1A and B). Additionally, we expressed and purified two known USP activity modulators: UAF1[21] and GMPS[19]. Cloning, expression and purification
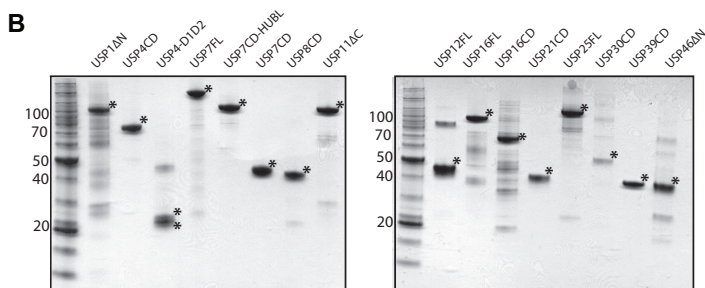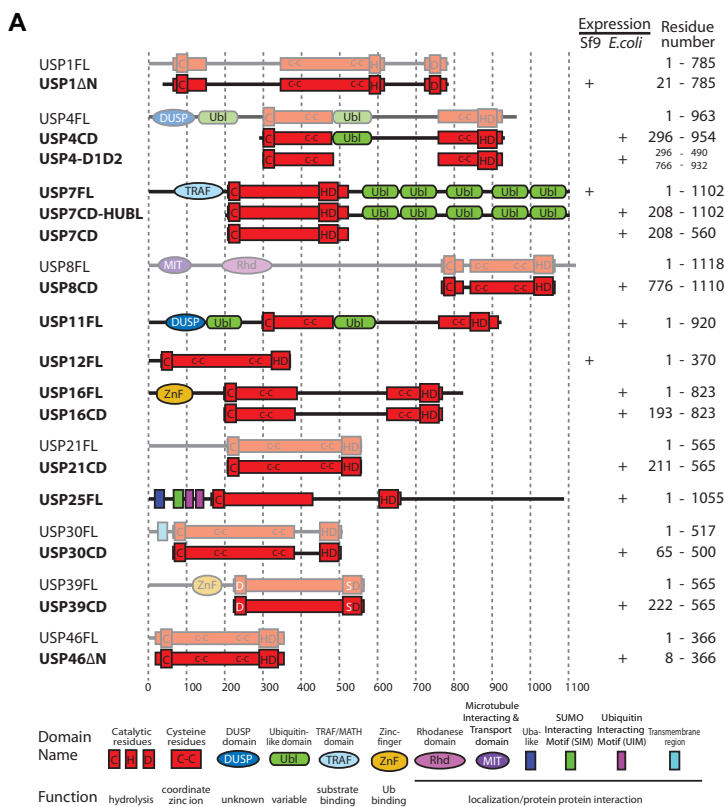

Figure 1: Overview of the characterized USPs. A. Domain architecture of the USPs used in this study. The constructs used in this manuscript are highlighted with corresponding residue numbers and expression system. **B.** Final purification product of the USP constructs shown on SDS-PAGE gel. An asterisk indicates the expressed USP. USP7FL has an N-terminal GST tag.

protocols are provided in the materials and methods section.

Large variations in both catalytic turnover and Ub binding

Although USP family members share a homologous catalytic domain, many contain insertions within their catalytic domain or have additional domains that could influence their activity[6,7] (Figure 1A). To study these effects, we determined the kinetic parameters of all the USPs. To this end, we produced a minimal synthetic Ub substrate with fused at its C-terminus the small molecule 7-amino-4-methylcoumarin (UbAMC)[22,24]. The UbAMC substrate is a widely used reagent to assay DUB activity. Upon hydrolysis by the DUB, the free AMC reporter molecule produces a fluorescent signal, which allows for a direct read-out of activity (Supplemental Figure S1). Since this universal DUB substrate contains an AMC moiety instead of the endogenous USP target, it is suitable for comparing the relative activity among the USP family members. With this substrate, we observed variations of several orders of magnitude in both K_M and k_{cat} between the USP constructs (Figure 2). Our data are in agreement with earlier reports for USP1, USP4,

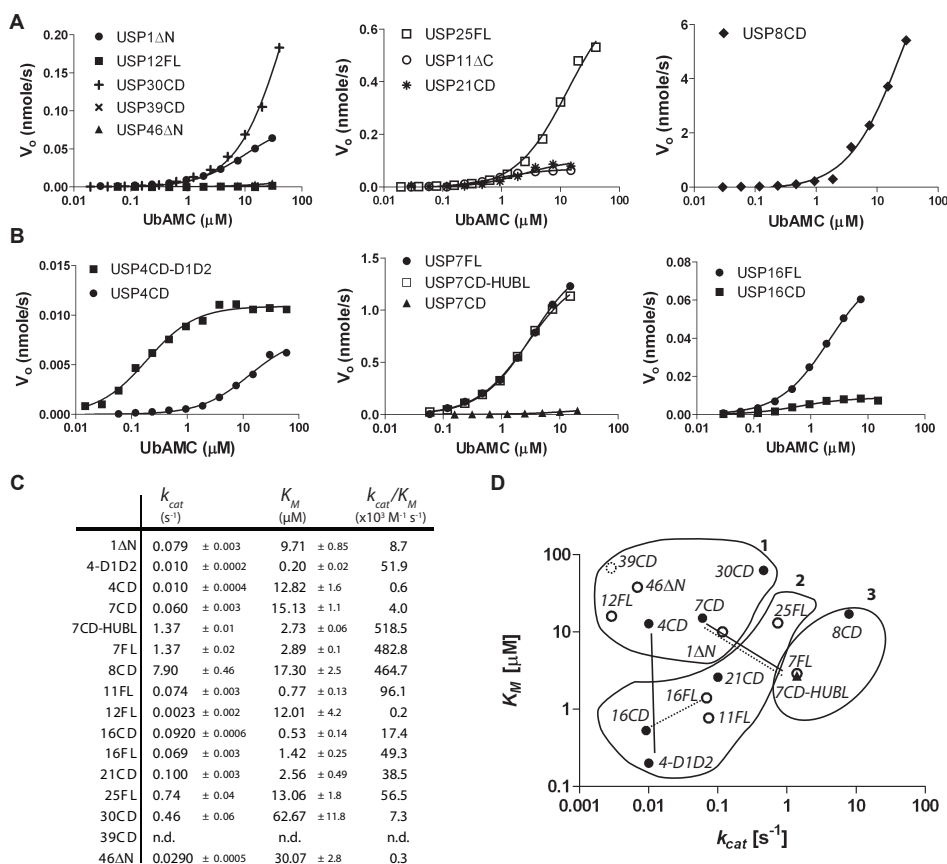|	k_{cat} (s^{-1})		K_M (µM)		k_{cat}/K_M (x10^3 M^{-1} s^{-1})
1ΔN	0.079	± 0.003	9.71	± 0.85	8.7
4-D1D2	0.010	± 0.0002	0.20	± 0.02	51.9
4CD	0.010	± 0.0004	12.82	± 1.6	0.6
7CD	0.060	± 0.003	15.13	± 1.1	4.0
7CD-HUBL	1.37	± 0.01	2.73	± 0.06	518.5
7FL	1.37	± 0.02	2.89	± 0.1	482.8
8CD	7.90	± 0.46	17.30	± 2.5	464.7
11FL	0.074	± 0.003	0.77	± 0.13	96.1
12FL	0.0023	± 0.002	12.01	± 4.2	0.2
16CD	0.0920	± 0.0006	0.53	± 0.14	17.4
16FL	0.069	± 0.003	1.42	± 0.25	49.3
21CD	0.100	± 0.003	2.56	± 0.49	38.5
25FL	0.74	± 0.04	13.06	± 1.8	56.5
30CD	0.46	± 0.06	62.67	±11.8	7.3
39CD	n.d.		n.d.		n.d.
46ΔN	0.0290	± 0.0005	30.07	± 2.8	0.3

Figure 2. Kinetic parameters using UbAMC. A. and B. The Michaelis-Menten curves for the different USPs obtained by determining the initial rates (V0) at different UbAMC concentration. (B) Shows the USPs with intra-molecular modulation. **C.** Overview of the kinetic parameters (k_{cat}, K_M and K_{cat}/K_M) for the different USPs. **D.** Activity classification of USPs, based on kinetic parameters, where group 1 represents the USPs with the lowest activity; group 2 contains USPs with intermediate activity and group 3 contains the USPs with the highest activity. Dashed lines link the catalytic domains with the corresponding full length USPs. Solid lines show the effect of intra-molecular activating and inhibiting domains.

USP7, USP8 and USP39 (Supplemental Table S1)[7,11,21,25,26]. Based on their K_M and k_{cat} values, the USPs could be classified in three groups (Figure 2D). Group 1 represents the USPs, whose activity is very limited due to a low k_{cat} (USP1ΔN, USP4CD, USP12, USP30CD, USP39CD and USP46ΔN). The "intermediate" group 2 contains the USPs that show moderate activity (USP4-D1D2, USP11FL, USP16CD, USP16FL, USP21CD and USP25FL), and group 3 contains very active USPs (USP7FL, USP7CD-HUBL and USP8CD).

As expected, group 1 contains USP39CD. It shows no activity, since it lacks the catalytic cysteine and histidine residues[3]. Group 1 also contains USP1ΔN, USP12FL and USP46ΔN, all three known to have low activity, which is enhanced by the external modulator UAF1[20,21]. Interestingly, also USP30CD shows very little activity. To date there is no known activator for USP30CD, although several interaction partners have been identified[16].

In contrast, group 3 represents the most active USPs, and contains both USP8CD and the USP7 constructs with activating C-terminal Hausp UBL (HUBL) domain[17]. Interestingly, USP8CD has an unusual high K_M, which is possibly due to an inserted α-helix in the catalytic domain, which is suggested to stabilize the observed closed conformation[11]. However, this is compensated by a very high catalytic turnover, rendering it a very active USP overall.

Intra-molecular modulation of USP activity

Not only do we observe differences in enzymatic behavior between the USPs, but we also observe differential effects of intra-molecular domains on the activity of the (minimal) catalytic domains in USP4, USP7 and USP16 (Figure 2B).

We recently showed that USP4 contains a UBL domain inserted in its catalytic domain[5] (USP4CD; Figure 1A), which inhibits the activity of USP4CD (group 1; Figure 2B,D). The presence of this UBL domain in USP4CD increases the K_M and is therefore less active than the minimal catalytic domain USP4-D1D2[7] (group 2; Figure 2D). In contrast, both k_{cat} and K_M are affected in USP7, where the minimal catalytic domain (group 1) shows far less activity than the full-

length enzyme (group 3). Here, the activity of USP7 is modulated by its HUBL domain which is essential for both activity and Ub binding *in vitro* and *in vivo*[17,25,27]. The activity of USP16CD is modulated by the zinc-finger Ub specific protease (ZnF-UBP) domain. Surprisingly, the activity is enhanced by increasing catalytic turnover, rather than the K_M (Figure 2B,D). Since it is a Ub binding domain, the effect of the zinc-finger could be more prominent in poly-Ub processing[28], which might add up to a bigger difference than observed here. USP39CD also contains a Znf-UBP domain, but it is unlikely that this will lead to enzymatic activation since USP39CD does not have the catalytic residues.

Overall, this shows that several intramolecular domains are able modulate USPs. The modulation can affect K_M (USP4), k_{cat} (USP16), or both (USP7), and both inhibitory and activating domains are found in USPs. Together, this creates an additional layer of regulation on the catalytic activity of USPs.

Some USPs show small preference for di-Ub topoisomers

Most studies of DUB specificity have focused on processing K48- and K63-linked poly-Ub. However, since the additional linkages serve equally important cellular functions, we synthesized all seven lysine-linked di-Ub topoisomers[22] and we used them in a qualitative assay to assess all linkage preferences of the panel of USPs (Figure 3 and Supplemental Figure S2). In agreement with the kinetic parameters from the UbAMC assay, the USPs from group 1 showed very little activity; USP8CD from group 3 is the most active USP, and most USPs from group 2 show an intermediate activity. However, there were two clear changes. Where USP7 was amongst the most active USPs in the UbAMC assay, now it shows an intermediate activity. In contrast, USP21CD showed intermediate activity in the UbAMC assay, but is very active in the di-Ub assay and displays activities almost matching the most active USP; USP8CD.

The USP family seems to be rather promiscuous compared to other DUB families. For example, Cezanne[29] (K11), OTUB1[30] (K48) and TRABID[31] (K29) from the OTU family display strong

linkage preferences for di-Ub topoisomers. However, figure 3 shows that the differential activity of the USPs is smaller. All the active USPs from this study hydrolyze all di-Ub topoisomers. Nevertheless, there are clear differences in efficiency. For instance, most USPs have difficulties in hydrolyzing K27- and, to a lesser extent, K29-linked di-Ub. For example, USP7 has limited activity towards hydrolyzing K27- and K29-linked di-Ub. In contrast, the K6, K11, K48 and K63 Ub topoisomers are hydrolyzed

relatively efficiently. Another clear example is USP4, for which K63-linked di-Ub is a better substrate than K48-linked di-Ub. Apparently, some USPs seem to prefer specific di-Ub isoforms.

We wondered whether the intramolecular modulating domains in USP4, USP7 and USP16 change the linkage preferences. However, this does not seem to be the case. The different USPs respond differently to modulation by internal

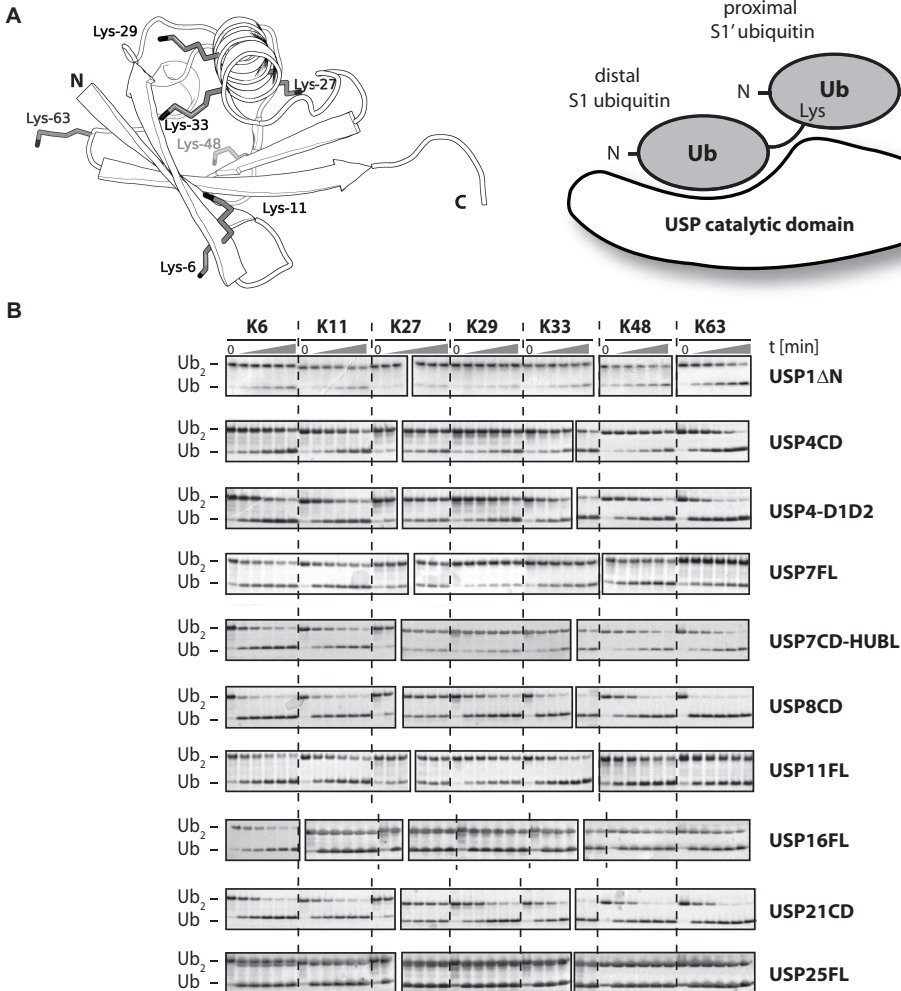**Figure 3. Di-Ub topoisomer preference for the different USPs. A.** Ubiquitin (1UBQ) showing all lysines. The distal ubiquitin binds the catalytic domain. **B.** Overview of a time-course using all seven different di-Ub topoisomers (5 µM) (K6, K11, K27, K29, K33, K48 and K63) for the active USPs (75 nM). Samples from each time-point (0, 5, 10, 30, 60, 180 min) were analyzed on coomassie stained SDS-PAGE gels.

domains, analogous to what was observed with UbAMC (Figure 3 and Supplemental Figure S2B,C). However, no change in linkage preference was seen between catalytic domain and longer constructs, showing that the modulation effects are substrate independent mechanisms.

Overall, this shows that USPs can hydrolyze all Ub lysine-linked di-Ub topoisomers, but with differences in efficiency. Moreover, these differences are preserved in the presence of the intra-molecular activity modulators.

In the case of USPs, isopeptide-linked Ub is not representative for di-Ub

To explain the Ub linkage preference, we might not need full-length di-Ub[32]. To test this in an activity assay, we designed and synthesized a panel of fluorescence polarization-based (FP) di-Ub mimics. In these reagents, TAMRA-labeled Ub peptides were linked via an isopeptide linkage to the carboxy-terminus of wild-type full-length mono-Ub[33] (Figure 4A and Supplemental Figure S3A,B). Therefore, in contrast to the peptide linkage in UbAMC, these FP-reagents use the natural isopeptide linkage. The proximal Ub is represented by 14-mer peptides, each representing one of the seven lysines of Ub (Figure 3A and 4A). In addition, the di-peptide (KG) was prepared to serve as a minimal substrate. Mass spectrometry and SDS-PAGE analysis of these new Ub substrates showed that the synthesis was successful for all eight different TAMRA labeled isopeptide-linked Ub FP-reagents (Supplemental Figure S3C,F).

As a proof of principle, we used the minimal ´KG´ FP-reagent to determine the kinetic parameters of USP4-D1D2 (Figure 4B and Supplemental Figure S3D,E,F,H). With this reagent we determined K_M (293 nM) and k_{cat} (0.07 s^{-1}) values similar to the kinetic parameters obtained using UbAMC. Only the k_{cat} is higher, possibly due to the difference in the chemical and steric nature of the linkage, since the FP-reagents contain a natural isopeptide linkage in contrast to the UbAMC reagent. However,
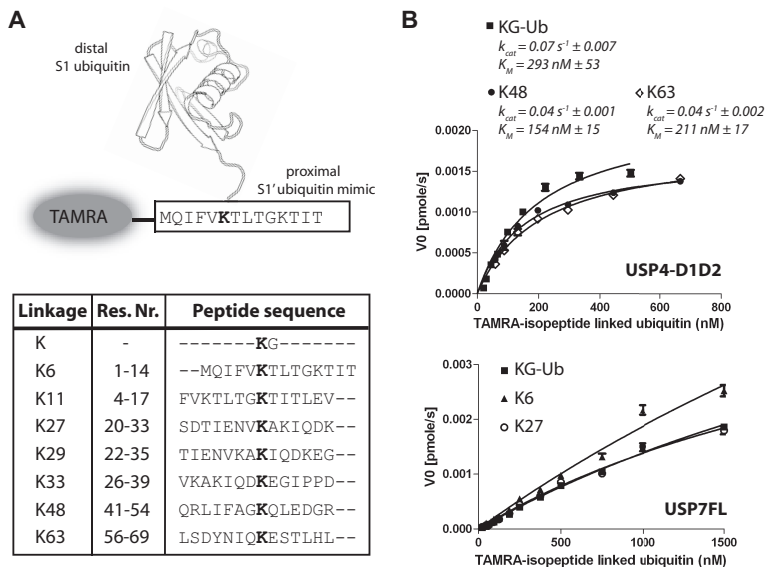
Figure 4. Isopeptide linked-ubiquitin FP reagents. A. Schematic view of N-terminal TAMRA labeled ubiquitin peptide (K6) conjugated with ubiquitin. Table shows the peptide sequences used with the corresponding residue numbers for the different types of ubiquitin linkages. The conjugated lysine is highlighted. **B.** Michaelis-Menten curves for USP4-D1D2 (top) and USP7FL (bottom) were obtained using the TAMRA labeled ubiquitin peptides in a FP hydrolysis assay. The curves for USP7 could not be fitted.

since the K_M values are similar, both represent comparable Ub reagents.

In the di-Ub time course assay, we observed linkage preferences of USP4-D1D2 and USP7; e.g. USP7 prefers the hydrolysis of K6- over K27-linked di-Ub, and USP4-D1D2 prefers K63- over K48-linked di-Ub (Figure 3B). Although difficult to fit for USP7, with our FP-reagents we observed no difference in activity for either USP4-D1D2 or USP7, and therefore could not recapitulate the preferences observed in the di-Ub assay (Figure 4B and Supplemental Figure S3G,H). This shows that these FP reagents do not contain the required information to mimic di-Ub for USPs.

The proximal Ub does not contribute, but rather hinders binding to USP7

Since the FP-reagents were not sufficient to reproduce the observed linkage preference, we used full-length di-Ubs to determine the kinetic parameters directly. We determined K_M and k_{cat} of the hydrolysis of all seven lysine linked di-Ubs by USP7, using initial rate experiments that monitored the appearance of mono-Ub (Figure 5). These experiments showed that the linkages that are efficiently hydrolyzed by USP7 (K6, K11, K33, K48 and K63) have similar kinetic behavior (Figure 5B). Interestingly, the K_M and k_{cat} values are similar to the minimal substrate UbAMC, which contains only a single Ub moiety. This suggests that there is no induced binding or catalysis effect by the proximal Ub moiety.

In the initial di-Ub assay, two linkages (K27 and K29) showed a clear delay in hydrolysis by USP7 (Figure 3). This was nicely reproduced in this kinetic di-Ub assay. Interestingly, there was hardly any change in k_{cat}, but rather the K_M increased far above the concentrations used in our assays. This suggests that the preference for the di-Ub topoisomers arises from steric hindrance, rather than an additional binding
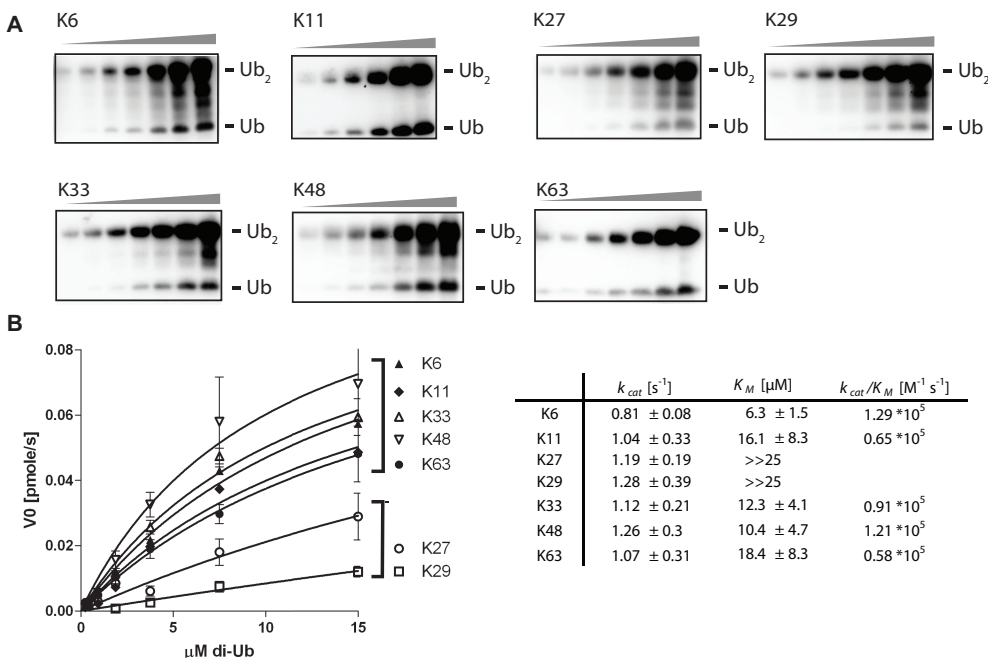

Figure 5. Michaelis-Menten kinetics of di-Ub hydrolysis by USP7. A. Representative western-blot Michaelis-Menten analysis di-Ub hydrolysis USP7. Assay performed using 2-fold dilutions of the di-Ub starting at 15 μM for 5 minutes at 37 degrees. **B.** Michaelis-Menten analysis for USP7FL for di-ubiquitin hydrolysis. Initial rate (V0) of di-Ub conversion into mono-Ub was determined at different substrate concentration from Western Blots shown in A. The conversion to mono-Ub was quantified using the di-Ub signal corrected for conversion.

	k_{cat} [s^{-1}]	K_M [μM]	k_{cat}/K_M [M^{-1} s^{-1}]
K6	0.81 ± 0.08	6.3 ± 1.5	1.29 *10^5
K11	1.04 ± 0.33	16.1 ± 8.3	0.65 *10^5
K27	1.19 ± 0.19	>>25	
K29	1.28 ± 0.39	>>25	
K33	1.12 ± 0.21	12.3 ± 4.1	0.91 *10^5
K48	1.26 ± 0.3	10.4 ± 4.7	1.21 *10^5
K63	1.07 ± 0.31	18.4 ± 8.3	0.58 *10^5

site for the proximal Ub moiety. Therefore the binding of some linkages to the catalytic domain is impaired, resulting in lower activity.

Intermolecular activation of USPs by UAF1 and GMPS only affects k_{cat}.

Besides their intrinsic activity, some USPs are activated by intermolecular modulation. For example, USP1, USP12 and USP46 are activated by the WD40-repeat containing UAF1, and USP7 is activated by GMPS[17,19-21]. Here, we used the UbAMC assay to quantify this activation (Figure 6A,B and Supplemental Figure S4). In agreement with previous data, we observe mainly a k_{cat} increase (7-fold) of USP1ΔN activity in the presence of UAF1. The USP1 used in this study has a mutation in the self-cleavage site (Gly671,672Ala)[21]. UAF1 also activates USP12FL and USP46ΔN, where the k_{cat} is increased by 66- and 70-fold, respectively. Also in the case of USP7 we observed a k_{cat} increase (5.5-fold) in the presence of its modulator GMPS. Interestingly, in contrast to variable modulation invoked by internal domains (Figure 2D), intermolecular modulation is achieved mainly by an increase

in the catalytic turnover rather than in substrate binding (Figure 6B).

To investigate whether this activation also induces new linkage preferences of these USPs, we repeated the di-Ub assay in the presence of UAF1 or GMPS (Figure 6C). As expected from the UbAMC kinetics, USP1ΔN shows limited activity in the absence of UAF1, while USP12FL and USP46CD show no activity. However, in the presence of UAF1, the activity of all three USPs is increased, albeit not to the same level. In complex with their activators, USP1ΔN and USP7CD-HUBL show most activity, but no change in chain type preference by UAF1 or GMPS. This agrees well with an activation mechanism that only increases k_{cat}, but does not induce binding, which should translate in changing K_M values.
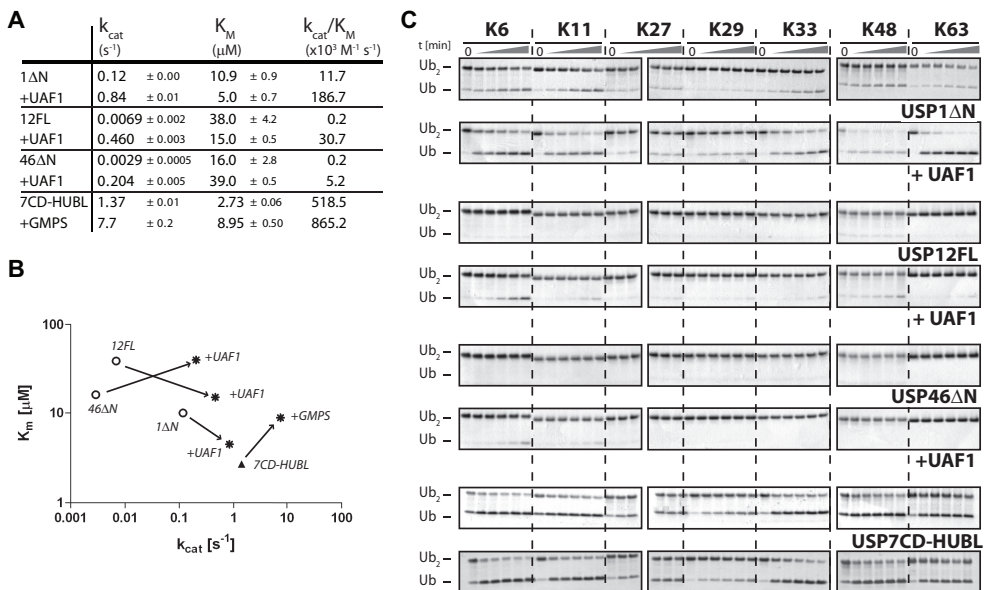

Figure 6. Intermolecular USP activity modulation is achieved by increasing kcat. A. Kinetic parameters (k_{cat}, K_m and k_{cat}/K_M) using UbAMC as substrate for USP1ΔN, USP12FL and USP46ΔN in presence of UAF1 and USP7CD-HUBL in presence of GMPS. **B.** Alternative representation of the kinetic parameters comparing the USP activity between the USPs and in the presence of their modulator. **C.** Activity modulation by UAF1 and GMPS towards all seven di-Ub topoisomers. Samples from each time-point (0, 5, 10, 30, 60, 180 min) were analyzed on coomassie stained SDS-PAGE gels.

Discussion

In this study, we used chemical reagents to determine the kinetic parameters of substrate independent activity of 12 USPs, their di-Ub linkage preference and characteristics of both intra- and intermolecular activity modulation. We observe large variations in both the catalytic turnover (k_{cat}) and Ub binding (K_M) between USPs, which can be further modulated by several intra-molecular domains. Interestingly, the interactors UAF1 and GMPS can activate USPs by increasing their catalytic turnover (k_{cat}). Additionally, the USPs have a small preference for individual di-Ub topoisomers. We show that in USP7 there is no additional Ub binding site, but rather that the differences in hydrolysis of the topoisomers are achieved by hindering binding (K_M) sterically. The combined data provide insights in the variation in the biochemical behavior of the USP enzyme family.

Based on their specific catalytic efficiency (Figure 2), the USPs can be classified into three groups: (1) a group of USPs showing very low DUB activity, (2) an ´intermediate´ group and (3) USPs that exhibit high activity. This variability in activity can be explained in several ways. First, the activity can be affected by structural rearrangements in both Ub binding sites and active sites, as shown by structural studies[11,12]. Secondly, intra-molecular domains of USPs can modulate the DUB activity, as seen here for USP4, USP7 and USP16. External modulator proteins can further regulate the activity of the USP by enhancing its activity, as seen for USP1, USP7, USP12 and USP46 (Figure 6A,B).

Here we report a few cases where intra-molecular modulators regulate the USP activity: either insertions within or additional domains outside the catalytic domain. For both USP7 and USP16 the enzymatic behavior is regulated by intra-molecular domains (the HUBL and ZnF-UBP domain, respectively) outside the catalytic domain, resulting in the increase of the activity. Additionally, variations in kinetics can be induced by (large) insertions in the catalytic domains themselves, as demonstrated for USP4, where a UBL containing insert is inhibiting the catalytic efficiency[7]. These variations and intra-

molecular modulations result in the unique activity of each USP.

For the last decade, the focus on DUB specificity has been on K48- and K63-linked poly-Ub chains. However, different Ub linkage topoisomers can result in different cellular fates, some of which are very specific[34-36] and others requiring a minimal chain length to invoke its function[37,38]. Our study presents the first complete and comprehensive study on di-Ub preference of all seven lysine linked di-ubiquitins for USP family members. Although none of the DUBs so far has been tested for all Ub linkages, some DUBs show remarkable specificity. For example the OTU protease DUBA[39] is K63-specific, OTUB1[30] is K48-specific, while AMSH[40] and BRCC3[41] both from the JAMM/MPN+ family are K63-specific. Next to CYLD[10], the USPs do not have strict chain-type specificity, but rather have preferences. Kinetic studies on USP7 showed us that there is no proximal S1' Ub binding site to induce Ub topoisomers preference, but rather the proximal Ub moiety induces steric constraints for binding to the USP in the case of K27 or K29 linkages. However, it is possible that linkage specificity is increased when using longer Ub chains.

Overall, the hydrolysis efficiency of the USPs towards K6-, K11-, K48- and K63-linked Ub was higher than for K27- and, to a lesser extent, K29- and K33-linked di-Ub. These residues localize in distinct regions on Ub (Figure 3A). The lysine residues involved in the easiest hydrolyzed linkages (K6, K11, K48 and K63) are in the β-sheet or loops. In contrast, the lysine residues of the more difficult linkages (K27, K29 and K33) are positioned on the other side of the Ub molecule, and are all in the α1-helix. Additionally, K27 is barely accessible, which possibly induces a steric constraint, resulting in the lower activity. This interesting bi-polar behavior needs future investigation.

Previous studies suggested that Ub-peptide reagents were sufficient to mimic di-Ub and discriminate between topoisomers in binding[32]. However, in our activity assays with the FP Ub-peptide reagents, we observed no difference between Ub linkages. This suggests

that the peptides do not contain enough information to mimic the proximal Ub for the USPs. Nevertheless, they may be sufficient for DUBs from families with more pronounced Ub specificity and be useful tools in those cases. In addition, the 'KG' FP-reagent might prove a good alternative for UbAMC, as the kinetic parameters are similar, while it contains the natural isopeptide linkage, which is not present in UbAMC.

This study confirmed that two known intermolecular USP activity modulators UAF1 and GMPS activate USP1, USP12, USP46, and USP7 respectively. This activation is mainly by increasing the k_{cat}. However, the biological roles of the UAF1 and GMPS activation are distinct. UAF1 activation is almost essential for USP activity of USP1, USP12 and USP46. This resembles the Ubp8 activation by Sgf11[14,15]. Surprisingly, USP12 in complex with UAF1 is still not very active, possibly requiring additional partners, like WDR20[42]. In a different manner, GMPS hyper-activates USP7, by allosterically stabilizing the active state of the enzyme induced by the HUBL domain[17]. Besides a general activation, the GMPS activity modulation most likely has additional substrate specific roles, as it induces H2B de-ubiquitination.

Although the function of an increasing number of USPs is elucidated, they still represent a relatively uncharacterized enzyme family. To aid in the biochemical understanding of these enzymes, we here report the large variations in kinetics and intra-molecular modulation (k_{cat} and K_M), the modest but surprising differential activity towards the seven di-Ub topoisomers (K_M), and a characterization of the activation by intermolecular interactions (k_{cat}).

Significance

Ubiquitination is a dynamic process, which is involved in numerous key cellular processes. The removal of the Ub molecules is an integral part of this process, and is carried out by Deubiquitinating enzymes (DUBs). These are increasingly recognized as interesting drug targets. However, to date we lack the markers to predict the biochemical behavior based on

sequence alignments and therefore a need exists for comprehensive kinetic studies. This is where chemical tools that allow fast and accurate read-outs will contribute to answer these biological questions. In this study, we designed and produced several of such chemical reagents to determine the kinetics and di-Ub linkage preferences of twelve USPs. Despite the homologous catalytic domain, the kinetic data underline the large variability within the USP family, and the intra- and intermolecular activity modulators create an additional layer of regulation.

In addition this study for the first time reports the linkage preference of twelve USPs against all seven-lysine linked di-Ubs. Kinetic analysis of the hydrolysis of the di-Ub topoisomers, suggest that within the USP family the preferences are induced by steric hindrance, rather than the induced binding, as seen in other DUB families.

Together, this data provides insight in the biochemical behavior in the USP family, and validates the chemical tools that now also can be applied in characterizing other DUB families.

Experimental procedures

General
General reagents were obtained from Sigma Aldrich, Fluka and Acros and used as received. Solvents were purchased from Biosolve or Aldrich. Peptide synthesis reagents were purchased from Novabiochem. USP25 cDNA was provided by Erik Meulmeester and Frauke Melchior.

General plasmids and proteins
Di-Ub moieties were produced as previously described[22]. USP4CD (aa 296-954), USP4-D1D2 (aa 296-490/766-932), USP8CD (aa 776-1110), USP11FL (aa 1-920), USP16FL (aa 1-823), USP16CD (aa 193-823), USP21CD (aa 211-565), USP30CD (aa 65-500), USP39CD (aa 222-565) and USP46ΔN (aa 8-366) are cloned into the pETNKI-LIC vector for expression in bacteria as described23. USP1ΔN (aa 21-785 self-cleavage site glycine 671 and 672 are mutated to alanine), USP7FL (aa 1-1102), USP12FL (aa1-355) and STREP-TEV-UAF1 (6-677) are cloned into the

pFastBac-HTb vector for expression in insect cells. Both USP7CD-HUBL (aa 208-1102) and USP7CD (aa 208-560) are cloned into the pGEX vector[17] and USP25FL is cloned in the pET11a vector[43]. Codon optimized full length USP7 and GMPS cDNA was obtained from DomainEx (Cambridge, UK). Both were amplified by PCR and subcloned (SpeI/NotI) into a pFastBac vector (Invitrogen) containing an N-terminal GST tag (BamHI/SpeI) and Prescission Protease cleavage site. cDNA for USP11 and USP16 were obtained from ImaGenes (Berlin, Germany).

Protein expression and purification

As specified in figure 1, the USPs were expressed in both *E.coli* and insect cells and purified as described[7,17]. GMPS was expressed and purified as before[17]. USP constructs and GMPS cloned both in bacterial and baculovirus expression vector are expressed and purified as described[17,23]. Depending on the type of vector, the tag was removed with either TEV or the HRV 3C protease. Bacmids were prepared following the manufacturer's guidelines. USP1, USP12 and UAF1 were produced using *Sf9* and *Sf21* insect cell expression. Infection was done using a low-MOI infection protocol[44]. The cells were harvested 72 hours after a baculovirus induced growth arrest was observed. USP46 was produced in *E.coli*. USP1, 12, 46 and UAF1 were purified using Ni2+ sepharose (GE Healthcare) in 20 mM Hepes (pH 7.5), 150 mM NaCl, 0.1 mM PMSF, and 0.1 mM DTT followed by elution using imidazole. His-tag was removed by overnight cleavage with TEV protease whilst dialyzing to remove imidazole. Uncleaved product was removed with Ni2+ sepharose. Size exclusion chromatography was performed using a Superdex 200 or 75 column (GE Healthcare), equilibrated against buffer containing 10 mM Hepes [pH 7.5], 100 mM NaCl and 1 mM DTT. All proteins were concentrated to ~10 mg/ml and stored at -80°C.

UbAMC assay

Kinetics were determined as described before[7]. UAF1 and GMPS were added in a 1:1 stoichiometry. USP concentration varied between 1 and 100 nM, depending on relative activity. In order to calculate the kinetic parameters for the hydrolysis of UbAMC, curves obtained by plotting the measured enzyme initial rates (v) versus the corresponding substrate concentrations ([S]). These were subjected to nonlinear regression fit using the Michaelis–Menten equation $V = (Vmax \cdot [S]) / ([S] + K_M)$ (eqn 1), where Vmax is the maximal velocity at saturating substrate concentrations and K_M the Michaelis constant. The k_{cat} value was derived from the equation $k_{cat} = Vmax / [Eo]$ (eqn 2) where [Eo] is the total enzyme concentration. Experimental data was processed using Prism 5.01 (GraphPad Software, Inc.).

Di-Ub assay

Di-Ub hydrolysis reactions were performed at 37°C in 50 mM Hepes buffer at pH 7.5, with 100 mM NaCl, 1 mM EDTA, 5 mM dithiothreitol and 0.05% (w/v) Tween-20 with constant enzyme concentration (75 nM). When indicated UAF1 was added in a 2-fold excess (150 nM) and GMPS in a 1:1 stoichiometry. Reactions were stopped by addition of SDS loading buffer and followed by SDS-PAGE analysis. For the kinetic analysis, the reaction mixture was pre-heated to 37 °C degrees before adding USP7. Samples were run on a 12% Bis-Tris NuPage gel (duplicates on one gel), and western blots were performed with anti-Ub antibody (Santa Cruz; P4D1). The ChemiDoc system (Biorad) was used to read the chemiluminence signal and subsequent quantification of mono-Ub was done using the quantification tools of ImageLab (Biorad) using the non-saturated di-Ub signal (corrected for conversion to mono-Ub). Experimental data was processed using Prism 5.01 (GraphPad Software, Inc.).

Solid Phase Peptide Synthesis (SPPS) of the TAMRA thiolysine peptides

SPPS was performed on a Syro II MultiSyntech Automated Peptide synthesizer using standard 9-fluorenylmethoxycarbonyl (Fmoc) based solid phase peptide chemistry at 25 μmol scale, using fourfold excess of amino acids relative to pre-loaded Fmoc amino acid Wang type resin (0.2 mmol/g, Applied Biosystems). The following protected amino acids were used during Ub peptide synthesis: Fmoc-L-Ala-OH, Fmoc-L-Arg-(Pbf)-OH, Fmoc-L-Asn (Trt)-OH, Fmoc-L-Asp (OtBu)-OH, Fmoc-L-Gln (Trt)-OH, Fmoc-L-Glu (OtBu)-OH, Fmoc-Gly-OH, Fmoc-L-His (Trt)-OH,

Fmoc-L-Ile-OH, Fmoc-L-Leu-OH, Fmoc-L-Lys (Boc)-OH, Fmoc-L-Met-OH; Fmoc-L-Phe-OH; Fmoc-L-Pro-OH; Fmoc-L-Ser (tBu)-OH; Fmoc-L-Thr (tBu)-OH, Fmoc-L-Tyr (tBu)-OH, Fmoc-L-Val-OH. Fmoc-5S- (methyldisulfanyl)- (L)-Lys (Boc)-OH was synthesized as described previously[22].

The coupling procedure starts off with single couplings in N-methylpyrrolidon (NMP) for 45 min using PyBOP (4 equiv) and DiPEA (12 equiv) in a total volume of 750 µL. Followed by the removal of Fmoc with 20% piperidine in NMP for 2×2 and 1×5 min. Finally the procedure ends with NMP wash steps after each coupling (3×) and deprotection (5×).

The resin was washed with diethylether and dried under high vacuum. Next, the polypeptide sequence was detached from the resin and deprotected by treatment with TFA/H2O/Phenol/iPr3SiH 90.5/5/2.5/2 v/v/v/v for 2.5 h. After washing the resin with 3×1 mL TFA, the crude protein was precipitated with cold Et2O/n-pentane 3:1 v/v. The precipitated protein was washed 3× with diethylether, the pellet was dissolved in a mixture of H2O/CH3CN/HOAc (65/25/10 v/v/v) and finally lyophilized. All peptides were analyzed by LC-MS and purified by RP-HPLC when necessary.

LC-MS
LC-MS measurements were performed on a Waters 2795 Seperation Module (Alliance HT), equipped with a Waters 2996 Photodiode Array Detector (190-750nm), Phenomenex Kinetex C18 column (2.1×50, 2.6 µm) and LCTTM Orthogonal Acceleration Time of Flight Mass Spectrometer. Samples were run using two mobile phases: A = 0.1% formic acid in water and B = 0.1% formic acid in acetonitrile. Flow rate = 0.8 mL/min, runtime = 6 min, column T = 40 °C. Gradient: 0 – 0.5 min: 5% B; 0.5 – 4 min: 5% to 95% B; 4 – 5.5 min: 95% B. Data processing was performed using Waters MassLynx Mass Spectrometry Software 4.1 (deconvulation with Maxent1 function).

Ligation of Ub to the peptides followed by desulphurization
Schematic overview of reaction scheme and final yields can be found in Supplemental

Figure S3. A mixture of 4-mercaptophenylacetic acid (MPAA, 100 mM) and TCEP (50 mM) in 6M Guanidinium ·HCl (1 mL, pH 7) was added to Ub-MesNa thioester (5 mg, prepared according to the procedure described previously [22]). To this the TAMRA thiolysine peptide (100 µL of a 20 mM stock solution in DMSO) was added and the whole mixture was incubated at 37 °C. After overnight incubation, all low-molecular weight material was removed using a 3 kDa cutoff spin-column (Amicon Ultra) in four centrifuge cycles. The crude material was taken up in 6M Guanidinium·HCl, 0.1M sodium phosphate (4 mL, pH 6.5) and to this was added TCEP (187 mg) and glutathione (30 mg), after which the pH of the mixture was adjusted to pH 6.5 by addition of 1M NaOH. Next, the mixture was degassed with argon, after which radical initiator VA-044 was added. The mixture was incubated at 37 °C overnight. All constructs were purified by RP-HPLC and analyzed by LC-MS and gel electrophoresis and were obtained as purple solids.

C18 RP-HPLC
Purification by RP-HPLC was performed on a Shimadzu system equipped with a LC-20AT liquid chromatography pump, CTO-20A column oven (T = 40 °C), SPD-20A UV/VIS detector (detection simultaneously at 230 nm and 254 nm), RF-10AXL fluorescence detector (ex/em = 540/600 nm) and an Atlantis Prep T3 column (10×150 mm, 5 µm). Samples were run using two mobile phases: A = 0.05% trifluoroacetic acid in water and B = 0.05% trifluoroacetic acid in acetonitrile. Flow rate = 7.5 mL/min, runtime = 30 min. Gradient: 0 – 6 min: 5% to 10% B; 6.5 – 26 min: 25% to 47% B; 26.5 – 29.5 min: 95% B. Pure fractions were pooled and lyophilized.

Isopeptide linked Ub FP hydrolysis assay
FP assays were performed on a PerkinElmer Wallac EnVision 2010 Multilabel Reader with a 531 nm excitation filter and two 579 nm emission filters. The confocal optics were adjusted with TAMRA-KG (synthesized by SPPS as described above) and the G factor was determined using a polarization value for TAMRA-KG (25 nM) of 50 mP. The assays were performed in "non binding surface flat bottom low flange" black 384-well plates (Corning) at

room temperature in a buffer containing 20 mM Tris•HCl, pH 7.5, 5 mM DTT, 100 mM NaCl, 1 mg/mL 3-[(3-cholamidopropyl) dimethylammonio] propanesulfonic acid (CHAPS) and 0.5 mg/mL bovine gamma globulin (BGG). Each well had a volume of 20 μL. Buffer and enzyme were predispensed and the reaction was started by the addition of substrate. Kinetic data was collected in intervals of 2.5 or 3 min. From the obtained polarization values (P) the amount of processed substrate (Pt) was calculated with to the following equation[45]: $S = S0 - S0 \cdot ((Pt - Pmin) / (Pmax - Pmin))$, where Pt is the polarization measured (in mP); Pmax is the polarization of 100% unprocessed substrate (determined for every reagent at all used substrate concentrations); Pmin is the polarization of 100% processed substrate (determined for every linkage at all used substrate concentrations by measuring the mP value for the corresponding deubiquitinated TAMRA-peptide, which were synthesized by SPPS according to the procedure describes above); S0 is the amount of substrate added to the reaction. From the obtained Pt values the values for initial velocities were calculated, which were used to determine the Michaelis-Menten constants. All experimental data was processed using Ms Excel and Prism 4.03 (GraphPad Software, Inc.).

Acknowledgements

Author contributions

USP expression and purification was performed by M.P.A.L.V. with assistance from W.J.v.D; enzyme assays were designed and analyzed by A.C.F. and executed by M.P.A.L.V and A.C.F.; USP1, 12, 46 and UAF1 were expressed, purified and analyzed by M.C.; UbAMC was designed and synthesized by R.M.; di-Ubs were designed by F.E. and H.O. and synthesized by D.S.H.; FP reagents were designed by F.E., P.P.G. and H.O. and synthesized by P.P.G. and F.E.; FP reagent assays were performed by P.P.G.; H.O. supervised all synthesis efforts and FP experiments; T.K.S. designed and supervised USP project; Data analysis and manuscript writing by A.C.F. with M.P.A.L.V. and T.K.S.

References

1. Hochstrasser, M. Origin and function of ubiquitin-like proteins. Nature 458, 422-9 (2009).
2. Pickart, C.M. Back to the future with ubiquitin. Cell 116, 181-90 (2004).
3. Nijman, S.M. et al. A genomic and functional inventory of deubiquitinating enzymes. Cell 123, 773-86 (2005).
4. Komander, D., Clague, M.J. & Urbe, S. Breaking the chains: structure and function of the deubiquitinases. Nat Rev Mol Cell Biol 10, 550-63 (2009).
5. Zhu, X., Menard, R. & Sulea, T. High incidence of ubiquitin-like domains in human ubiquitin-specific proteases. Proteins 69, 1-7 (2007).
6. Ye, Y., Scheel, H., Hofmann, K. & Komander, D. Dissection of USP catalytic domains reveals five common insertion points. Mol Biosyst 5, 1797-808 (2009).
7. Luna-Vargas, M.P. et al. Ubiquitin-specific protease 4 is inhibited by its ubiquitin-like domain. EMBO Rep (2011).
8. Reyes-Turcu, F.E., Shanks, J.R., Komander, D. & Wilkinson, K.D. Recognition of polyubiquitin isoforms by the multiple ubiquitin binding modules of isopeptidase T. J Biol Chem 283, 19581-92 (2008).
9. Borodovsky, A. et al. A novel active site-directed probe specific for deubiquitylating enzymes reveals proteasome association of USP14. Embo J 20, 5187-96 (2001).
10. Komander, D. et al. The structure of the CYLD USP domain explains its specificity for Lys63-linked polyubiquitin and reveals a B box module. Mol Cell 29, 451-64 (2008).
11. Avvakumov, G.V. et al. Amino-terminal dimerization, NRDP1-rhodanese interaction, and inhibited catalytic domain conformation of the ubiquitin-specific protease 8 (USP8). J Biol Chem 281, 38061-70 (2006).
12. Hu, M. et al. Crystal structure of a UBP-family deubiquitinating enzyme in isolation and in complex with ubiquitin aldehyde. Cell 111, 1041-54 (2002).
13. Hu, M. et al. Structure and mechanisms of the proteasome-associated deubiquitinating enzyme USP14. Embo J 24, 3747-56 (2005).
14. Kohler, A., Zimmerman, E., Schneider, M., Hurt, E. & Zheng, N. Structural basis for assembly and activation of the heterotetrameric SAGA histone H2B deubiquitinase module. Cell 141, 606-17 (2010).
15. Samara, N.L. et al. Structural insights into the assembly and function of the SAGA deubiquitinating module. Science 328, 1025-9 (2010).
16. Sowa, M.E., Bennett, E.J., Gygi, S.P. & Harper, J.W. Defining the human deubiquitinating enzyme interaction landscape. Cell 138, 389-403 (2009).
17. Faesen, A.C. et al. Mechanism of USP7/HAUSP activation by its C-terminal Ubiquitin-like domain and allosteric regulation by GMP-synthetase. *Mol Cell* **44**, 1-14 (2011).
18. Sarkari, F. et al. EBNA1-mediated recruitment of a histone H2B deubiquitylating complex to the Epstein-Barr virus latent origin of DNA replication. PLoS Pathog 5, e1000624 (2009).
19. van der Knaap, J.A. et al. GMP synthetase stimulates histone H2B deubiquitylation by the epigenetic silencer USP7. Mol Cell 17, 695-707 (2005).
20. Cohn, M.A., Kee, Y., Haas, W., Gygi, S.P. & D'Andrea, A.D. UAF1 is a subunit of multiple deubiquitinating enzyme complexes. J Biol Chem 284, 5343-51 (2009).
21. Cohn, M.A. et al. A UAF1-containing multisubunit protein complex regulates the Fanconi anemia pathway. Mol Cell 28, 786-97 (2007).
22. El Oualid, F. et al. Chemical synthesis of ubiquitin, ubiquitin-based probes, and diubiquitin. Angew Chem Int Ed Engl 49, 10149-53 (2010).
23. Luna-Vargas, M.P. et al. Enabling High-Throughput Ligation-Independent Cloning and Protein Expression for the Family of Ubiquitin Specific Proteases. J Struct Biol (2011).
24. Dang, L.C., Melandri, F.D. & Stein, R.L. Kinetic and mechanistic studies on the hydrolysis

of ubiquitin C-terminal 7-amido-4-methylcoumarin by deubiquitinating enzymes. Biochemistry 37, 1868-79 (1998).

25. Fernandez-Montalvan, A. et al. Biochemical characterization of USP7 reveals post-translational modification sites and structural requirements for substrate processing and subcellular localization. Febs J 274, 4256-70 (2007).

26. van Leuken, R.J., Luna-Vargas, M.P., Sixma, T.K., Wolthuis, R.M. & Medema, R.H. Usp39 is essential for mitotic spindle checkpoint integrity and controls mRNA-levels of aurora B. Cell Cycle 7, 2710-9 (2008).

27. Ma, J. et al. C-terminal region of USP7/HAUSP is critical for deubiquitination activity and contains a second mdm2/p53 binding site. Arch Biochem Biophys 503, 207-12 (2010).

28. Pai, M.T. et al. Solution structure of the Ubp-M BUZ domain, a highly specific protein module that recognizes the C-terminal tail of free ubiquitin. J Mol Biol 370, 290-302 (2007).

29. Bremm, A., Freund, S.M. & Komander, D. Lys11-linked ubiquitin chains adopt compact conformations and are preferentially hydrolyzed by the deubiquitinase Cezanne. Nat Struct Mol Biol 17, 939-47 (2010).

30. Edelmann, M.J. et al. Structural basis and specificity of human otubain 1-mediated deubiquitination. Biochem J 418, 379-90 (2009).

31. Virdee, S., Ye, Y., Nguyen, D.P., Komander, D. & Chin, J.W. Engineered diubiquitin synthesis reveals Lys29-isopeptide specificity of an OTU deubiquitinase. Nat Chem Biol 6, 750-7 (2010).

32. Shanmugham, A. et al. Nonhydrolyzable ubiquitin-isopeptide isosteres as deubiquitinating enzyme probes. J Am Chem Soc 132, 8834-5 (2010).

33. Tirat, A. et al. Synthesis and characterization of fluorescent ubiquitin derivatives as highly sensitive substrates for the deubiquitinating enzymes UCH-L3 and USP-2. Anal Biochem 343, 244-55 (2005).

34. Jin, L., Williamson, A., Banerjee, S., Philipp, I. & Rape, M. Mechanism of ubiquitin-chain formation by the human anaphase-promoting complex. Cell 133, 653-65 (2008).

35. Matsumoto, M.L. et al. K11-linked polyubiquitination in cell cycle control revealed by a K11 linkage-specific antibody. Mol Cell 39, 477-84 (2010).

36. Wu, T. et al. UBE2S drives elongation of K11-linked ubiquitin chains by the anaphase-promoting complex. Proc Natl Acad Sci U S A 107, 1355-60.

37. Cook, W.J., Jeffrey, L.C., Kasperek, E. & Pickart, C.M. Structure of tetraubiquitin shows how multiubiquitin chains can be formed. J Mol Biol 236, 601-9 (1994).

38. Thrower, J.S., Hoffman, L., Rechsteiner, M. & Pickart, C.M. Recognition of the polyubiquitin proteolytic signal. Embo J 19, 94-102 (2000).

39. Kayagaki, N. et al. DUBA: a deubiquitinase that regulates type I interferon production. Science 318, 1628-32 (2007).

40. McCullough, J., Clague, M.J. & Urbe, S. AMSH is an endosome-associated ubiquitin isopeptidase. J Cell Biol 166, 487-92 (2004).

41. Cooper, E.M. et al. K63-specific deubiquitination by two JAMM/MPN+ complexes: BRISC-associated Brcc36 and proteasomal Poh1. Embo J 28, 621-31 (2009).

42. Kee, Y. et al. WDR20 regulates activity of the USP12 x UAF1 deubiquitinating enzyme complex. J Biol Chem 285, 11252-7 (2010).

43. Meulmeester, E., Kunze, M., Hsiao, H.H., Urlaub, H. & Melchior, F. Mechanism and consequences for paralog-specific sumoylation of ubiquitin-specific protease 25. Mol Cell 30, 610-9 (2008).

44. Fitzgerald, D.J. et al. Protein complex expression by using multigene baculoviral vectors. Nat Methods 3, 1021-32 (2006).

45. Levine, L.M., Michener, M.L., Toth, M.V. & Holwerda, B.C. Measurement of specific protease activity utilizing fluorescence polarization. Anal Biochem 247, 83-8 (1997).

# Table of contents Supplementary information

2

	k_{cat}	K_M	k_{cat}/K_M	Reference
	$[s^{-1}]$	$[\mu M]$	$[x10^3\ M^{-1}\ s^{-1}]$	
USP1FL	0.014	1.4	10.2	Cohn et al. (2007)
USP1FL+UAF1	0.26	0.7	371	Cohn et al. (2007)
Ubp8/SAGA	0.17	1.5	110	Samara et al. (2011)
USP2CD	0.62	2.5	250	Zhang et al. (2011)
USP2CD	0.14	0.55	252	Renatus et al. (2006)
USP7FL	3.56	17.5	203	Fernandez-Montalvan et al. (2007)
USP7CD	0.077	44.2	1.7	Fernandez-Montalvan et al. (2007)
USP7CD-HUBL	0.805	22.8	35	Fernandez-Montalvan et al. (2007)
USP8CD	2.4	10.2	235	Avvakumov et al. (2006)
USP21CD	0.041	0.26	158	Ye et al. (2011)
USP25FL	0.12	5	24	Meulmeester et al. (2008)

Supplemental Table S1. Related to Figure 1. Published UbAMC kinetics of USPs.
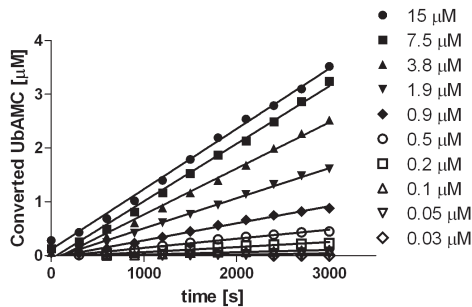
Supplemental Figure S1. Related to Figure 2. Exemplary raw data of UbAMC hydrolysis by USP7CD-HUBL. Measurements were done using a five minute interval. The signal was stable for at least one hour.
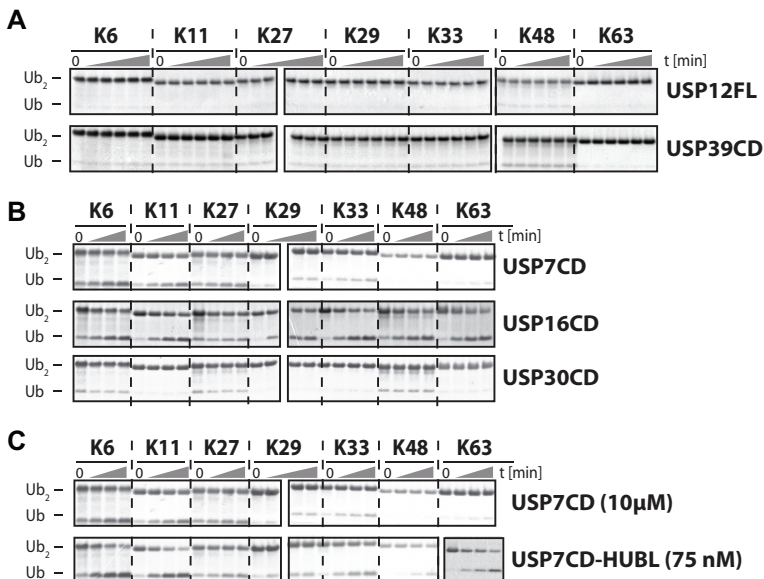
Supplemental Figure S2. Related to Figure 3. Di-Ub assay for inactive USPs and comparison USP7CD versus USP7CD-HUBL. A. and B. Di-Ub assay for USP12FL, USP39CD, USP46FL, USP7CD, USP16CD and USP30CD. Time-course using all di-Ub topoisomers (5 µM) (Linear, K6, K11, K27, K29, K33, K48 and K63) for USPs (75 nM). Samples from each time-point (0, 5, 10, 30, 60, 180 min) (A) and (0, 10, 30, 60 min) (B) were analyzed on coomassie stained SDS-PAGE gels. **C.** Di-Ub assay USP7CD versus USP7CD-HUBL. Time-course using all di-Ub topoisomers (5 µM) (Linear, K6, K11, K27, K29, K33, K48 and K63) for USP7 constructs (10 µM and 75 nM). Samples from each time-point (0, 10, 30, 60 min) were analyzed on coomassie stained SDS-PAGE gels.

A

B

Linkage type	Peptide sequence	MW (Da)	Yield
KG	**TAMRA**-K(**Ub**)G	9162	1.3 mg (25%)
K6 (Ub 1-14)	**TAMRA**-MQIFVK(**Ub**)TLTGKTIT	10540	0.8 mg (16%)
K11 (Ub 4-17)	**TAMRA**-FVKTLTGK(**Ub**)TITLEV	10509	1.0 mg (18%)
K27 (Ub 20-33)	**TAMRA**-SDTIENVK(**Ub**)AKIQDK	10548	0.5 mg (10%)
K29 (Ub 22-35)	**TAMRA**-TIENVKAK(**Ub**)IQDKEG	10532	1.8 mg (30%)
K33 (Ub 26-39)	**TAMRA**-VKAKIQDK(**Ub**)EGIPPD	10497	1.7 mg (28%)
K48 (Ub 41-54)	**TAMRA**-QRLIFAGK(**Ub**)QLEDGR	10590	0.6 mg (12%)
K63 (Ub 56-69)	**TAMRA**-LSDYNIQK(**Ub**)ESTLHL	10620	1.6 mg (32%)

C

D

USP4-D1D2

	k_{cat} [s^{-1}]	K_m [nM]	k_{cat}/K_m [M^{-1} s^{-1}]
KG	0.068 ± 0.006	271.8 ± 43.2	2.51 ×10^5
K6	0.157 ± 0.015	1532 ± 256	1.03 ×10^5
K11	0.060 ± 0.001	229.2 ± 16.0	2.61 ×10^5
K27	0.038 ± 0.001	150.1 ± 11.4	2.56 ×10^5
K29	0.060 ± 0.002	299.7 ± 20.5	1.99 ×10^5
K33	0.048 ± 0.002	330.5 ± 31.6	1.46 ×10^5
K48	0.044 ± 0.001	165.5 ± 11.7	2.65 ×10^5
K63	0.047 ± 0.001	220.7 ± 12.2	2.12 ×10^5

E

Supplemental Figure S3. Related to Figure 4. Synthesis, LC-MS of FP reagents, exemplary raw data and Michaelis-Menten curves of USP4 and USP7. A. Ligation of Ub to the peptides. **B.** Peptide sequence, molecular weight and typical yield of the reaction. **C.** Coomassie staining and fluorescence scan of SDS electrophoresis analysis of the FP-reagent. **D.** Kinetic parameters of USP4-D1D2 using the FP-reagents. **E.** Exemplary data of hydrolysis of FP reagents (K29 with USP4-D1D2).

Figure and legend continue on next page

F

KG-Ub

K6-Ub

K11-Ub

K27-Ub

K29-Ub

K33-Ub

K48-Ub

K63-Ub

G

Figure and legend continued from previous page.

Supplemental Figure S3. Related to Figure 4. Synthesis, LC-MS of FP reagents, exemplary raw data and Michaelis-Menten curves of USP4 and USP7. F. LC-MS spectra of the FP-reagents. **G.** Michaelis-Menten analysis of USP7 hydrolysis of the FP reagents. Data could not be fitted with an exponential Michealis-Menten curve.

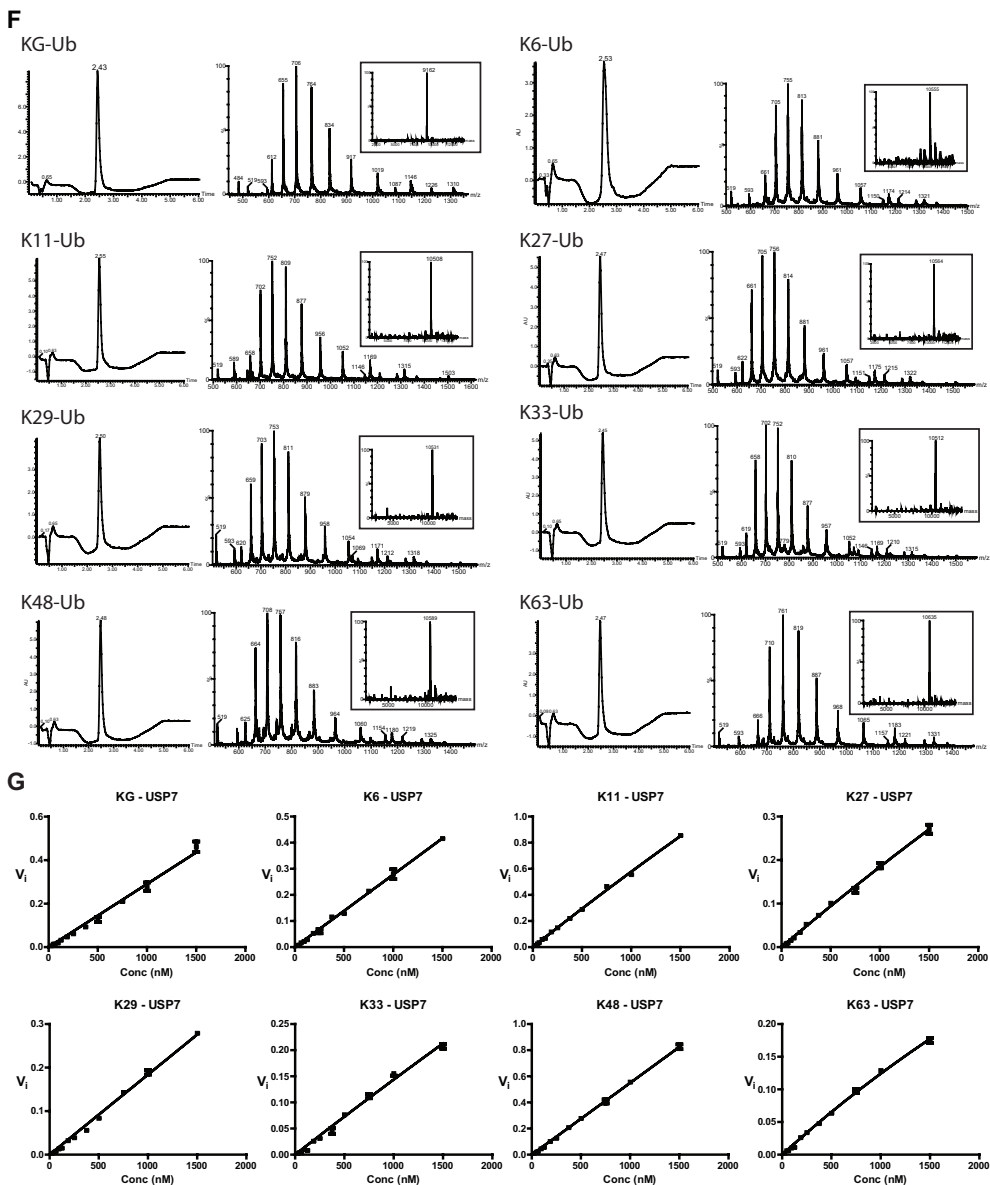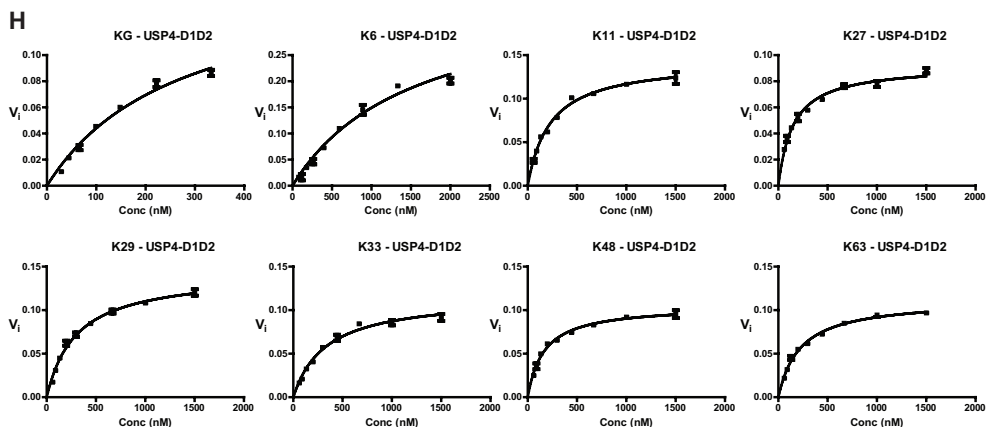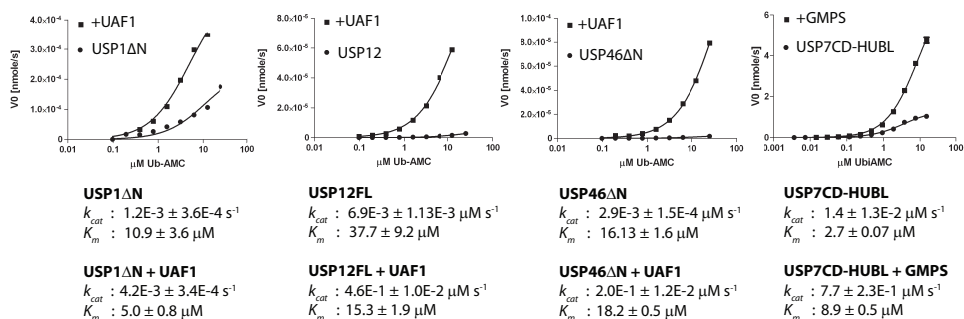*Figure and legend continue on next page*

H

Figure and legend continued from previous page.

Supplemental Figure S3. Related to Figure 4. Synthesis, LC-MS of FP reagents, exemplary raw data and Michaelis-Menten curves of USP4 and USP7. H. Michaelis-Menten analysis of USP4 hydrolysis of the FP reagents. Kinetic pararameters are in (D).

USP1ΔN
k_{cat} : 1.2E-3 ± 3.6E-4 s^{-1}
K_m : 10.9 ± 3.6 μM

USP12FL
k_{cat} : 6.9E-3 ± 1.13E-3 μM s^{-1}
K_m : 37.7 ± 9.2 μM

USP46ΔN
k_{cat} : 2.9E-3 ± 1.5E-4 μM s^{-1}
K_m : 16.13 ± 1.6 μM

USP7CD-HUBL
k_{cat} : 1.4 ± 1.3E-2 μM s^{-1}
K_m : 2.7 ± 0.07 μM

USP1ΔN + UAF1
k_{cat} : 4.2E-3 ± 3.4E-4 s^{-1}
K_m : 5.0 ± 0.8 μM

USP12FL + UAF1
k_{cat} : 4.6E-1 ± 1.0E-2 μM s^{-1}
K_m : 15.3 ± 1.9 μM

USP46ΔN + UAF1
k_{cat} : 2.0E-1 ± 1.2E-2 μM s^{-1}
K_m : 18.2 ± 0.5 μM

USP7CD-HUBL + GMPS
k_{cat} : 7.7 ± 2.3E-1 μM s^{-1}
K_m : 8.9 ± 0.5 μM

Supplemental Figure S4. Related to Figure 6. Curves of the Michaelis-Menten analysis of the UAF1 and GMPS modulation. The Michaelis-Menten curves for the different USPs obtained by determining the initial rates (V0) at 2-fold serial dilutions of UbAMC.

$\leftrightarrow$

Chapter 3

Ubiquitin Specific Protease 4 is inhibited by its Ubiquitin-like domain

Mark P A Luna-Vargas[1], Alex C Faesen[1], Willem J van Dijk[1], Michael Rape[2], Alexander Fish[1] and Titia K Sixma[1]

[1] Division of Biochemistry and Center for Biomedical Genetics, The Netherlands Cancer Institute, Plesmanlaan 121, 1066 CX Amsterdam, The Netherlands
[2] Department of Molecular and Cell Biology, University of California at Berkeley, Berkeley, California 94720, USA

Abstract

USP4 is a member of the ubiquitin-specific protease (USP) family of deubiquitinating enzymes that has a role in spliceosome regulation. Here, we show that the crystal structure of the minimal catalytic domain of USP4 has the conserved USP-like fold with its typical ubiquitin-binding site. A ubiquitin-like (Ubl) domain inserted into the catalytic domain has autoregulatory function. This Ubl domain can bind to the catalytic domain and compete with the ubiquitin substrate, partially inhibiting USP4 activity against different substrates. Interestingly, other USPs, such as USP39, could relieve this inhibition.

Introduction

Post-translational modification by the small, highly conserved ubiquitin (Ub) protein has an essential role in the regulation of many cellular processes in eukaryotes[1,2]. In this process, the carboxy-terminus of Ub forms an isopeptide with lysines on the target proteins, or on Ub itself, to form poly-Ub chains. The activity of the conjugating enzymes E1–E2–E3 is actively balanced through hydrolysis by deubiquitinating enzymes (DUBs)[1,3,4,5,6]. Deregulation of the ubiquitination pathway can lead to cancer and neurodegenerative diseases[7,8].

More than 100 putative DUBs are known so far, belonging to five subfamilies of isopeptidases. The Ub-specific protease (USP) family is the largest, with more than 60 members in the human genome[4,6,9]. USPs share a papain-like catalytic domain and crystal structures show a conserved catalytic core that undergoes conformational changes after Ub binding[10,11,12,13,14].

USPs are variable in size with modular domain architecture including, for example, TRAF-like, DUSP or Znf domains[4,6]. Sequence analysis predicted the presence of Ub-like (Ubl) domains in 17 different USPs[15]. Integrated Ubl domains are stretches of 45–80 amino acids that share the β-grasp fold of Ub, but often have poor sequence conservation among subfamilies[16,17]. The Ubl domains in the USP family are located amino-terminally, within or C-terminally to the catalytic domain. Structural studies of the N-terminal Ubl domain of USP14 confirmed the Ubl-fold (Protein Data Bank (PDB): 1WGG) and showed involvement in proteasome binding that promotes the DUB activity of USP14[18]. Similar to USP14, USP4 has a Ubl domain N-terminal of its catalytic domain, but it has an additional Ubl domain embedded in the catalytic domain.

USP4 was previously known as ubiquitous nuclear protein (UNP)[19]. Identified as a proto-oncogene related to Tre 2/Tre 17 (USP6), USP4 shows a consistently elevated gene expression level in small cell tumours and lung adenocarcinomas, suggesting that it may have a possible causative role in neoplasia[20]. Besides possible roles in Wnt signalling[21] and recruitment to the A2A receptor[22], USP4 is recruited to the spliceosome by complex formation with Sart3[23]. Here, it preferentially deubiquitinates K63-linked chains on the U4 component Prp3. Another component of the spliceosome complex is the catalytically inactive USP39[23,24], which controls the messenger RNA levels of Aurora B[25].

Here, we report on the crystal structure of the catalytic domain of USP4 without the internal Ubl domain, and show how this Ubl domain acts as an autoregulatory domain that partially inhibits catalytic activity by competitive inhibition.

Results

Identification of USP4–D1D2

To gain insight into the structure and function of USP4, we expressed and purified the USP4 catalytic domain (amino acids 296–954, Figure 1A) in *Escherichia coli*. To improve the chances for crystallization, we used limited proteolysis. After treatment with thermolysin, two fragments (domain 1 (D1) and 2 (D2)) were obtained, which copurified on size exclusion chromatography and together retained DUB activity (supplementary Figure S1A,B). We

identified the composition of D1 and D2 using mass spectrometry and N-terminal sequencing (supplementary Figure S1C) and compared them against a multi-sequence alignment of USP family members. This showed that the protease treatment removed an insertion between Leu 481 and Leu 766 (supplementary Figure S2), yielding an enzymatically active complex of two fragments: USP4–D1D2

Structure of the USP4–D1D2 catalytic domain

We crystallized and determined the USP4–D1D2 structure by molecular replacement using the USP8 catalytic domain (PDB: 2GFO) as the search molecule, and refined it to 2.4 Å resolution with an R/Rfree of 0.178/0.21 and good geometry (Figure 1B; supplementary Table S1). There are six molecules of USP4–D1D2 per asymmetric unit, with a pairwise root-mean-square deviation of approximately 0.7 Å over 344 residues using the PISA program[26].
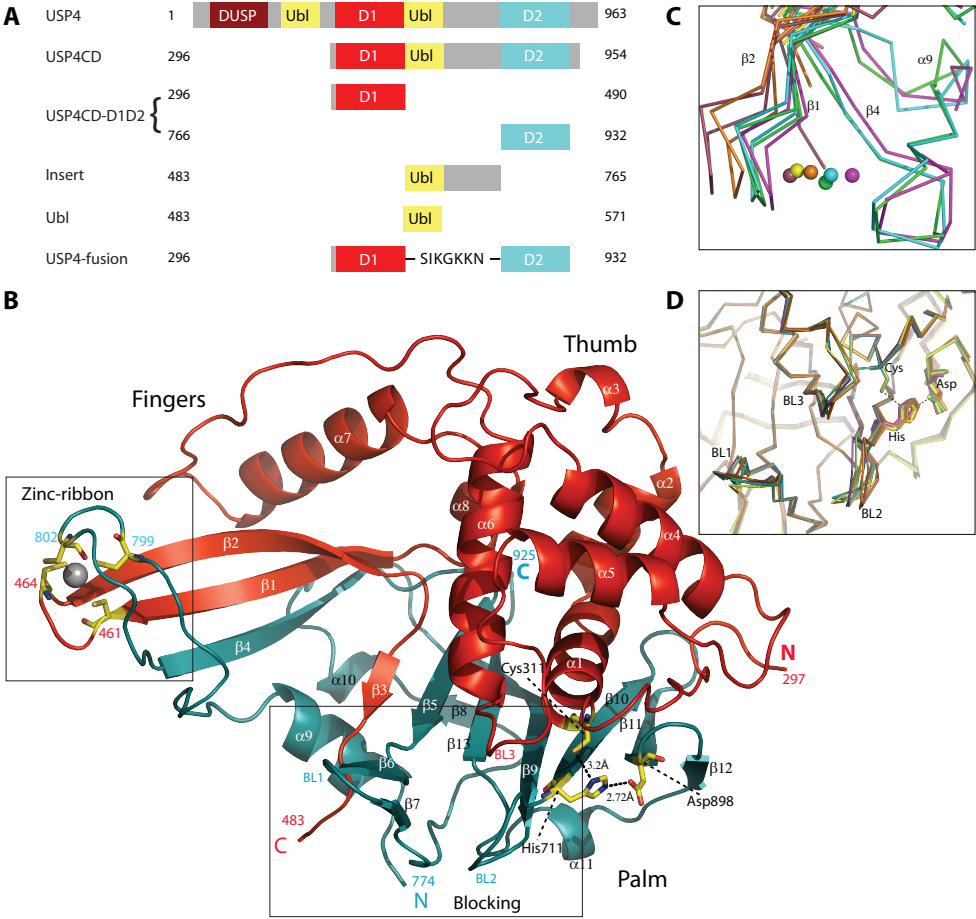

Figure 1: The catalytic domain of USP4–D1D2. A. Domain architecture of USP4 and fragments expressed. **B.** Crystal structure of USP4–D1D2 catalytic domain in cartoon representation, with secondary structure elements labelled. D1 and D2 are coloured as in (A). Catalytic triad and the cysteines (yellow) coordinating zinc (grey sphere) are shown in stick representation. **C,D.** Superposition of six non-crystallographic symmetry-related copies in the asymmetric unit showing flexibility in (C) the zinc-finger ribbon and (D) blocking loops, BL1–3.

Similar to crystal structures of other USPs, the catalytic domain of USP4–D1D2 resembles an extended right hand comprising three domains: Fingers, Thumb and Palm (Figure 1B; supplementary Figure S3). The D1 fragment contains the Thumb domain and part of the Fingers domain with the Cys box (amino acids 303–320) and QQD box (amino acids 390–403) of the active site, whereas the D2 fragment completes the active site with the His box (amino acids 864–885, 894–903, 915–922) and makes the remaining part of the Fingers and the Palm9) (supplementary Figure S2). Like other USP structures[11,12,13,14,18], except USP7[10], the catalytic triad is in a catalytically competent configuration, wherein His 711-ND1 is 3.2 Å away from Cys 311-SG and His 711-ND2 is hydrogen bonding with Asp 898-OD1 (2.7 Å; Figure 1B).

The zinc-finger ribbon observed in USP2 and USP8 is present in USP4 (Figure 1B,C). The Zn^{2+} ion brings together the D1 and D2 domains, tetrahedrally coordinated by cysteines on anti-parallel β-strands β1 and β2 in D1, and β4 in D2. This zinc-finger ribbon in the Fingers domain seems to be in the contracted 'closed-hand' configuration seen in USP8 that blocks access of Ub to its binding site[11]. A similar role was assigned to the two Ub-binding surface loops (BL1 and BL2) in USP14[18] that block the active site, but relocate after Ub binding. In USP4, both loops (Figure 1D), as well as a third blocking loop (BL3) that hinders access of the C-terminal tail of Ub to the binding pocket, are observed.

Superposition of the six non-crystallographic symmetry-related molecules of USP4–D1D2 shows that both the zinc-finger ribbon and the three blocking loops show flexibility (maximal Cα displacement 4 Å; Figure 1C,D), which is in agreement with their role in activation[10,11].

The insert inhibits deubiquitinating activity
We compared the catalytic activity of the USP4 catalytic domain with and without the large insert, by using *in vitro* deubiquitinating assays. In these assays we followed the hydrolysis of K63- and K48-linked di-Ub into mono-Ub (Figure 2A,B; supplementary Figure S4A,B). We observed that K63 di-Ub is more efficiently

degraded than K48, in agreement with the role of USP4 in splicing23. Interestingly, quantification (Figure 2D; supplementary Figure S4D) shows that USP4–D1D2 without insert is more efficient at degrading both di-Ubs than the complete catalytic domain. When D1 and D2 are fused through a short linker, as found in USP7 (supplementary Figure S2), their activity is similar to that of USP4–D1D2, showing that the cause of the activation is the lack of insert and not the chain break (Figure 2C; supplementary Figure S4C).

In Ub-7-amido-4-methylcoumarin (Ub-AMC) assays the intact USP4 catalytic domain is also less active than USP4–D1D2 or the fusion protein. As only AMC is cleaved off, the inhibition is not dependent on the protein target. When analysed by Michaelis–Menten kinetic analysis (Figure 2E) the Vmax values were similar, but the K_M for the intact catalytic domain (13.5 µM) was weaker than that for USP4–D1D2 (0.20 µM), leading to approximately 90-fold lower catalytic efficiency overall (k_{cat}/K_M) for USP4CD than for USP4–D1D2.

As the insert seems to inhibit the DUB activity of USP4, we tested whether it could do so *in trans*. We expressed and purified the insert (amino acids 483–765) and added it in increasing amounts to USP4–D1D2 in the Ub-AMC assay (supplementary Figure S5A). We observed that the insert slows deubiquitination by USP4–D1D2. To investigate whether this reduction in DUB activity is due to molecular crowding, we repeated the *in trans* inhibition assay with USP4–D1D2 in the presence of either SUMO or BSA (supplementary Figure S6). Neither of these reduced DUB activity, confirming that the insert is intrinsically able to inhibit the catalytic activity of USP4.

Competitive inhibition of the USP4 insert
We tested whether USP4–D1D2 would directly interact with the insert. In a surface plasmon resonance (SPR; Figure 3B) experiment, we observed binding of USP4–D1D2 to the insert, with a Kd of 1.32 µM after equilibrium fitting. This affinity closely resembled the affinity of USP4–D1D2 for Ub itself (Kd of 1.39 µM; Figure 3A).

Therefore, we tested whether the insert could compete with Ub for binding to USP4–D1D2, experiment we flowed USP4–D1D2 over a glutathione S-transferase (GST)-tagged insert in the presence of increasing amounts of Ub (Figure 3D). We observed decreasing binding of USP4–D1D2 to the GST-insert as the Ub concentration increased. The data could be fitted with a one-site competition binding model with a Ki of 1.4 μM, showing that the USP4 insert competes with Ub for binding to USP4–D1D2.

Interestingly, the Kd of intact USP4CD for Ub is only fourfold less, compared to USP4–D1D2 in an isothermal titration calorimetry (ITC) experiment (Figure 3E). Although the exact Kds are slightly tighter in the ITC experiment, qualitative analysis of SPR experiments agrees with this assessment. Non-specific binding at high concentrations precluded detailed fitting of these data (supplementary Figure S7), but the curves show that binding of Ub to USP4CD has a slower off-rate than that of Ub to USP4–D1D2, and together with the Kd value also suggest that it has a slower on-rate. As the K_M is dependent on Kd as well as the binding rate, the combination of slow kinetics and slightly lower affinity explains the differences in K_M values. Apparently, the insert prevents rapid binding as well as rapid release of the Ub substrate, allowing competitive binding.

3

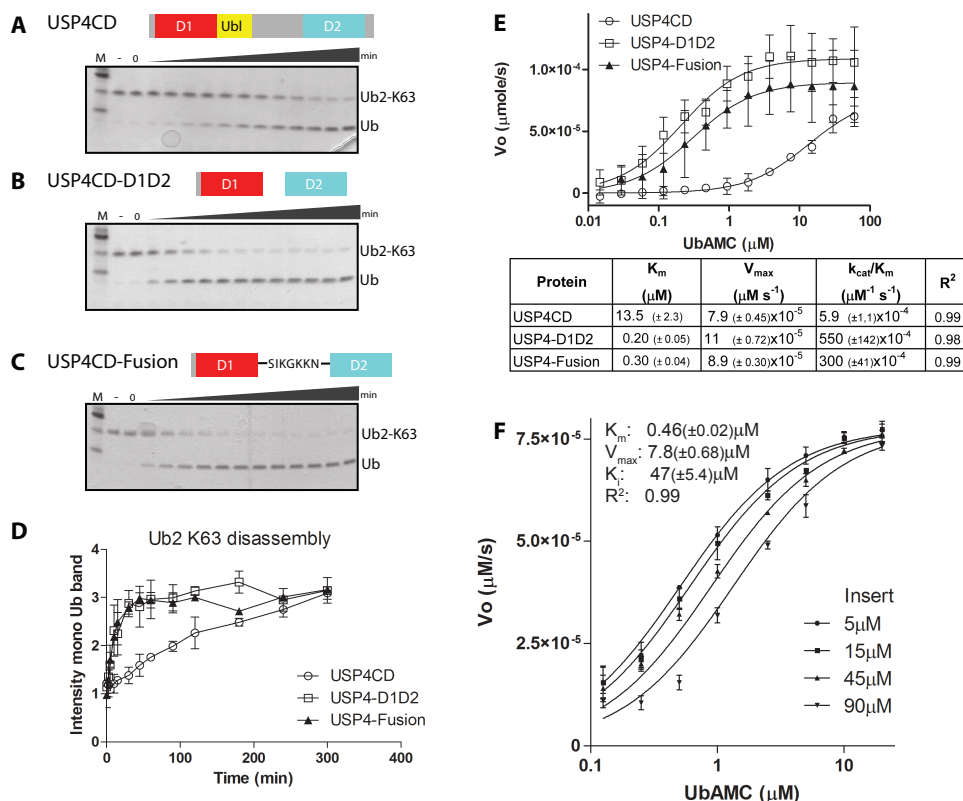| Protein	K_m (μM)	V_{max} (μM s^{-1})	k_{cat}/K_m (μM^{-1} s^{-1})	R^2
USP4CD	13.5 (± 2.3)	7.9 (± 0.45)x10^{-5}	5.9 (±1.1)x10^{-4}	0.99
USP4-D1D2	0.20 (± 0.05)	11 (± 0.72)x10^{-5}	550 (±142)x10^{-4}	0.98
USP4-Fusion	0.30 (± 0.04)	8.9 (± 0.30)x10^{-5}	300 (±41)x10^{-4}	0.99

Figure 2: Insert inhibits the DUB activity of USP4CD. A–C. The full-length USP4 catalytic domain (A) is much less active than (B) USP4–D1D2 or (C) USP4 fusion in deubiquitinating K63 di-Ub (Coomassie-stained SDS–PAGE gels). **D.** Quantification of mono-Ub in K63 di-Ub cleavage assays. The intensity of the mono-Ub band is plotted against time. **E.** The inhibitory effect of the insert is observed in a Ub-AMC assay. On comparing K_{cat}/K_m between USP4CD and D1D2, we observed a 90 times lower enzyme efficiency for the insert containing USP4CD. **F.** Inhibition of USP4–D1D2 in trans in Ub-AMC assays at different Ubl-insert concentrations (5, 15, 45 and 90 μM) can be jointly fit as a competitive inhibitor.

Finally we analysed whether the enzymatic activity is competitively inhibited by the addition of the insert *in trans*. We tested the enzymatic activity with varying inhibitor concentrations against a range of substrate concentrations (Figure 2F), and fitted the data against different inhibition models[27]. We found that the data were best explained by competitive inhibition with Ki=47 µM.

Although this value is lower than expected on the basis of the binding data alone, it explains why the USP4CD is not completely inhibited in the continuous presence of the insert. It seems

that additional conformational changes take place. One possibility is that the enzyme reaches a state after turnover that has lower affinity for the insert, and is therefore not as effectively inhibited.

The Ubl domain is sufficient for inhibition.
The presence of a Ubl domain within the insert was predicted (supplementary Figure S2)[15]. To test whether the Ubl domain is sufficient for binding to the USP4 catalytic domain, we performed the SPR experiment with the purified Ubl domain (amino acids 483–571, Figure 1A) and found a K_d of 1.36 µM towards USP4–D1D2,
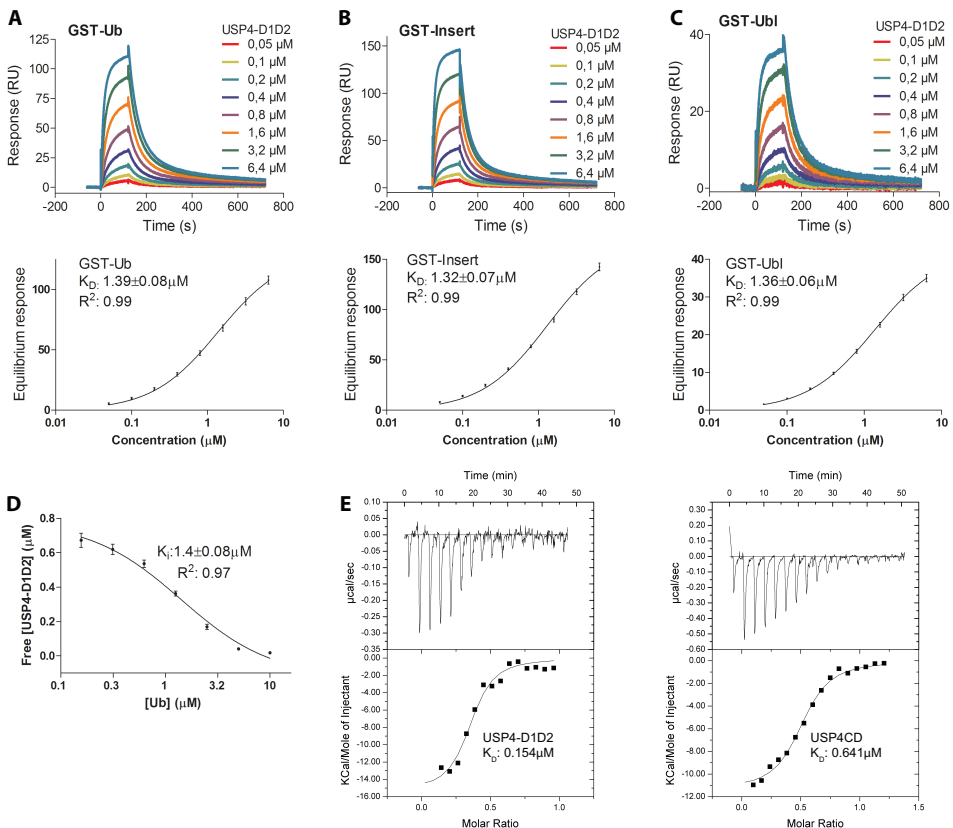

Figure 3: Ubiquitin competes with the insert or Ubl-domain for binding to USP4–D1D2. A–C. Interaction of Ub and the insert fragments with USP4–D1D2 was studied by SPR experiments. Top: (A) GST-tagged Ub, (B) GST-insert and (C) GST-Ubl domain were immobilized on anti-GST antibodies coupled to a CM5 Biacore chip and USP4–D1D2 was flowed over the chip at different concentrations. Bottom: Langmuir binding curves. **D.** Competition experiment with immobilized GST insert on USP4–D1D2 with varying concentrations of Ub. A one-site competition binding model was fitted (Ki=1.4 µM). **E.** The interaction of Ub with USP4–D1D2 (left) and with full-length USP4CD (right) were studied by ITC. Thermodynamic values for USP4–D1D2 (ΔH=−14.3 kcal/mol and ΔS=−16.9 cal/mol/deg), for USP4CD (ΔH=−11.4 kcal/mol and ΔS=−10.0 cal/mol/deg).

which is similar to that for the complete insert (Figure 3C). This suggests that the Ubl domain is the functional part of the insert.

To test whether the Ubl domain can inhibit the DUB activity of USP4, we repeated the *in trans* inhibition assay with USP4–D1D2 in the presence of increasing amounts of the Ubl domain (supplementary Figure S6) and found that it provides inhibition equal to the insert. We therefore conclude that the Ubl domain is sufficient to inhibit the DUB activity of USP4, through competitive inhibition of Ub binding.

Regulation by other USP enzymes.
As the Ubl domain seems to bind in the substrate Ub-binding site of USP4, we wondered whether other USP enzymes could also bind to the Ubl domain. We tested whether our Ubl domain containing insert could bind to the catalytic domain of USP39 and USP8, and found similarly high affinities as for USP4CD (Figure 4B,C).

Then, we analysed whether these DUBs could modulate USP4CD activity. We repeated the *in trans* Ub-AMC assay with USP4CD in the presence of the intrinsically inactive USP39CD or an inactive variant of the USP8 catalytic domain, USP8CD-mut (Figure 4A). For both USPs we observe a modest activation of USP4CD that was dependent on the presence of the Ubl-containing insert, as it does not increase the

DUB activity of USP4–D1D2 in this manner.

Apparently, other USP enzymes can regulate USP4 activity by competing for binding to the Ubl domain. This effect could be larger when the USPs have further interactions. As USP39 forms a stable complex with USP4 in cells[23,24], it is a prime candidate for an activating role *in vivo*.

Discussion

We show that the predicted Ubl domain within a large insert embedded in the USP4 catalytic domain partially inhibits DUB activity by competing with Ub for binding. Superposition of the crystal structure of USP4–D1D2 and any Ubl domain on USP7 in complex with Ub-aldehyde (PDB: 1NBF), respectively, shows that the Ubl domain would fit like a Ub molecule into the hand of USP4–D1D2 (Figure 5A), only requiring movements in the blocking loops and the zinc-finger ribbon. Hence, we propose a model in which the Ubl domain partially inhibits DUB activity through competitive inhibition by binding into the hand of USP4 and thus preventing Ub substrate binding (Figure 5B)

This function of an integrated Ubl domain is relatively new. The Ubl domains in proteasomal shuttle factors Rad23 and Dsk2, as well as in
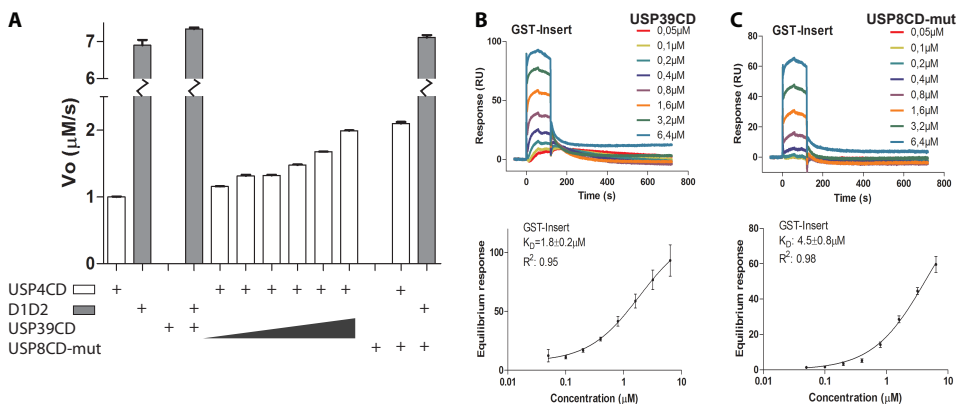
Figure 4: USP39CD binds to the Ubl domain and increases the deubiquitinating-enzyme activity of USP4CD. A. Other USPs activate the DUB activity of USP4CD in trans in a Ub-AMC assay (USP39CD: 10, 20, 50, 100, 500 and 1,000 nM; USP8CD-mut: 1,000 nM). **B.** USP39 and **C.** USP8-mut bind to Ubl insert, in an SPR assay analogous to Figure 2B.

Parkin and USP14, function in recruitment of ubiquitinated proteins to the proteasome[18,28]. Other Ubl domains regulate the enzymatic activities of immune-response inducible kinases such as IKKβ (a subunit of IκB kinase complex)[29], or as PB1 (Phox and Bem1) domains, have a role in the regulation of signal transduction in proteins such as P62, MEK5 and protein kinaseC[30,31]. However, all these Ubl-domain families have low sequence similarities, indicating that their functions are probably distinct between subfamilies.

The activity of USPs is regulated through an inactive conformation of the catalytic triad, as in USP7, or through a series of blocking loops or a blocking zinc-finger ribbon. USP4 seems to combine the blocking loops and zinc-finger ribbon with a further regulation through the Ubl domain.

Whether Ubl domains provide a common regulation mechanism for the DUB activity of USPs is an interesting question for future research. A second Ubl domain is found within USP4, at its N-terminus. A recent crystal structure (PDB: 3JYU, amino acids 139–226) shows that this Ubl domain interacts extensively with the adjacent DUSP (domain in USP) domain (amino acids 27–125). This region of the protein is primarily important for interaction with Sart3[23] and hence might not have this function.

However, USP4 is not the only DUB with a Ubl fold within its catalytic domain. Sequence analysis identified an integrated Ubl fold within the catalytic domain of USPs 6, 11, 15, 19, 31, 32 and 43, embedded in a larger insert, like in USP4[15]. In particular, USP11 and USP15 are closely related to USP4. This subgroup of USPs probably also regulates DUB activity through its Ubl domain.

The way in which Ubl-domain inhibition itself is regulated is an exciting question. One could imagine that further post-translational modification by, for example, phosphorylation or acetylation would enable the release of the
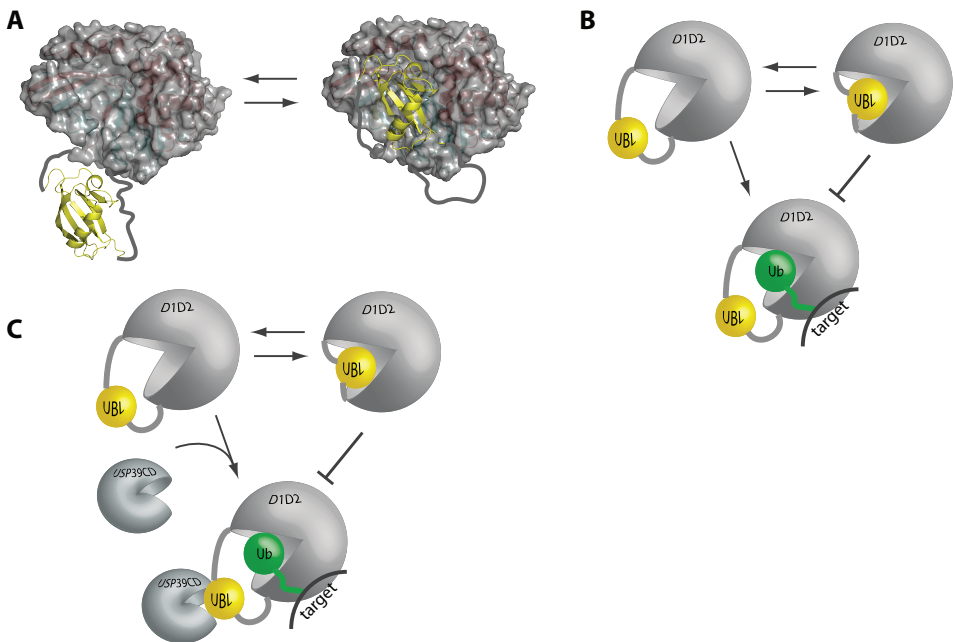

Figure 5: Model for Ubl domain inhibition on USP4. A. Structural model in which interaction of the Ubl domain with USP4CD inhibits the binding of Ub. **B.** Schematic model of the auto-inhibitory role of the Ubl domain in USP4. **C.** Other USP enzymes, such as USP39, may relieve the inhibition by binding to the Ubl domain.

full activity of the DUB enzyme. In addition, we have shown that binding partners such as USP39, can activate USP4 function by binding to the Ubl domain (Figure 5C). Although the activation is modest (Figure 4A), this could be increased by further interactions, as observed in the spliceosome complex.

Regardless of the mechanisms that regulate USP4 activation, it is clear that this type of internal regulation by a Ubl domain allows the creation of an extremely fast response element to external signals.

Experimental procedures

Plasmids and cloning
cDNA for human USP4 and USP8 was a gift from Hidde Ploegh and cDNA for USP39 was a gift from R. Medema. USP4CD (aa 296-954) and the D1 fragment (aa 296-490) of human USP4, USP39CD (aa 219-565) and USP8CD (aa 771-1118) were cloned using ligation independent cloning into pET-46 Ek/LIC vector (Novagen). The D2 fragment (aa 766-932) of USP4 was cloned into the pET-NKI b/3C32. The fused USP4-D1D2 was created by inserting aa 353-359 of USP7 (SIKGKNN) between residues Leu479 and Leu777. The USP4 insert (aa 483-765), Ubl domain (aa 483-571) and Ub were cloned into pGEX-6P-1 (GE Healthcare). The USP8CD mutant was generated by site-directed mutagenesis of the catalytic cysteine (C786A).

Protein preparation
Purification of E2-25K[33], Ubc13/Mms2[34] was as described. GST-tagged proteins were overexpressed in Escherichia coli strain Rosetta2(DE3)-T1R using IPTG (200μM) induction overnight at 15°C. Cells were lysed by microfluidizer into buffer A (50mM Hepes pH7.5, 150mM NaCl, 5mM β-mercaptoethanol, 1mM PMSF). The fusion protein was purified using glutathione sepharose resin, eluted, followed by removal of the GST-tag with 3C protease and size-exclusion using HiLoad 16/60 Superdex 200 (GE Healthcare). Peak fractions were concentrated to 10mg/ml in 25mM Hepes (pH7.5), 200mM NaCl and 5mM β- mercaptoethanol. D1 and D2 co-expression, other USP4 variants, USP39CD and USP8CD-

mut were overexpressed as above, with 200μM ZnCl2 during induction and lysed in buffer A supplemented with 1mM ZnCl2 and 10mM Imidazole. These His-tagged proteins were purified by a Co2+-affinity (Talon resin) step. Upon Imidazole elution the Histag was removed by TEV cleavage at 4°C overnight during dialysis in buffer B (25mM Hepes pH7.5, 150mM NaCl, 5mM β-mercaptoethanol). This was followed by POROS Q affinity chromatography and size-exclusion using HiLoad 16/60 Superdex 200 (GE Healthcare), where the protein eluted as a monomer. The peak fractions were concentrated to 5mg/ml in buffer B.

Limited Proteolysis and protein identification
Purified USP4CD (9mg/ml) was incubated with Thermolysin (0.8units) for 1,5hr at room temperature and subjected to size exclusion chromatography using Superdex75 16/60. Fractions containing USP4-D1 and –D2 were subjected to LC-MS analysis. LC-MS measurements were performed on a system equipped with a Waters 2795 Seperation Module (Alliance HT), Waters 2996 Photodiode Array Detector (190-750nm), Waters Alltime C18 (2.1x100mm, 3μm), Waters Symmetry300TM C4 (2.1x100mm, 3.5μm) and LCTTM Orthogonal Acceleration Time of Flight Mass Spectrometer. Data processing was performed using Waters MassLynx Mass Spectrometry Software 4.1 (deconvolution with Maxent 1 function). N-terminal sequencing of USP4-D1 and –D2 were performed by AltaBioscience in Birmingham, England.

Crystallization and structure determination of the USP4-D1D2
Crystals were grown overnight in sitting-drops mixing 200nl USP4-D1D2 (~3.5mg/ml) with 200 nl 100mM Bis-Tris propane [pH8.5], 25mM Na_2SO_4 and 18% PEG3350 (w/v) at 19°C. Crystals were cryoprotected in mother liquor with 25% ethyleneglycol. The crystals belong to the space group $P2_12_12_1$ with six molecules per asymmetric unit (supplementary Table S1). Diffraction data were collected at the ESRF (Grenoble, France) beamline ID14-2 and processed with MOSFLM[35] and SCALA[36]. The structure was solved by molecular replacement with PHASER[37] using

USP8CD (PDB: 2GFO) as search model. Iterative rebuilding and refinement were done with Coot[38] and PHENIX[39] and BUSTER[40]. The structure was validated with MOLPROBITY[41] and WHAT-CHECK[42] and structure figures were generated using PYMOL (Delano, 2002). Cysteine residue 311 in all chains have been chemically modified by β-mercaptoethanol.

Ub-AMC assays.

UbAMC assays were done in 50mM Hepes [pH7.5], 100mM NaCl, 5mM DTT, 0.05% Tween-20 and 1mM EDTA and reaction progress was monitored with a Fluostar Optima plate-reader (BMG Tech) by the increase in fluorescence emission at 460nm (λex = 355nm) generated by Ub-AMC cleavage. Quantitative activity (triplicate) and *in trans* inhibition (duplicate) assays or USP modulation assays (triplicate) were performed using Ub-AMC with 10 nM enzyme in 30 μl reaction volume in 384-well plates and preincubated for 15 min at 21° C, for inhibition assays with Ubl insert and with other DUBs for modulation assays. Initial velocities against Ub-AMC concentration were computed to derive steady-state kinetic parameters using GraphPad Prism5 (GraphPad Software Inc.). Non-linear fitting of four inhibition models was compared in GraphPad.

Di-Ub assays.

Di-Ub assays were performed in similar buffer as in UbAMC assays at 37°C in 75μl reaction volume. Aliquots (5μl) were stopped by addition of 4x SDS-sample loading buffer and subjected to SDS-PAGE analysis on a 4- 12% coomassie stained gel (Invitrogen). K48 and K63 di-Ub substrates were produced and purified as described[43]. 75 nM enzyme was incubated with 3 μM di-Ub, subjected to SDS–polyacrylamide gel electrophoresis and image analysis, and quantitation was performed in duplicate with TINA 2.09 (Raytest Co.).

SPR and ITC.

SPR was performed on a Biacore T-100, with GST-Ub, GST-insert and GST-Ubl domain immobilized on anti-GST antibodies coupled to a CM5 chip. Quantitative binding analysis was done in duplicate at 25°C on a Biacore T-100 instrument (GE Healthcare). GST fused Ub, insert and Ubl domain were immobilized on α-GST antibodies lysine-coupled to a CM5 chip. USPs were injected in varying concentrations over the sensor chip at 30μl/min with a 120s association phase followed by a 10min dissociation phase. For the binding inhibition assay Ub was added in varying concentrations to USP4-D1D2. Standard double referencing data subtraction methods were used before and equilibrium curve fitting with BiaEvaluation (GE Healthcare) and GraphPad software (GraphPad Software Inc). Data (duplicate) were processed using BiaEvaluation (GE Healthcare) and GraphPad Prism5.

Isothermal titration calorimetry (ITC) experiments were performed with the VP-ITC Micro Calorimeter (MicroCal, Inc.) at 25°C. Stock solutions of USP4CD, USP4-D1D2 and Ub were prepared by dialysis of the purified proteins against a buffer containing 25mM Hepes pH8.0, 150mM NaCl and 5mM β-mercaptoethanol at 4°C and were degassed before use. The sample cell (1.8ml) contained USP4-D1D2 (10μM) or USP4CD (20μM) which was titrated with 100μM Ub or 200μM Ub respectively using 16 injections. The injections after saturation were used to determine the background signal. Corrected data were analyzed using software supplied by the ITC manufacturer to calculate the dissociation constant Kd and fitted with a one to one binding model.

Accession numbers

Coordinates and structure factors were deposited in the Protein Data Bank under identification code 2Y6E.

Acknowledgements

References

1. Pickart, C.M. Back to the future with ubiquitin. Cell 116, 181-90 (2004).
2. Hochstrasser, M. Origin and function of ubiquitin-like proteins. Nature 458, 422-9 (2009).
3. Amerik, A.Y. & Hochstrasser, M. Mechanism and function of deubiquitinating enzymes. Biochim Biophys Acta 1695, 189-207 (2004).
4. Nijman, S.M. et al. A genomic and functional inventory of deubiquitinating enzymes. Cell 123, 773-86 (2005).
5. Deshaies, R.J. & Joazeiro, C.A. RING domain E3 ubiquitin ligases. Annu Rev Biochem 78, 399-434 (2009).
6. Komander, D., Clague, M.J. & Urbe, S. Breaking the chains: structure and function of the deubiquitinases. Nat Rev Mol Cell Biol 10, 550-63 (2009).
7. Hoeller, D. & Dikic, I. Targeting the ubiquitin system in cancer therapy. Nature 458, 438-44 (2009).
8. Lopez-Otin, C. & Hunter, T. The regulatory crosstalk between kinases and proteases in cancer. Nat Rev Cancer 10, 278-92.
9. Quesada, V. et al. Cloning and enzymatic analysis of 22 novel human ubiquitin-specific proteases. Biochem Biophys Res Commun 314, 54-62 (2004).
10. Hu, M. et al. Crystal structure of a UBP-family deubiquitinating enzyme in isolation and in complex with ubiquitin aldehyde. Cell 111, 1041-54 (2002).
11. Avvakumov, G.V. et al. Amino-terminal dimerization, NRDP1-rhodanese interaction, and inhibited catalytic domain conformation of the ubiquitin-specific protease 8 (USP8). J Biol Chem 281, 38061-70 (2006).
12. Renatus, M. et al. Structural basis of ubiquitin recognition by the deubiquitinating protease USP2. Structure 14, 1293-302 (2006).
13. Kohler, A., Zimmerman, E., Schneider, M., Hurt, E. & Zheng, N. Structural basis for assembly and activation of the heterotetrameric SAGA histone H2B deubiquitinase module. Cell 141, 606-17 (2010).
14. Samara, N.L. et al. Structural insights into the assembly and function of the SAGA deubiquitinating module. Science 328, 1025-9 (2010).
15. Zhu, X., Menard, R. & Sulea, T. High incidence of ubiquitin-like domains in human ubiquitin-specific proteases. Proteins 69, 1-7 (2007).
16. Kiel, C. & Serrano, L. The ubiquitin domain superfold: structure-based sequence alignments and characterization of binding epitopes. J Mol Biol 355, 821-44 (2006).
17. Burroughs, A.M., Balaji, S., Iyer, L.M. & Aravind, L. Small but versatile: the extraordinary functional and structural diversity of the beta-grasp fold. Biol Direct 2, 18 (2007).
18. Hu, M. et al. Structure and mechanisms of the proteasome-associated deubiquitinating enzyme USP14. Embo J 24, 3747-56 (2005).
19. Gupta, K., Copeland, N.G., Gilbert, D.J., Jenkins, N.A. & Gray, D.A. Unp, a mouse gene related to the tre oncogene. Oncogene 8, 2307-10 (1993).
20. Gray, D.A. et al. Elevated expression of Unph, a proto-oncogene at 3p21.3, in human lung tumors. Oncogene 10, 2179-83 (1995).
21. Zhao, B., Schlesiger, C., Masucci, M.G. & Lindsten, K. The ubiquitin specific protease 4 (USP4) is a new player in the Wnt signalling pathway. J Cell Mol Med 13, 1886-95 (2009).
22. Milojevic, T. et al. The ubiquitin-specific protease Usp4 regulates the cell surface level of the A2A receptor. Mol Pharmacol 69, 1083-94 (2006).
23. Song, E.J. et al. The Prp19 complex and the Usp4Sart3 deubiquitinating enzyme control reversible ubiquitination at the spliceosome. Genes Dev 24, 1434-47 (2010).
24. Sowa, M.E., Bennett, E.J., Gygi, S.P. & Harper, J.W. Defining the human deubiquitinating enzyme interaction landscape. Cell 138, 389-403 (2009).
25. van Leuken, R.J., Luna-Vargas, M.P., Sixma, T.K., Wolthuis, R.M. & Medema, R.H. Usp39 is

essential for mitotic spindle checkpoint integrity and controls mRNA-levels of aurora B. Cell Cycle 7, 2710-9 (2008).

26. Krissinel, E. & Henrick, K. Secondary-structure matching (SSM), a new tool for fast protein structure alignment in three dimensions. Acta Crystallogr D Biol Crystallogr 60, 2256-68 (2004).

27. Copeland, R.A. Enzymes: A Practical Introduction to Structure, Mechanism and Data Analysis. pp 270–290, UK: Wiley (2000).

28. Sakata, E. et al. Parkin binds the Rpn10 subunit of 26S proteasomes through its ubiquitin-like domain. EMBO Rep 4, 301-6 (2003).

29. May, M.J., Larsen, S.E., Shim, J.H., Madge, L.A. & Ghosh, S. A novel ubiquitin-like domain in IkappaB kinase beta is required for functional activity of the kinase. J Biol Chem 279, 45528-39 (2004).

30. Terasawa, H. et al. Structure and ligand recognition of the PB1 domain: a novel protein module binding to the PC motif. Embo J 20, 3947-56 (2001).

31. Sumimoto, H., Kamakura, S. & Ito, T. Structure and function of the PB1 domain, a protein interaction module conserved in animals, fungi, amoebas, and plants. Sci STKE 2007, re6 (2007).

32. Luna-Vargas, M.P. et al. Enabling high-throughput ligation-independent cloning and protein expression for the family of ubiquitin specific proteases. J Struct Biol (2011).

33. Pichler, A. et al. SUMO modification of the ubiquitin-conjugating enzyme E2-25K. Nat Struct Mol Biol 12, 264-9 (2005).

34. Marteijn, J.A. et al. The ubiquitin ligase Triad1 inhibits myelopoiesis through UbcH7 and Ubc13 interacting domains. Leukemia 23, 1480-9 (2009).

35. Leslie, A.G. The integration of macromolecular diffraction data. Acta Crystallogr D Biol Crystallogr 62, 48-57 (2006).

36. Evans, P. Scaling and assessment of data quality. Acta Crystallogr D Biol Crystallogr 62, 72-82 (2006).

37. McCoy, A.J. Solving structures of protein complexes by molecular replacement with Phaser. Acta Crystallogr D Biol Crystallogr 63, 32-41 (2007).

38. Emsley, P. & Cowtan, K. Coot: model-building tools for molecular graphics. Acta Crystallogr D Biol Crystallogr 60, 2126-32 (2004).

39. Terwilliger, T.C. et al. Iterative model building, structure refinement and density modification with the PHENIX AutoBuild wizard. Acta Crystallogr D Biol Crystallogr 64, 61-9 (2008).

40. Blanc, E. et al. Refinement of severely incomplete structures with maximum likelihood in BUSTER-TNT. Acta Crystallogr D Biol Crystallogr 60, 2210-21 (2004).

41. Davis, I.W. et al. MolProbity: all-atom contacts and structure validation for proteins and nucleic acids. Nucleic Acids Res 35, W375-83 (2007).

42. Hooft, R.W., Vriend, G., Sander, C. & Abola, E.E. Errors in protein structures. Nature 381, 272 (1996).

43. Raasi, S. & Pickart, C.M. Ubiquitin chain synthesis. Methods Mol Biol 301, 47-55 (2005).

Table of contents Supplementary information

3

Data collection statistics	Native
Wavelength (Å)	0.993
Space group	$P2_12_12_1$
Unit cell (Å)	110.5, 151.0, 178.7
Molecules per asymmetric unit	6
Resolution (Å)[a]	47.0 - 2.4 (2.53 - 2.4)
R_{merge} (%)	8.8 (66.1)
$<I/\sigma(I)>$	11.0 (1.1)
Completeness (%)	94.9 (74.0)
Redundancy	3.4 (2.4)
Refinement	
R_{work}/R_{free} (%)	17.5/21.3
Number of reflections	111078
Number of protein atoms	15775
Number of zinc ions	6
Number of waters	867
RMSD from ideal geometry	
Bond lengths (Å)	0.009
Bond angles (°)	1.01
Ramachandran statistic[b] (prefered/allowed/outliers)	1849 / 66 / 2

[a] Numbers in parentheses are for the highest-resolution shell

[b] Calculated using Molprobity

Supplemental Table S1. Data collection and refinement statistics.

Supplemental Figure S1. Identification of USP4-D1D2. A Limited proteolysis analysis of thermolysin cleavage on USP4CD at 37°C. Samples at different time-points were taken and analyzed on a SDS-PAGE gel. **B** Proteolytic sample of USP4CD was subjected to a size exclusion chromatography and fraction samples were analyzed on a SDSPAGE gel. **C** Mass Spectrometry analysis and N-terminal sequencing determined the identity of the two fragments, D1 and D2.

Supplemental Figure S2. Structure based multiple sequence alignment. Secondary structure elements are colored and labeled according to structure of USP4-D1D2 in Figure 1. The internal Ubl is depicted as a yellow bar and the two black arrows indicate where the protease thermolysin cleaved in the catalytic domain of USP4. The catalytic triad residues are indicated with an asterisk. The four black triangles indicate the positions of the Cys residues coordinating the zinc ion.

USP4-D1D2 [2Y6E]

Ubp8 [3MM9]

CYLD [2VHF]

USP21 [3I3T]

USP2 [2HD5]

USP8 [2GFO]

USP14 [2AYO]

USP7 [1NB8]

Supplemental Figure S3. Overview and superposition of USP catalytic domain structures with USP4-D1D2. Comparison between catalytic domains depicted in cartoon representation of USP4-D1D2 (red-cyan), Ubp8 (brown, PDB: 3MM9), CYLD (orange, PDB: 2VHF), USP21 (marine blue, PDB: 3I3T), USP2 (yellow, PDB: 2HD5), USP8 (purple, PDB:2GFO), USP14 (green, PDB: 2AYO) and USP7 (light pink, PDB:1NB8). The structures depicted in ribbon representation were superposed in Coot (RMSD of 2.1Å over 323 residues).

A USP4CD

B USP4CD-D1D2

C USP4CD-Fusion

D
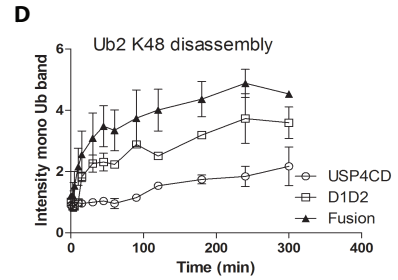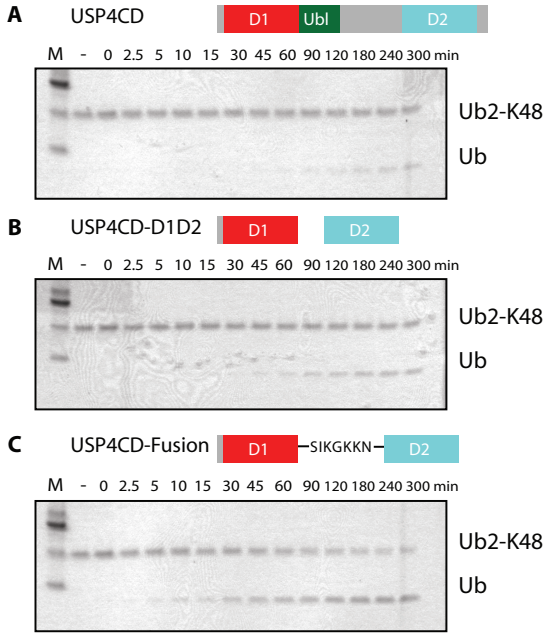
Supplemental Figure S4. Deubiquitinating assay with K48 di-Ub as substrate A-C The full-length USP4 catalytic domain (A) is much less active than USP4-D1D2 (B) or USP4-fusion (C) in a deubiquitinating assay using K48 di-Ub as substrate on coomassie-stained SDS-PAGE gels. **(D)** Quantification of mono-Ub in K48 di-Ub cleavage assays. The intensity of the mono Ub band is plotted against time.

A

B
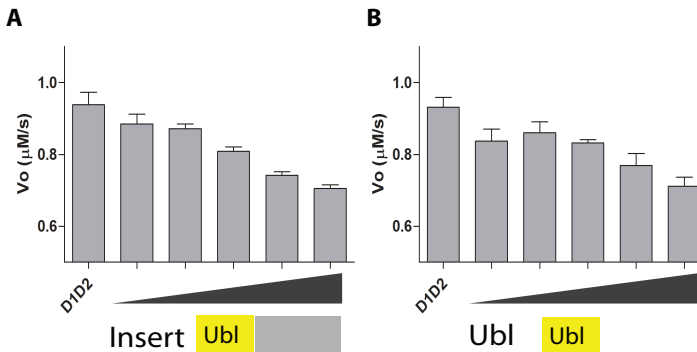
Supplemental Figure S5. In trans inhibition of USP4-D1D2 DUB activity A The inhibitory effect of the insert is observed in a Ub-AMC assay with increasing amounts of insert (5, 10, 25, 50 and 75µM). **B** The Ubl domain (5, 10, 25, 50 and 100µM) is sufficient to show this in trans inhibition.
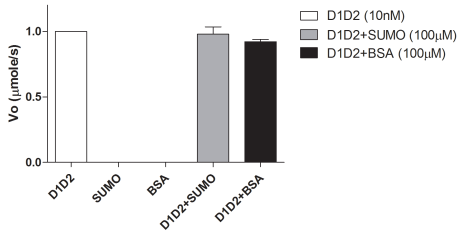
Supplemental Figure S6. The molecular crowding of high concentrations of SUMO or BSA (100μM) does not have an effect on USP4-D1D2 DUB activity.

Supplemental Figure S7. Kinetic comparison of USP4-D1D2 and USP4CD binding to Ub, Ubl and insert on SPR. Binding curve of 0.8 μM of USP4-D1D2 and of 1 μM of USP4CD were normalized for maximum binding in order to compare offrates.

$\rightarrow$
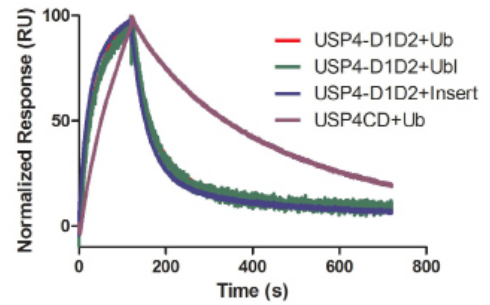
Chapter 4

Mechanism of USP7/HAUSP activation by its C-terminal ubiquitin-like domain (HUBL) and allosteric regulation by GMP-synthetase

Alex C. Faesen[1], Annette M.G. Dirac[2], Anitha Shanmugham[3], Huib Ovaa[3], Anastassis Perrakis[1] and Titia K. Sixma[1]

[1]Division of Biochemistry and Center for Biomedical Genetics, [2]Division of Molecular Carcinogenesis, [3]Division of Cell Biology, The Netherlands Cancer Institute, Plesmanlaan 121, 1066 CX Amsterdam, The Netherlands.

Abstract

The ubiquitin specific protease USP7/HAUSP regulates p53 and MDM2 levels, and cellular localization of FOXO4 and PTEN, and hence is critically important for their role in cellular processes. Here we show how the 64kDa C-terminal region of USP7 can positively regulate deubiquitinating activity. We present the crystal structure of this USP7/HAUSP Ubiquitin-Like domain (HUBL), comprised of five ubiquitin-like domains (Ubl) organized in 2-1-2 Ubl units. The last di-Ubl unit, HUBL-45, is sufficient to activate USP7, through binding to a 'switching' loop in the catalytic domain, which promotes ubiquitin binding and increases activity 100-fold. This activation can be enhanced allosterically by the metabolic enzyme GMPS. It binds to the first three Ubl domains (HUBL-123), and hyper-activates USP7 by stabilization of the HUBL-45 dependent active state.

Introduction

The deubiquitinating enzyme (DUB) Ubiquitin Specific Protease 7 (USP7), also known as Herpes-virus Associated Ubiquitin-Specific Protease (HAUSP), regulates the function of the tumor suppressor p53 that is mutated or inactivated in approximately 50% of human cancers[1]. USP7 removes ubiquitin from p53 itself, but also from the p53 E3 ubiquitin-ligase MDM2[2-5]. These combined effects determine functional p53 levels, creating an important role for USP7 in p53-dependent stress responses[6-8]. Precise regulation of USP7 expression and activity is therefore necessary for maintaining proper cell proliferation, and both up and down regulation of USP7 inhibit colon cancer cell proliferation[9]. USP7 also counteracts mono-ubiquitination of the transcription factor FOXO4 oncogene, and the phosphatase PTEN tumor suppressor, regulating their nuclear localization[10-12]. Consequently, USP7 over-expression in prostate cancer was directly associated with tumor aggressiveness, most likely through PTEN mislocalization. Altogether, USP7 activity regulates important pathways for cell survival, proliferation and apoptosis, misregulation of which often lead to tumorigenesis. Better understanding of USP7 activity may therefore contribute to insights in the role of these pathways in cancer.

USP7 is a cysteine isopeptidase of the ubiquitin specific proteases (USP) family[13]. It contains an N-terminal TRAF/Math domain, a catalytic domain and a 64 kDa C-terminal region (Figure 1A). The N-terminal TRAF domain directly interacts with the substrates of USP7 such as p53, MDM2 and TSPYL5[14-17]. The catalytic domain of USP7 has the conserved fold of the USP family[16,18,19]. It shows a papain-like architecture plus an extended, fingers-like domain that forms the ubiquitin binding pocket. Interestingly, the USP7 crystal structures show that the catalytic domain is maintained in a non-functional state, with the active site residues in a non-reactive conformation. The active conformation involves rearrangements of the catalytic domain that allow ubiquitin binding and organization of the catalytic triad, as shown in the structure of USP7 in complex with the suicide substrate ubiquitin aldehyde[18].

The C-terminal region of USP7 is essential for effective catalytic activity against a minimal synthetic substrate[20,21]. It harbors additional MDM2 and p53 binding sites and promotes sequence specific DNA binding of p53[21,22]. It was predicted to contain at least 4 domains with a Ubiquitin-Like (Ubl) β-grasp fold[23], and a NMR structure of one of these is reported (2KVR). Ubl domains are also predicted at various positions in sixteen additional USP enzymes. Two more Ubl domain structures are available: the N-terminal domains in USP14 (1WGG) and in USP4 (3JYU, residues 134-222). Among the USP family enzymes, USP7 is unique in containing a large number of consecutive Ubls.

Ubl domains share the ubiquitin fold, but lack the C-terminal Gly-Gly residues required for conjugation to a target. Although many Ubl domains are found in the human genome, mostly as part of multi-domain proteins, only few of these have been studied functionally[24,25]. Among these, distinct subclasses have different

functions[26]. Most classes of Ubl domains however, have not yet been characterized. Moreover, since different classes have only limited sequence similarity they may have very different functions.

A number of interaction partners of USP7 have been identified[27], but for most neither function nor interaction site are known. So far, the TRAF domain seems dedicated to binding substrate proteins MDM2, p53 and TSPYL5. The C-terminal domain is also used for interactions, as was shown for Ataxin-1[28] and the viral E3-ligase ICP0[29]. The metabolic enzyme GMP-synthetase (GMPS) interacts with USP7 in *Drosophila*[30] and human cells[31]. GMPS was found upregulated in tumorigenic cells[32,33], and together with USP7 is involved in cell survival, chromatin maintenance and transcriptional regulation of ecdysteroid target genes[34]. This interaction promotes USP7 activity towards H2B as well as enhancing activity against p53 in Drosophila. The activation mechanism is unclear, but possibly involves both general and target specific aspects.

Here we investigate how Ubl domains in the C-terminal region of USP7 promote activity. We show that USP7 exists in two states, an active and an inactive state. In the active state the C-terminal Ubl domains HUBL-45 interact with a 'switching loop' in the catalytic domain. We identified point mutations that interfere with the activation to validate its relevance in cells. Finally we show that GMPS can allosterically stabilize the interaction between HUBL-45 and the catalytic domain and thus promote the active state.

Results

The HUBL domain is essential for USP7 activity *in vitro* and *in vivo*

To study the function of the 64 kDa C-terminal HUBL domain of USP7 we purified a series of different USP7 constructs (Figure 1A,B), and compared their activity against ubiquitinated p53. In this assay, purified p53 was ubiquitinated *in vitro* with human MDM2/MDMX and then incubated with the USP7 constructs. p53 could only be efficiently deubiquitinated by USP7 constructs that contain the HUBL domain (Figure 1C, top panel). Removal of the N-terminal p53-binding domain (TRAF) does not affect the role of the HUBL domain, and has a relatively limited influence on the activity in these experiments (Figure 1C, bottom panel).

We then analyzed the importance of the HUBL domain for activity against ubiquitin chains, by monitoring hydrolysis of K48-linked di-ubiquitin into mono-ubiquitin. Consistently, we saw robust activity in the presence of the HUBL domain, whereas in its absence no activity was observed (Figure 1D). Only when the concentration of the catalytic domain was 1000-fold increased, activity could be observed (Figure S1B). Thus the HUBL domain is essential for full enzymatic activity of the USP7 catalytic domain.

To study the *in vivo* significance of the HUBL domain, we transfected U2OS cells with GFP-fused full-length USP7 and USP7N-CD and investigated protein levels of two USP7 substrates, p53 and MDM2. Our experiments showed an accumulation of p53 and MDM2 in the presence of full length USP7 compared to USP7N-CD (Figure 1E). This suggests that the HUBL domain is required to de-ubiquitinate p53 and MDM2, and thereby prevents degradation, resulting in a net stabilization. This shows that the HUBL domain is important for the activity of USP7 *in vivo*, and therefore essential for its biological function.

To quantify the HUBL-mediated activation we used a minimal synthetic substrate, ubiquitin fused to a C-terminal fluorescent group, 7-amido-4-methylcoumarin (Ub-AMC). Full-length USP7 and a construct that lacks the TRAF domain (USP7CD-HUBL) showed very similar activity, with similar Michaelis-Menten kinetic parameters (Vmax 1.4 nmole s^{-1} and K_M 3 µM) (Figure 1F and Table S2). In contrast, the catalytic domain alone (USP7CD) was much less active, with a decrease in Vmax to 0.06 nmole/s (22-fold) and an increase in K_M to 15 µM (5.5-fold). Altogether, the enzyme efficiency (k_{cat}/K_M) decreases 120-fold, suggesting that the C-terminal HUBL domain is essential to achieve full enzymatic efficiency and therefore activates the catalytic domain.

Since all USP7 constructs eluted as monomers from gel filtration, it is likely that this activation occurs within the same molecule. However, we wondered whether the HUBL domain could activate the catalytic domain when it is not part of the same chain, in trans. First we showed that the HUBL domain itself has no DUB activity on Ub-AMC, and then we mixed the catalytic domain with the HUBL domain. Adding 10 µM HUBL domain to the catalytic domain resulted in a 2-fold increase of catalytic turnover (Figure

S1A). However, when adding a higher excess of the HUBL domain (50 µM), a clear activation can be observed (Figure 1F). This result shows that the catalytically inactive HUBL domain can indirectly activate the USP7 catalytic domain also in trans, at least at high concentrations.

To exclude the possibility that the observed in vitro activation was due to assay conditions, we tested the effect of pH and salt concentration. The USP7 activity is strongly dependent on
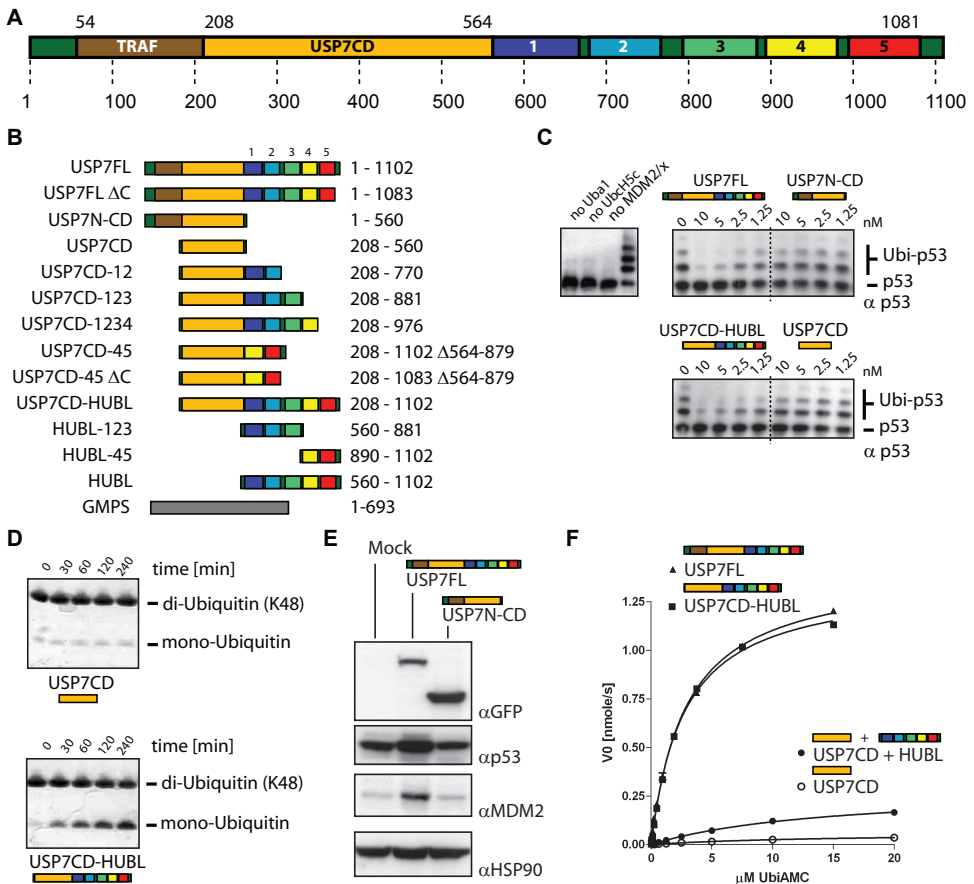
Figure 1. The HUBL domain is essential for USP7 activity. A. USP7 contains a TRAF substrate binding domain (brown) a catalytic domain (orange) and five Ubl domains (rainbow). **B.** USP7 constructs used in this study. **C.** Only in the presence of the HUBL domain can p53 be deubiquitinated. The presence of the N-terminal TRAF domain has a minor additional effect. **D.** Using 10 µM di-ubiquitin and 1 nM USP7, only USP7CD-HUBL is able to hydrolyse the substrate to mono-ubiquitin. **E.** In U2OS cells, p53 and MDM2 protein levels increase compared to control levels by over-expression of full-length USP7. However, with over-expression of USP7N-CD, this stabilization is not observed. HSP90 was used as a loading control. **F.** Kinetic analysis of Ub-AMC hydrolysis shows similar activity for USP7FL and USP7CD-HUBL, while USP7CD is 90-fold decrease in K_M/k_{cat}. Kinetic parameters can be found in Table S2.

pH (Figure S1C), with an optimum between pH 8 and 9, and also shows considerable dependence on ionic strength (Figure S1D). Since p53 is responsible for stress responses, these pH and ionic strength dependencies may well be relevant in cells. However, the presence of the HUBL domain has no effect on the pH response and only a mildly positive effect on the response to salt (Figure S1C, D, right panels). Thus, although activation may have an electrostatic component, we concluded that neither ionic strength nor pH effects explain how the activation is achieved.

Altogether these data confirm and extend the observation that the C-terminal domain is essential for full activity against Ub-AMC. As expected, the N-terminal TRAF domain

Figure 2. Crystal structure of the HUBL domain shows five Ubl domains. A. Secondary structure assignment of the HUBL domain. The residues are coloured to the corresponding Ubl. Disordered residues (1084-1102) are boxed. **B.** Cartoon representation of the HUBL domain with surface representation of the Ubls. See Table S1 for crystallographic information. **C.** Structure superposition shows that the Ubls share the β -grasp fold with ubiquitin, with variations in the length of the loop regions. (red: α-helix; blue: β-strand; green: ubiquitin). **D.** Di-Ubl units HUBL-12 and HUBL-45 are somewhat similar in Ubl orientation, showing a relative 30 degree rotation of HUBL-5 compared to HUBL-2. The ubiquitin Ile44 equivalents in the HUBL domains are labelled and depicted in sticks.

increases the activity against p53, but not against the minimal target Ub-AMC and has therefore no effect on the HUBL activation itself. We thus show that the catalytically inactive HUBL domain indirectly activates USP7 catalytic domain in a target-independent manner.

The USP7 HUBL structure shows five Ubl domains in three units

To investigate the mechanism underlying USP7 activation by its HUBL domain, we determined the crystal structure of the HUBL domain (residues 560 to 1102) using single anomalous dispersion (SAD) phasing from seleno-methionines (Figure 2A,B). The final model was refined to 2.7Å with Rfree of 0.216 (Supplementary Table S1), and includes residues 560 to 1083 with no Ramachandran outliers. The HUBL domain comprises five modules with the ubiquitin-like ββαβαβ-fold, one more than previously predicted based on consensus fold recognition[23]. The Ubl domains adopt an extended conformation, linked through regions of varying size that contain either one or two α-helices. The helices connecting HUBL-2 and -3 interact with HUBL-2 (Figure S2A), but otherwise these linkers have little contact with the individual domains.

The Ubl domains closely resemble ubiquitin (rmsd 1.9-2.5 Å, Figure 2C and S2B,C) and SUMO-2 (rmsd 2.2-2.9 Å), according to SSM[35] and DALI[36] structural similarity searches against all structures in the PDB. Despite the structural similarities, the sequence identities with ubiquitin are very limited, varying from 6-19% (Figure S2B). There are no obvious specific resemblances to other ubiquitin-like domains beyond the conserved fold, and hence it is not obvious that there is a shared function with other classes of Ubl domains.

Although the five Ubl domains share the ubiquitin fold they are no more similar to each other than to other ubiquitin-like structures (rmsd 2.1-2.9 Å), and they are widely divergent in sequence (3-15% sequence identity) (Figure S2B). This leads to large variations in charge distribution, such that under physiological conditions HUBL-1 and -2 are negatively charged (calculated pI 4.4 and 4.5 respectively), HUBL-3

is positively charged (pI 9.8) and HUBL-4 and -5 are neutral (pI 5.6 and 6.0 respectively) (Figure S5D). Mutations in these charged patches do not affect the enzymatic activity of USP7 (Figure S5C), although they may play a role in other functions of the protein, such as protein-protein interactions with its binding partners.

The HUBL domain is organized in an elongated arrangement, where HUBL-3 has limited contacts with the other domains (Figure 2B) and HUBL-1 and -2, as well as HUBL-4 and -5 form di-Ubl units. Analysis with PISA35, shows that the di-Ubl interfaces bury a large surface area (total ~1200 and ~740 Å2, respectively) with negative solvation energies ΔiG (Figure S2D), suggesting that they are stable in solution. This was supported by the degradation pattern of semi-purified USP7CD-HUBL, which degrades to three stable fragments that correspond to the masses of USP7CD-123, USP7CD-12 and USP7CD (Figure S2E). From this we concluded that the HUBL domain is organised in a 2-1-2 fashion that contains three units: HUBL-12, HUBL-3 and HUBL-45.

Structural comparison of these di-Ubl units reveals that HUBL-12 and HUBL-45 are similarly arranged (Figure 2D). Superposing the N-terminal domains HUBL-1 and HUBL-4 shows that equivalent interfaces are buried on the first Ubl in each pair, including the residue that is equivalent to the canonical Ile-44 of ubiquitin (Trp-623 and Leu-942, respectively). The second Ubl domains do not bury their Ile-44 equivalent residues (Tyr 735 and Ala 1041) and they are arranged slightly differently with a relative rotation of ~30 degrees resulting in small differences in detailed contacts. In both di-Ubl units the interfaces are mediated by extensive hydrophobic contacts as well as hydrogen bonds and electrostatic interactions (Figure S2D). This suggests that these di-Ubl units are functionally relevant.

SAXS analysis suggests flexibility and interaction between USP7CD and HUBL

We were intrigued by the extended structure of the HUBL domain and wondered whether it was relevant in solution. To address this question we used Small Angle X-ray Scattering (SAXS).

When we compared SAXS curves recorded for the USP7CD, HUBL-123 and HUBL-45 domains to scattering curves calculated from their corresponding crystal structures, we obtained a good fit between the experimental and calculated curves (Figure 3A). The calculated molecular weights (Mw), radii of gyration (Rg) and maximum interatomic distance (Dmax), also correspond well with the expected values (Figure 3B), with only the Rg of HUBL-45 approximately 30% larger than expected from the structure. These data show that USP7CD, HUBL-123 and HUBL-45 are structurally stable sub-domains of USP7 also in solution.

In contrast, the scattering curve for the complete HUBL domain does not fit the calculated scattering curve (Figure 3A). The interatomic distance probability distribution P(r) shows a non-symmetrical shape, including a significant proportion of long distances (Figure 3C). This suggests that the extended conformation is retained in solution. Since rigid body modelling did not yield a single model, we conclude that the structure of the HUBL domain in solution is not static, most likely exhibiting considerable flexibility between the two stable domains, HUBL-123 and HUBL-45.

The HUBL domain and USP7CD-HUBL have a similar radius, with the HUBL domain being marginally smaller as expected (Figure 3B,C). However, in the USP7CD-HUBL domain P(r) plot (Figure 3C) the asymmetry due to long interatomic distances mostly disappears, indicating a more compact molecule, despite the addition of the catalytic domain. This suggests that the HUBL domain folds back to the catalytic domain, resulting in a more compact shape. Since rigid body modelling did not yield a single solution, the interaction between the catalytic domain and the HUBL domain could be dynamic.
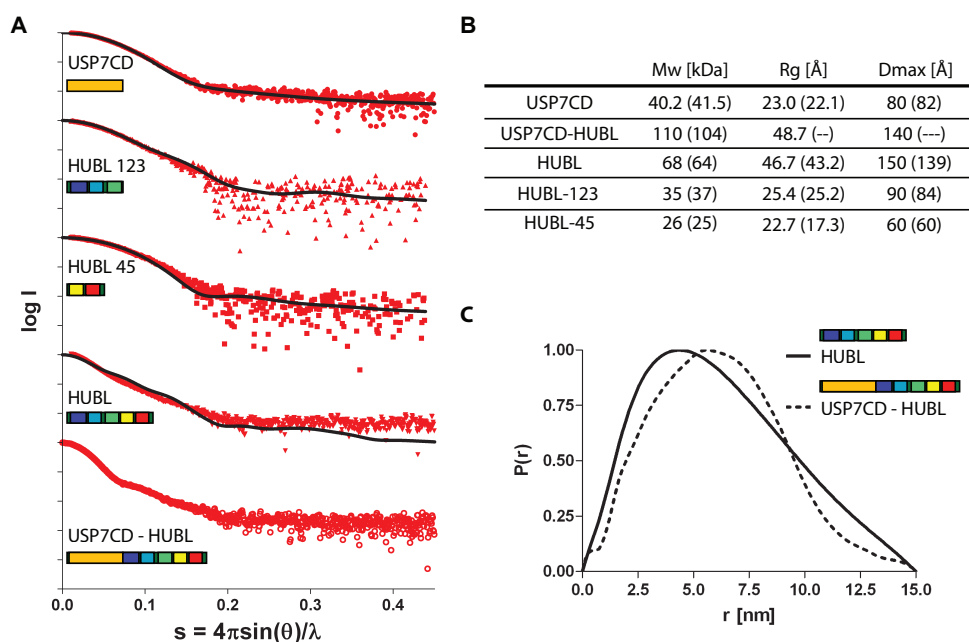

Figure 3. SAXS analysis of the HUBL domain. A. Scattering curves of the USP7 fragments (red symbols) with corresponding scattering curves calculated from the crystal structures (black lines). **B.** Overview of the SAXS analysis results. **C.** The symmetrical interatomic distance probability distribution (P(r)) of USP7CD-HUBL shows that it has less extended shape than the HUBL domain, indicating that the HUBL domain folds back onto the CD.

HUBL-45 is sufficient for USP7 activation

To identify the minimal region in the HUBL domain that is required for activation of the USP7 enzymatic activity, we produced C-terminal deletion constructs (Figure 1B). Upon deletion of the last one or two Ubl domains, the resulting USP7CD-1234 and USP7CD-123 has a severely compromised catalytic turnover, similar to the catalytic domain alone (Figure 4A). As HUBL-45 is an independent folding unit that seemed essential for *in vitro* activity, we tested if deleting it would affect USP7 function *in vivo*.

After transfecting U2OS cells with full-length USP7, USP7N-CD or USP7N-CD-123, we monitored p53 and MDM2 protein levels. Our experiments showed an accumulation of p53 and MDM2 in the presence of the full length USP7, which is not observed in absence of HUBL-45 (USP7N-CD-123) (Figure 4B), suggesting that it is required to de-ubiquitinate p53 and MDM2. This shows that HUBL-45 is essential for USP7 function *in vivo*.

Then we analyzed whether HUBL-45 alone is enough to reconstitute full activity. We deleted HUBL-123, coupling the HUBL-45 unit directly to the catalytic domain via a 2-amino acid linker (USP7CD-45). This variant had Vmax and K_M values almost identical to the complete USP7CD-HUBL (Figure 4D) in the Ub-AMC assay. In addition, USP7CD-HUBL and USP7CD-45
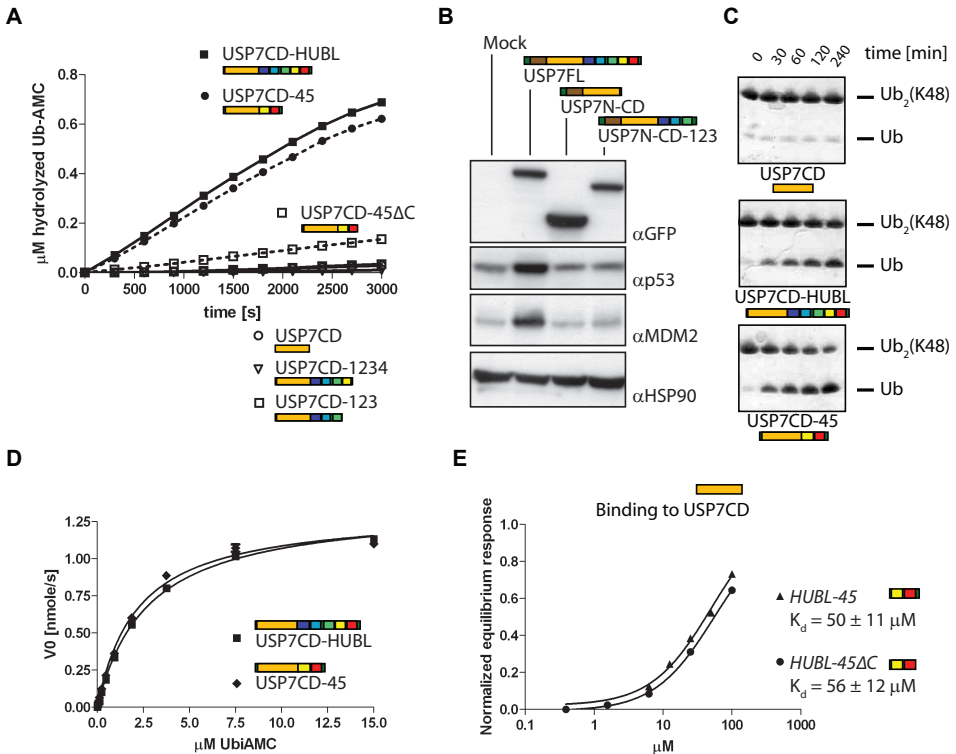

Figure 4. HUBL-45 is sufficient for activation. A. Any C-terminal deletion reduces activity to similar levels as USP7CD in Ub-AMC assays. However, the USP7CD-45 construct showed similar activity as USP7CD-HUBL. Removing the C-terminal peptide (USP7CD-45 ΔC) resulted in greatly reduced activity. **B.** Loss of HUBL-45 reduces USP7 activity in U2OS cells: protein levels of p53 and MDM2 did not increase as seen with the wild type full length USP7. HSP90 was used as a loading control. **C.** USP7CD-HUBL and USP7CD-45 have similar activity towards 10 μM di-ubiquitin (K48), while USP7CD did not show any activity. **D.** USP7CD-45 still showed full activity in Ub-AMC assays. **E.** SPR binding experiments, show an interaction with a K_d of 50 (± 11) μM between GST-USP7CD and HUBL-45.

have similar efficiency against a di-ubiquitin substrate (Figure 4C). These results show that HUBL-45 is sufficient to reconstitute the USP7 activation.

HUBL-45 consists of the di-Ubl unit and a flexible C-terminal 19 residue peptide that is disordered in the crystal structure. When we deleted this C-terminal tail of HUBL-45 (USP7CD-45ΔC) we observed a greatly reduced activity, similar to USP7CD (Figure 4A), showing that the C-terminal peptide is critical for the activation. To see whether this peptide alone was sufficient to promote activation, we performed in trans activation experiments with Ub-AMC using the peptide alone versus complete HUBL-45, including the peptide. In these assays (Figure S3A), the peptide marginally activates USP7CD in trans, whereas the full HUBL-45 domain provides robust levels of activation (Figure S3A). Therefore, we conclude that the C-terminal activation peptide is essential to increase the activity of USP7CD, but only in the context of HUBL-45.

Collectively, the activation of the catalytic domain and the SAXS data imply that the activation mechanism is through a direct interaction between the catalytic domain and HUBL-45. Indeed, when using a Surface Plasmon-Resonance (SPR) binding assay with immobilized GST-USP7CD, we observed a 50 μM dissociation constant (K_d) for HUBL-45 (Figure 4E), in agreement with the concentrations required for trans activation by the HUBL domain (Figure 1F and S3A). When the flexible C-terminal peptide was removed (HUBL-45ΔC), the affinity for the catalytic domain did not change (Figure 4E). Since no binding was detected between the catalytic domain and the peptide (Figure S3B), we concluded that although the peptide is essential for activity, the HUBL-45 di-Ubl unit is required for binding to the catalytic domain. This brings the flexible C-terminal activation peptide close to the catalytic domain, resulting in its activation.

The HUBL domain promotes ubiquitin binding

When considering the mechanism of USP7 activation, we realized that the lower K_M value in the catalytically efficient constructs suggested an increase in substrate affinity. Therefore we tested whether the HUBL domain affected the ubiquitin affinity of USP7CD. We incubated with the suicide substrate ubiquitin-VME (20 μM)[37]. While USP7CD alone was loaded only partially, USP7CD-45 loading was essentially complete (Figure S4A).

Since this could indicate an increase of ubiquitin affinity, we decided to validate this by SPR experiments. Neither USP7CD nor USP7CD-12 show appreciable ubiquitin binding, with almost no responses measured up to 17 μM, suggesting very little affinity for ubiquitin (Figure 5A and S4B). Also, no ubiquitin binding was observed for the HUBL domain itself (Figure 5A). However, the catalytically efficient USP7CD-HUBL construct showed a clear association and dissociation from ubiquitin. Both the kinetic and equilibrium data could be fitted with a K_d of 1.5 μM (Figure 5B,E). This indicates that the catalytic and HUBL domains cooperate to achieve ubiquitin binding. USP7CD-45 also binds ubiquitin with a K_d of 4 μM, similar to USP7CD-HUBL (Figure 5C,E), confirming that HUBL-45 is sufficient for the activation of USP7. Interestingly, although these Ubl domains may resemble ubiquitin, they do not compete for ubiquitin binding to USP7. Instead, they promote this interaction.

In the kinetic analyses, we observed that the catalytic domain and the HUBL domain cooperate in trans (Figure 1F). To test if that also translates to ubiquitin binding, different concentrations of USP7CD were flowed over the GST-ubiquitin chip in the presence of 50 μM HUBL. A partial reconstitution of the ubiquitin binding to a K_d of 13 μM was achieved, confirming that trans activation of the catalytic domain translates in an increased ubiquitin affinity (Figure 5D,E). The observed ubiquitin affinities correlate with the K_M values for Ub-AMC derived in the kinetic analysis, and therefore show that the increase of K_M can be explained by the increase of K_d (Table S2).

4

Point mutants prevent HUBL auto-activation
To understand how HUBL-45 conveys the activation to the catalytic domain, we used site-directed mutagenesis and tested a number of different options (Figure S5). In USP7 the residues forming the catalytic triad adopt an inactive conformation[18] (Figure S5A). However upon ubiquitin binding, the active site is remodelled to the active conformation. With this conformational change a small loop close to the active site (residues 285 to 291), that we name 'switching loop', shows dramatic changes (Figure 6A).

We mutated several residues in this 'switching loop', both in the context of USP7CD and USP7CD-45, and tested their activity using Ub-AMC (Figure 6B and Table S2). These mutations show a limited activating effect when tested in the catalytic domain alone. However, in the context of USP7CD-45, two switching loop mutants, W285D and E286A, greatly reduce
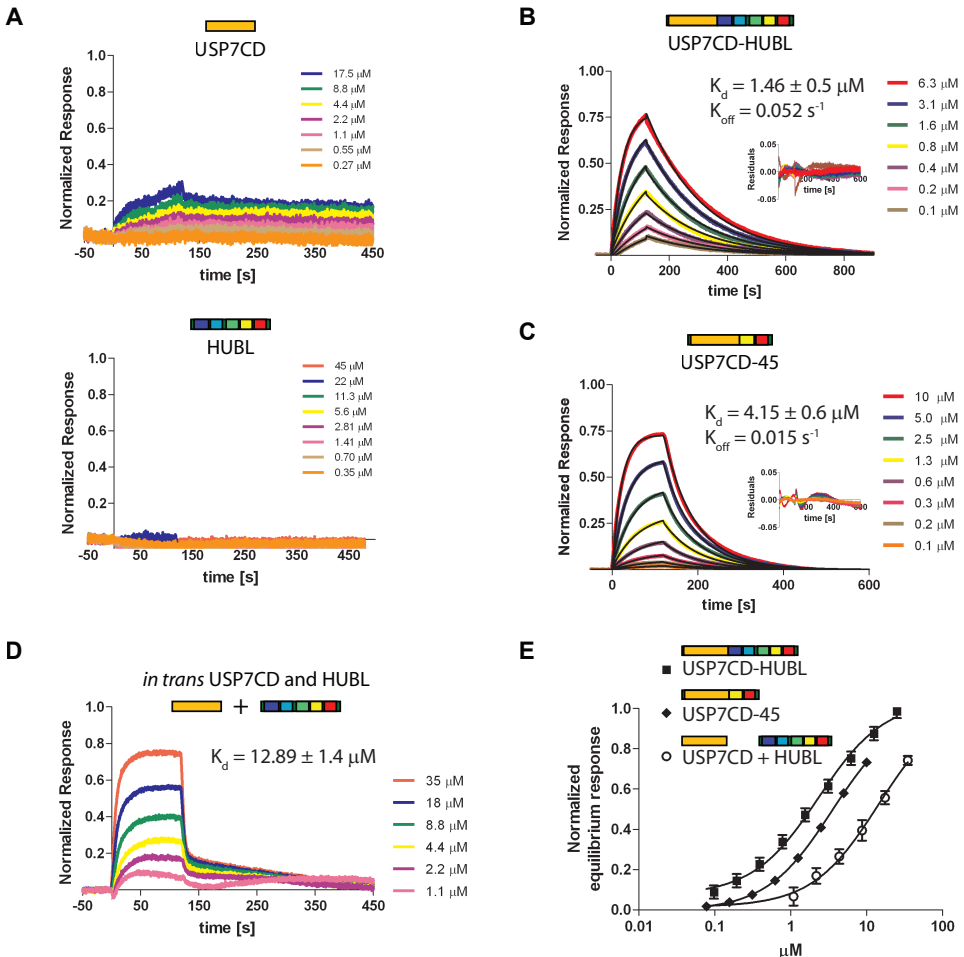

Figure 5. Ubiquitin affinity is increased by the HUBL domain. A. SPR binding studies using GST-tagged ubiquitin, showed weak ubiquitin binding for USP7CD, and no responses with the HUBL domain. **B.** USP7CD-HUBL binds to ubiquitin, which could be fitted using the binding kinetics (black line) to a K_d 1.5 (± 0.5) μM. The inset shows the residuals. **C.** USP7CD-45 binds ubiquitin with a dissociation constant of 4.15 (± 0.6) μM. The inset shows the residuals. **D.** The dissociation constant for ubiquitin of the USP7CD is increased to 12.90 (± 1.4) μM in the presence of 50 μM of the HUBL domain. **E.** Overlay of the normalized equilibrium responses.
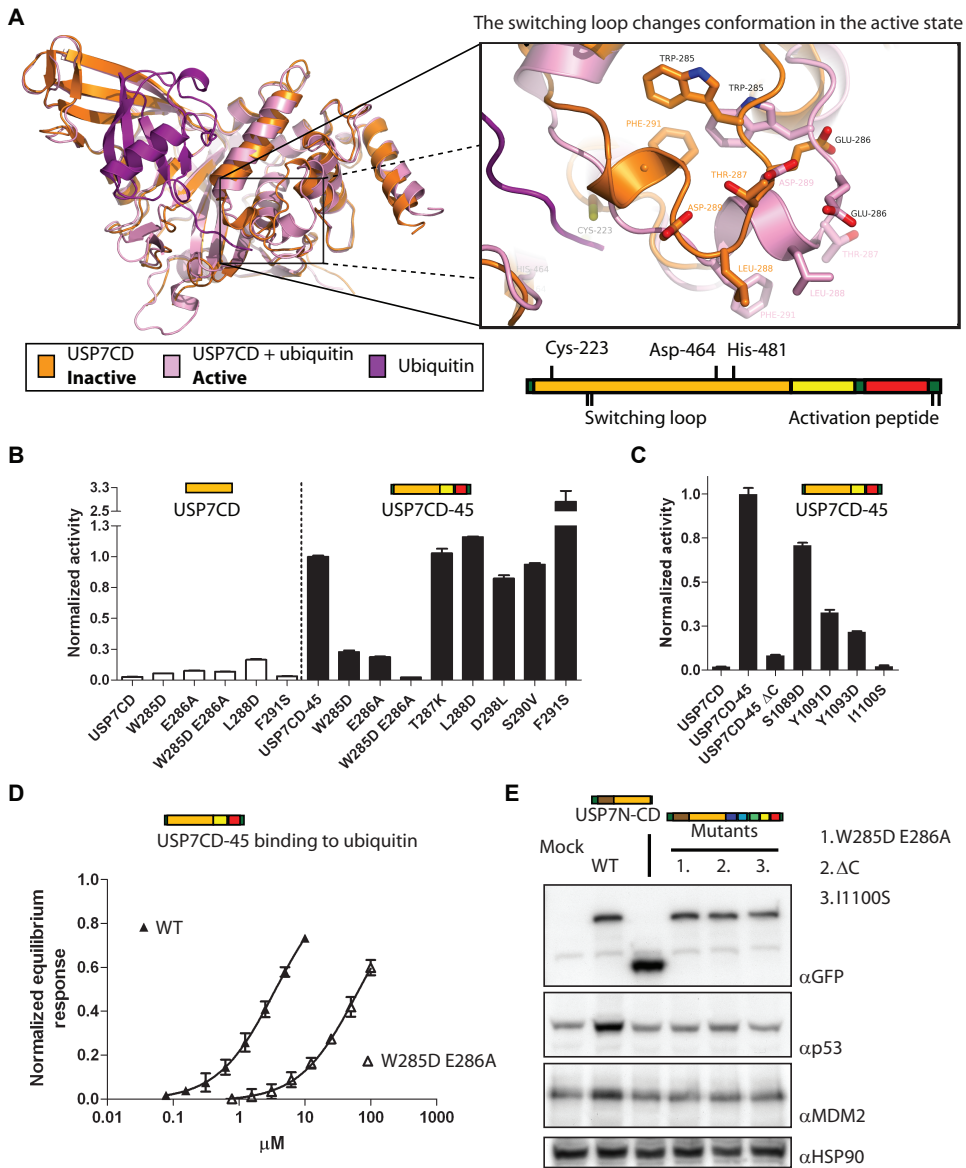
Figure 6. Mutants in the catalytic domain and HUBL-45 prevent activation. A. Crystal structures of the USP7 catalytic domain (1NB8 and 1NBF) show a remodelling of the "switching–loop" (residues W285 - F291) and active site upon binding of ubiquitin aldehyde. Schematic diagram of USP7CD-45 shows catalytic residues, the switching loop and activation peptide. **B.** Mutating 'switching loop' residues W285 and E286 in the catalytic domain dramatically reduced the activity of USP7CD-45. In USP7CD a limited activating effect is seen, due to destabilization of the inactive form. Mutating F291 resulted in extra HUBL activation. The activity is normalized to full length USP7. **C.** Mutating conserved residues in the C-terminal activation peptide of HUBL-45 resulted in decreased activity on Ub-AMC, with a complete loss of activation for mutant Ile1100Ser. **D.** SPR shows dramatic decrease in ubiquitin binding for USP7CD-45 W285D E286A ($K_d = 67.9 \pm 5.3 \ \mu$M). **E.** USP7FL activity in U2OS cells is reduced for mutants in the switching loop (1. W285D E286A), or in the activation peptide (2. ΔC; 3. I1100S) since protein levels of p53 and MDM2 only increase with wild-type USP7. HSP90 was used as a loading control.

the activation effect conferred by HUBL-45. Moreover, the W285D E286A double mutant has a greatly reduced ubiquitin affinity (Figure 6D and S4C,D).

The 19 residues in the flexible C-terminal peptide of HUBL-45 are essential for the activation (Figure S3A and 6C). Several single point mutants of conserved residues displayed a reduction in activating capacity (Figure 6C). Strikingly, the single point mutant I1100S completely abolished the HUBL activation and greatly reduced ubiquitin binding (Figure 6C, S4D and Table S2). Consistently, over-expressing these USP7 mutants in U2OS cells completely abolished the stabilisation of p53 and MDM2 observed for the wild-type enzyme (Figure 6E). This shows that, although they are not in direct contact with ubiquitin, both the switching loop and the C-terminal peptide of the HUBL domain are required for the HUBL mediated increase of activity and ubiquitin affinity.

GMPS binds to HUBL-123 and allosterically promotes activation

Due to the intrinsic flexibility and weak interactions with the catalytic domain, the HUBL domain may not always be in the activated state. Therefore, the HUBL activation mechanism may be susceptible to regulation. A prime candidate for this regulation is GMPS, a metabolic enzyme that binds and activates USP7 in *Drosophila*[30] and humans[31]. To analyze whether the HUBL domain intrinsically and constitutively activates USP7, or whether it can be further regulated, we studied the modulation of USP7 activity by GMPS.

First, we wondered which USP7 domains are involved in GMPS binding. Using pull-down experiments with various GST-tagged USP7 constructs we show that GMPS binds to USP7 only when HUBL-123 is present (Figure S7A). USP7CD-HUBL, USP7CD-123 and HUBL-123 have a very tight interaction with GMPS (K_d of 30-40 nM), as shown by SPR (Figure 7A and S7B,C). Neither USP7CD or USP7CD-45 showed any appreciable binding to GMPS (Figure 7A and S7C), confirming that HUBL-123 is sufficient for the USP7-GMPS interaction.

Next, we wanted to see if GMPS binding affects USP7 activity. Indeed, the activity of USP7CD-HUBL in Ub-AMC assays is increased 5.5-fold in the presence of GMPS (Figure 7B and Table S2). Kinetic analysis reveals an increased k_{cat}, with only a slightly increased K_M, consistent with the observation that the ubiquitin affinity of the complex does not change (K_d 2.5 ± 0.17 μM) (Figure S7D). The presence of GMPS does not activate USP7CD-123 even if they interact tightly (Figure S7E). Importantly when we introduced the W285D E286A and I1100S mutations to USP7CD-HUBL, the mutant proteins bound GMPS equally well as the wild type (Figure S7A,B,C), but could no longer be activated by GMPS (Figure 7C). This shows that GMPS hyper-activation of USP7 requires a functional switching loop in the catalytic domain and works through the HUBL-45 dependent activation.

To confirm whether the GMPS-dependent activation indeed acts through HUBL-45 we analyzed whether GMPS changed the affinity of the HUBL-45 region for the catalytic domain. Strikingly, whereas the HUBL-123 has no affinity for the catalytic domain in the presence of GMPS, the dissociation constant between the full HUBL domain and the catalytic domain increases from 48 (± 9.7) μM to 1.8 (± 0.42) μM in the presence of GMPS (Figure 7D). This shows that GMPS can allosterically activate USP7 by binding to HUBL-123, stabilizing the contact between HUBL-45 and USP7CD, thus promoting the activated state.

Discussion

We show here that the C-terminal HUBL-45 domain is required, and sufficient for full activity of the USP7/HAUSP deubiquitinating enzyme. This mechanism depends on contacts between the C-terminal tail of HUBL-45 and a 'switching loop' in the catalytic domain, which leads to organization of the active site and an increased affinity for ubiquitin. Single point mutants in the switching loop or C-terminal tail interfere with USP7 activity *in vivo* and *in vitro*.

Apparently USP7 has the unusual ability to switch the active site between an active and an inactive state, resulting in the change in both
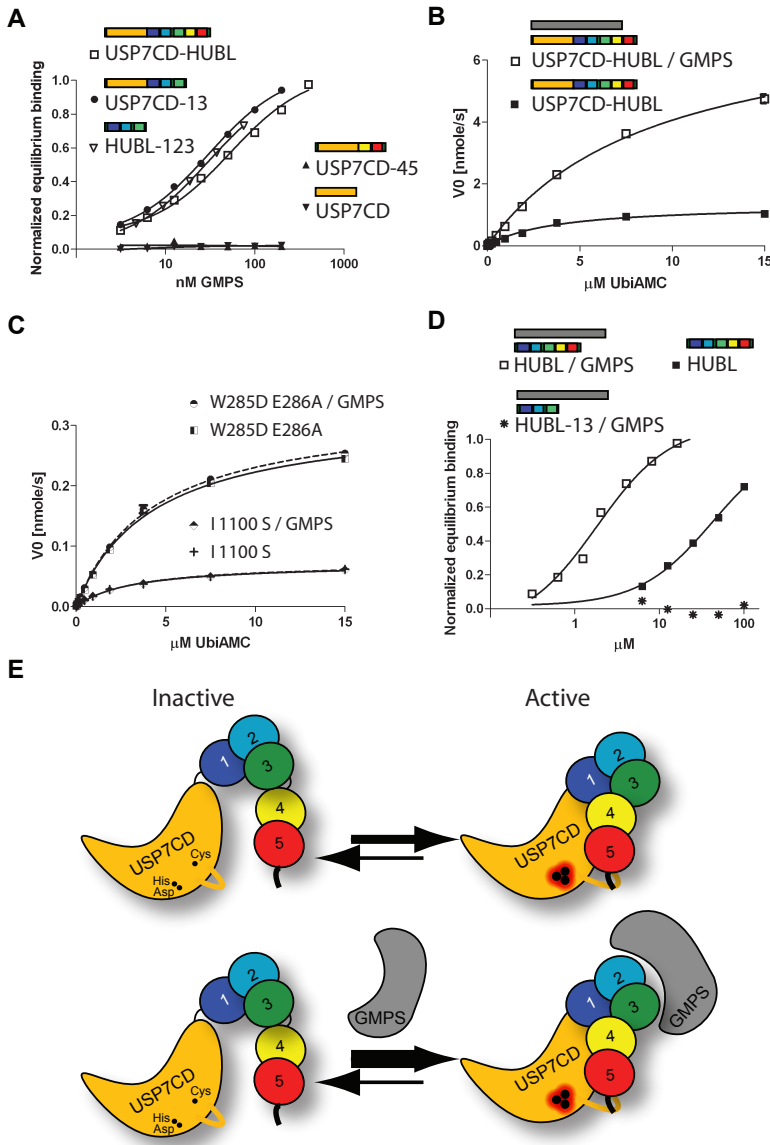
Figure 7. GMPS can hyper-activate the HUBL auto-activation. A. SPR experiments show that GMPS binds to USP7 constructs containing HUBL-123 with a K_d of 30-40 nM. **B.** Kinetic analysis of USP7CD-HUBL / GMPS complex showed a 5.5-fold increase of k_{cat}. **C.** The W285D E286A and I1100S mutants in USP7CD-HUBL (solid lines), prevent hyper-activation by GMPS (dashed lines) in the Ub-AMC assays. **D.** In complex with GMPS the binding of the HUBL domain for GST-USP7CD increased from a K_d of 48 ($\pm$ 9.7) μM to 1.8 ($\pm$ 0.42) μM. **E.** Model for the auto-activation of the USP7 catalytic domain by the HUBL domain, which is allosterically promoted by GMPS. In its resting state, the catalytic triad is in a misaligned and inactive conformation resulting in an almost inactive enzyme. However, the HUBL-45 domain interacts with the USP7 catalytic domain, and through its flexible C-terminal activating peptide mediates a conformational change of the switching loop, resulting in a re-arrangement of the catalytic triad to the active conformation. This increases both catalytic turnover and ubiquitin affinity (top panel). Subsequent binding of GMPS, allosterically stabilizes the activated state by binding to HUBL-123, in a mechanism that requires HUBL-45 and results in an increased affinity between the catalytic domain and the HUBL-45 unit of the HUBL domain (bottom panel).

k_{cat} and K_M. This was observed in the crystal structures of the catalytic domain, with and without ubiquitin. Most USP catalytic domains, USP8 (2GFO), USP14 (2AYN), USP4 (2Y6E) and CYLD (2VHF), do not have this non-organized state of the catalytic triad. USP14 is activated by binding to the proteasome[38], which is mediated by a single Ubl domain[37]. However only for USP7 and Ubp8, a member of the SAGA complex, the two states are suggested based on biochemical and structural data[39,40]. Here we show USP7 is able to switch, since in trans activation is possible. Apparently, the pre-folded catalytic domain can still be activated by the HUBL domain.

At first glance, full-length USP7 is continuously in the active state. However, we show that binding of GMPS can further activate USP7. The HUBL-123 domain, which is dispensable for USP7 intrinsic activity, serves as a binding platform for GMPS. This binding results in hyper-activation of USP7 through a mechanism that is completely dependent on a functional HUBL activation, since point-mutants in this interface can not be activated by GMPS. Rather, GMPS binding results in an increased affinity between the catalytic domain and the HUBL-45 unit of the HUBL domain, stabilizing the interaction.

Therefore we propose a model where USP7 exists in equilibrium between an active and an inactive state (Figure 7E, top panel). The switch between states involves an increase of ubiquitin binding and remodelling of the active site and switching loop, due to interactions with the HUBL-45 domain. Allosteric interaction with GMPS stabilizes the active state, promoting the interaction between HUBL-45 and switching loop (Figure 7E, bottom panel). It does not affect ubiquitin binding or K_M but activates through k_{cat}, resulting in substantially more molecules in the active state.

Since the interaction between USP7CD and the HUBL domain is weak, and single point mutants can completely prevent HUBL activation, USP7 is not always in the "on" state, but rather displays flexibility, as seen in the SAXS experiments. That would explain how GMPS could hyper-activate USP7 through an increase of HUBL affinity

for USP7CD, by serving as a molecular lock to reduce HUBL flexibility.

GMPS most likely has additional target specific regulatory functions in cells[30,31]. Since not all USP7 is found in complex with GMPS or vice versa[34], it is clear that USP7 is not always in this activated state in cells.

This opens the interesting possibility that other regulators could further modulate the interaction between the catalytic domain and the HUBL domain, either promoting the 'on-state', like GMPS, or by sequestering HUBL-45 from the catalytic domain and promoting the 'off-state'. Since USP7 is an important player in key cellular processes, such ability to hundred-fold modulate - increase or decrease - catalytic efficiency, provides a very fast response to external stimuli. The subsequent regulation could be achieved by post-translational modification, by interaction with other partners[27] or even by substrate interactions, since e.g. MDM2 and p53 were shown to interact with the HUBL domain.

Regulation of USP catalytic activity through allosteric interaction has been observed before, e.g. for the SAGA complex, where binding of Sgf11 is necessary to maintain the catalytic residues of Ubp8 in the proteolytically active conformation[39,40]. Interestingly, this allosteric activation depends on the topologically equivalent 'switching loop' as in USP7. Moreover, USP7 and Upb8 share the conserved W285 that is involved in the switching of USP7, confirming its importance. However, the mechanism in Ubp8 is distinct, since it relies on inter-molecular interactions, rather than an intra-molecular interaction as in USP7.

Surprisingly, both the activation of USP7 and the GMPS binding are conveyed by Ubl domains. None of these Ubl domains seem to resemble ubiquitin enough to compete for ubiquitin binding in the substrate binding site. This is in contrast to the internal Ubl domain in USP4, which competitively inhibits catalytic activity[41]. In USP7 the Ubl domains behave as larger units, with different functions. Although Ubl domains were predicted in other USPs, the large number of Ubl domain in the HUBL domain itself seems

to be unique for USP7.

The importance of USP7 for localisation and stability of critical cancer targets such as FOXO4, PTEN and p53/MDM2 make it into an interesting drug target. The unique features of its regulation may well offer specific opportunities for drug development.

Experimental procedures

General plasmids, proteins, antibodies

Plasmids for human MDM2, MDMX were a gift from Martin Scheffner, plasmids encoding ubiquitin variants for chain formation were a gift from Shaari Rahzi. Purified hyperstable p53[42] was a gift from Caroline Blair and Alan Fersht, UBA1, UBCH5c, ubiquitin were purified as described[43,44]; human MDM2/MDMX was purified using Martin Scheffner's protocol[45], di-ubiquitin with a K48 linkage was produced as previously described[44].

Generation of plasmids, bacmids and baculoviruses

Codon optimized full length USP7 and GMPS cDNA was obtained from DomainEx (Cambridge, UK). Both were amplified by PCR and subcloned (SpeI/NotI) into a pFastBac vector (Invitrogen) containing an N-terminal GST tag (BamHI/SpeI) and Prescission Protease cleavage site. Bacmids were prepared following the manufacturer's guidelines. Virus was produced using the low-MOI infection protocol[46]. DNAs coding for the truncation and deletion constructs of USP7 were amplified with 5'-BamHI and 3'-NotI overhangs and subcloned into the pGEX-6P-1 vector (GE Healthcare) or by introducing stop codons using the QuickChange mutagenesis kit from Stratagene (La Jolla, CA, USA). All constructs were checked by sequencing. USP7CD-45 was produced by amplifying the catalytic domain (residues 208 to 564) with 5'-BamHI and 3'-XhoI overhangs and HUBL-45 (residues 890 to 1102) 5'-XhoI and 3'-NotI overhangs and both fragment subsequently subcloned into the pGEX-6P-1 vector (GE Healthcare). This resulted in the addition of two extra residues (Leu-Glu) between the catalytic domain and HUBL-45. Mutants were created with the QuickChange mutagenesis kit (Stratagene).

Protein expression and purification

Full length USP7 and GMPS were produced using *Sf9* and *Sf21* insect cell expression. Infection was done using a low-MOI infection protocol[46]. The cells were harvested 72 hours after a baculovirus induced growth arrest was observed. All USP7 truncation constructs, USP7 mutants and GST-ubiquitin were expressed in *E.coli* BL21(DE3) T1-R cells using auto-induction medium47 overnight at 15°C. Selenomethionine HUBL was produced for crystallization and was expressed in *E.coli* B834(DE3) T1-R cells using SelenoMet Medium Base (Athena Enzyme Systems). All proteins were purified using GST sepharose (GE Healthcare) in 50 mM Hepes (pH 7.5), 250 mM NaCl, 0.1 mM PMSF, 1 mM EDTA and 1 mM DTT followed by elution in 50 mM reduced glutathione and overnight cleavage by Prescission Protease (GE Healthcare). Size exclusion chromatography was performed using a Superdex 200 or 75 column (GE Healthcare), equilibrated against buffer containing 10 mM Hepes [pH 7.5], 100 mM NaCl and 1 mM DTT. All proteins eluted as monomers from the gel filtration. When necessary the cleaved GST-tag was removed by attaching a GST FF column (GE Healthcare) to the end of the gel filtration column. USP7/GMPS complexes were purified using co-lysis, or mixing of the individual proteins before the last gel-filtration. Protein was concentrated to ~10 mg/ml and stored at -80°C.

In vitro p53 de-ubiquitination assay

Purified hyperstable p53[42] was ubiquitinated using 0.5 µM Uba1, 3 µM UbcH5c, human MDM2/MDMX, 250nM p53, 2 µM ubiquitin and 10mM ATP in 25 mM Tris (pH 8.0), 150 mM NaCl, 10 mM MgCl2, 2 µM ZnCl2, 5 µM β-mercapto-ethanol and 1 mM DTT for 1 hour at 37 degrees. The reaction was stopped by adding 11 mM EDTA and incubated with varying concentrations of USP7 for 1 hour at 37 degrees. Western blot was performed using mouse 1:1000 p53 antibody (PAB240 Santa Cruz) and the Pierce Fast Western Blot Kit.

Cell cultures, transient transfections

U2OS cells were cultured in Dulbecco's modified eagle medium (DMEM), supplemented with

10% foetal calf serum. Transfections were done with the calcium phosphate method. Cells were transfected with 10 μg GFP-USP7 construct and 0.5 μg pBabePuro per 10 cm dish. 48 hours after transfection, cells were selected with puromycin. Puromycin selected cells were lysed in RIPA buffer supplemented with "complete" protease inhibitors (Roche). Western blots were performed using whole cell extracts, separated on 8% SDS-PAGE gels and transferred to polyvinylidine difluoride membranes (Millipore). Western blots were probed with the indicated antibodies. Antibodies used were anti-GFP (FL), p53 (DO-1), and MDM2 (SMP-14), Hsp90 α/β (H-114), all from Santa Cruz.

Di-ubiquitin assay
Di-ubiquitin hydrolysis reactions were performed at 37°C in 50 mM Hepes buffer (pH 7.5), 100mM NaCl, 1 mM EDTA, 5 mM DTT and 0.05% (w/v) Tween-20 with either constant enzyme concentration (50nM) or constant substrate concentration (10 μM) with two-fold serial dilutions of the USP7 construct (starting from 20 μM). Reactions were stopped by addition of SDS loading buffer.

Ubiquitin-AMC assay
Activity towards Ub-AMC (Sigma) was assayed at 25°C in 50 mM Hepes buffer (pH 7.5), 100mM NaCl, 1 mM EDTA, 5 mM DTT and 0.05% (w/v) Tween-20. Assays were performed in "Non binding surface flat bottom low flange" black 384-well plates (Corning) in a 30 μl reaction volume. Fluorescence was measured in intervals of 5 min using a Fluostar Optima plate reader (BMG Labtechnologies) at excitation and emission wavelengths of 355 nm and 460 nm, respectively. All assays were performed in triplicate.

Kinetic analysis with Ubiquitin-AMC assay
To determine the assay linearity range, serial dilutions (from 200 nM) of each USP7 construct were used to completely hydrolyze 1 μM of Ub-AMC. For Michaelis-Menten analysis, constant enzyme concentrations (1nM for full length USP7, USP7CD-HUBL and USP7CD45; 10 nM for USP7CD) were used to hydrolyze varying substrate concentrations (from 15 μM in two-fold dilutions). In order to calculate the kinetic parameters for the hydrolysis of Ub-AMC, curves obtained by plotting the measured enzyme initial rates (v) versus the corresponding substrate concentrations ([S]). These were subjected to nonlinear regression fit using the Michaelis–Menten equation $V = (V_{max} \cdot [S]) / ([S] + K_M)$ (eqn 1), where V_{max} is the maximal velocity at saturating substrate concentrations and K_M the Michaelis constant. The k_{cat} value was derived from the equation $k_{cat} = V_{max}/[Eo]$ (eqn 2) where [Eo] is the total enzyme concentration. Experimental data was processed using Prism 4.03 (GraphPad Software, Inc.).

Crystal structure determination
For data collection statistics, see Supplementary Table S1. HUBL (residues 560 to 1102) was crystallized at 4°C in sitting drops against 10% (w/v) PEG4000, 200 mM sodium chloride, and 100 mM MES at pH 6.0 and cryoprotected in mother liquor supplemented with 20% (w/v) glycerol. A single-wavelength anomalous diffraction (SAD) experiment at the selenium anomalous peak wavelength, was performed at the PX beamline at the Swiss Light Source (SLS), while a native data set was collected at the ESRF microfocus beamline ID23-2. Both data sets were collected from a single crystal at 100K. Diffraction images were integrated with iMOSFLM[48] and scaled with SCALA[49], to 3Å for the selenomethionine crystal and 2.7Å for the native crystal. Structure solution was carried out using SHARP/autoSHARP[50], and resulted to a phase probability distribution with an overall figure of merit of 0.47 before solvent flattening. ARP/wARP[51] was used to built an initial incomplete model (375 out of 547 residues) which was used as a template to build a model manually in Coot[52]. This refined in iterative cycles with PHENIX[53] and Buster[54]. For crystallographic parameters, see Supplementary Table S1. For residues 1084-1102, no electron density has been observed. Structure figures were generated using PyMOL (http://www.pymol.org). Pictures of the electrostatic potential mapped on the protein surface were generated using CCP4MG[55]. Further structural analysis was performed with Espript[56], PISA[57], DSSP[58] and SSM[35].

4

SAXS analysis

Samples for the SAXS experiments were prepared immediately after gel filtration in buffer containing 10 mM Hepes [pH 7.5], 100 mM NaCl and 1 mM DTT with an additional 5% (v/v) glycerol as a radiation scavenger. Samples were taken during concentration and the flow-through was collected and used for the blank measurements. Typically five concentrations were measured, ranging from 0.5 to 10 mg/ml. Data were collected at the ESRF beamline ID14-3. Data were processed, analysed and modelled using programs from the ATSAS software package[59]. For the HUBL domain aggregation was observed and only the lowest concentration was used. The interatomic distance distribution probability function P(r) was calculated using Gnom. Rigid body modeling was performed using SASREF, using individual Ubl domains and/or the di-Ubl units. Distance constraints to define covalent links, or linkers when the connecting loops were removed, yielded similar results as using no distance restraints. Where possible, multiple merged scattering curves were used when the constructs overlapped. The ab initio models were calculated by DAMMIF and averaged over ten models using DAMAVER.

Surface Plasmon Resonance (SPR)

SPR was performed at 25°C on a Biacore T100. A CM5 sensor chip was prepared with monoclonal GST antibody via amino coupling (~20000 response units). This chip was used to load roughly 50 response units of GST-ubiquitin or 400 response units of GST-USP7CD. Biotinylated peptides were coupled to a SA chip (200 RU's). Concentration series of the USP7 constructs in running buffer (10 mM HEPES [pH 7.5], 100mM NaCl, 5 mM DTT, and 0.05% Tween-20) were tested at 30 µl/min. Saturation binding values were plotted against concentration (GST as reference) and fit to a steady-state affinity model for calculation of apparent dissociation (K_d) and association (K_a) constants (Prism 4.03, GraphPad Software, Inc.). All experiments have been repeated at least three times.

Accession numbers

Coordinates and structure factors were deposited in the Protein Data Bank under identification code 2YLM.

Author contributions

AF designed, performed and analyzed all *in vitro* experiments and wrote the manuscript. AMGD designed, performed and analyzed all *in vivo* experiments. AS observed the increase of ubiquitin affinity for the first time using ubiquitin-isopeptide isosteres. HO supervised ubiquitin-isopeptide research. AP supervised X-ray data collection and analysis. TKS designed research and supervised all *in vitro* experiments and manuscript writing.

4

References

1. Vogelstein, B., Lane, D. & Levine, A.J. Surfing the p53 network. Nature 408, 307-10 (2000).
2. Li, M., Brooks, C.L., Kon, N. & Gu, W. A dynamic role of HAUSP in the p53-Mdm2 pathway. Mol Cell 13, 879-86 (2004).
3. Li, M. et al. Deubiquitination of p53 by HAUSP is an important pathway for p53 stabilization. Nature 416, 648-53 (2002).
4. Cummins, J.M. et al. Tumour suppression: disruption of HAUSP gene stabilizes p53. Nature 428, 1 p following 486 (2004).
5. Cummins, J.M. & Vogelstein, B. HAUSP is required for p53 destabilization. Cell Cycle 3, 689-92 (2004).
6. Marchenko, N.D., Wolff, S., Erster, S., Becker, K. & Moll, U.M. Monoubiquitylation promotes mitochondrial p53 translocation. Embo J 26, 923-34 (2007).
7. Meulmeester, E. et al. Loss of HAUSP-mediated deubiquitination contributes to DNA damage-induced destabilization of Hdmx and Hdm2. Mol Cell 18, 565-76 (2005).
8. Kon, N. et al. Inactivation of HAUSP in vivo modulates p53 function. Oncogene 29, 1270-9 (2010).
9. Becker, K., Marchenko, N.D., Palacios, G. & Moll, U.M. A role of HAUSP in tumor suppression in a human colon carcinoma xenograft model. Cell Cycle 7, 1205-13 (2008).
10. Song, M.S. et al. Nuclear PTEN regulates the APC-CDH1 tumor-suppressive complex in a phosphatase-independent manner. Cell 144, 187-99 (2011).
11. Trotman, L.C. et al. Ubiquitination regulates PTEN nuclear import and tumor suppression. Cell 128, 141-56 (2007).
12. van der Horst, A. et al. FOXO4 transcriptional activity is regulated by monoubiquitination and USP7/HAUSP. Nat Cell Biol 8, 1064-73 (2006).
13. Nijman, S.M. et al. A genomic and functional inventory of deubiquitinating enzymes. Cell 123, 773-86 (2005).
14. Saridakis, V. et al. Structure of the p53 binding domain of HAUSP/USP7 bound to Epstein-Barr nuclear antigen 1 implications for EBV-mediated immortalization. Mol Cell 18, 25-36 (2005).
15. Sheng, Y. et al. Molecular recognition of p53 and MDM2 by USP7/HAUSP. Nat Struct Mol Biol 13, 285-91 (2006).
16. Hu, M. et al. Structural basis of competitive recognition of p53 and MDM2 by HAUSP/USP7: implications for the regulation of the p53-MDM2 pathway. PLoS Biol 4, e27 (2006).
17. Epping, M.T. et al. TSPYL5 suppresses p53 levels and function by physical interaction with USP7. Nat Cell Biol 13, 102-8 (2011).
18. Hu, M. et al. Crystal structure of a UBP-family deubiquitinating enzyme in isolation and in complex with ubiquitin aldehyde. Cell 111, 1041-54 (2002).
19. Komander, D. et al. The structure of the CYLD USP domain explains its specificity for Lys63-linked polyubiquitin and reveals a B box module. Mol Cell 29, 451-64 (2008).
20. Fernandez-Montalvan, A. et al. Biochemical characterization of USP7 reveals post-translational modification sites and structural requirements for substrate processing and subcellular localization. Febs J 274, 4256-70 (2007).
21. Ma, J. et al. C-terminal region of USP7/HAUSP is critical for deubiquitination activity and contains a second mdm2/p53 binding site. Arch Biochem Biophys 503, 207-12 (2010).
22. Sarkari, F., Sheng, Y. & Frappier, L. USP7/HAUSP Promotes the Sequence-Specific DNA Binding Activity of p53. PLoS One 5, e13040 (2010).
23. Zhu, X., Menard, R. & Sulea, T. High incidence of ubiquitin-like domains in human ubiquitin-specific proteases. Proteins 69, 1-7 (2007).
24. Grabbe, C. & Dikic, I. Functional roles of ubiquitin-like domain (ULD) and ubiquitin-binding domain (UBD) containing proteins. Chem Rev 109, 1481-94 (2009).

25. Madsen, L., Schulze, A., Seeger, M. & Hartmann-Petersen, R. Ubiquitin domain proteins in disease. BMC Biochem 8 Suppl 1, S1 (2007).
26. Burroughs, A.M., Balaji, S., Iyer, L.M. & Aravind, L. Small but versatile: the extraordinary functional and structural diversity of the beta-grasp fold. Biol Direct 2, 18 (2007).
27. Sowa, M.E., Bennett, E.J., Gygi, S.P. & Harper, J.W. Defining the human deubiquitinating enzyme interaction landscape. Cell 138, 389-403 (2009).
28. Hong, S., Kim, S.J., Ka, S., Choi, I. & Kang, S. USP7, a ubiquitin-specific protease, interacts with ataxin-1, the SCA1 gene product. Mol Cell Neurosci 20, 298-306 (2002).
29. Canning, M., Boutell, C., Parkinson, J. & Everett, R.D. A RING finger ubiquitin ligase is protected from autocatalyzed ubiquitination and degradation by binding to ubiquitin-specific protease USP7. J Biol Chem 279, 38160-8 (2004).
30. van der Knaap, J.A. et al. GMP synthetase stimulates histone H2B deubiquitylation by the epigenetic silencer USP7. Mol Cell 17, 695-707 (2005).
31. Sarkari, F. et al. EBNA1-mediated recruitment of a histone H2B deubiquitylating complex to the Epstein-Barr virus latent origin of DNA replication. PLoS Pathog 5, e1000624 (2009).
32. Boritzki, T.J., Jackson, R.C., Morris, H.P. & Weber, G. Guanosine-5'-phosphate synthetase and guanosine-5'-phosphate kinase in rat hepatomas and kidney tumors. Biochim Biophys Acta 658, 102-10 (1981).
33. Weber, G. et al. Purine and pyrimidine enzymic programs and nucleotide pattern in sarcoma. Cancer Res 43, 1019-23 (1983).
34. van der Knaap, J.A., Kozhevnikova, E., Langenberg, K., Moshkin, Y.M. & Verrijzer, C.P. Biosynthetic enzyme GMP synthetase cooperates with ubiquitin-specific protease 7 in transcriptional regulation of ecdysteroid target genes. Mol Cell Biol 30, 736-44 (2010).
35. Krissinel, E. & Henrick, K. Secondary-structure matching (SSM), a new tool for fast protein structure alignment in three dimensions. Acta Crystallogr D Biol Crystallogr 60, 2256-68 (2004).
36. Holm, L., Kaariainen, S., Rosenstrom, P. & Schenkel, A. Searching protein structure databases with DaliLite v.3. Bioinformatics 24, 2780-1 (2008).
37. Borodovsky, A. et al. A novel active site-directed probe specific for deubiquitylating enzymes reveals proteasome association of USP14. Embo J 20, 5187-96 (2001).
38. Leggett, D.S. et al. Multiple associated proteins regulate proteasome structure and function. Mol Cell 10, 495-507 (2002).
39. Kohler, A., Zimmerman, E., Schneider, M., Hurt, E. & Zheng, N. Structural basis for assembly and activation of the heterotetrameric SAGA histone H2B deubiquitinase module. Cell 141, 606-17 (2010).
40. Samara, N.L. et al. Structural insights into the assembly and function of the SAGA deubiquitinating module. Science 328, 1025-9 (2010).
41. Luna-Vargas, M.P. et al. Ubiquitin-specific protease 4 is inhibited by its ubiquitin-like domain. EMBO Rep 12, 365-72 (2011).
42. Khoo, K.H., Joerger, A.C., Freund, S.M. & Fersht, A.R. Stabilising the DNA-binding domain of p53 by rational design of its hydrophobic core. Protein Eng Des Sel 22, 421-30 (2009).
43. Buchwald, G. et al. Structure and E3-ligase activity of the Ring-Ring complex of polycomb proteins Bmi1 and Ring1b. Embo J 25, 2465-74 (2006).
44. Pickart, C.M. & Raasi, S. Controlled synthesis of polyubiquitin chains. Methods Enzymol 399, 21-36 (2005).
45. Linares, L.K., Hengstermann, A., Ciechanover, A., Muller, S. & Scheffner, M. HdmX stimulates Hdm2-mediated ubiquitination and degradation of p53. Proc Natl Acad Sci USA 100, 12009-14 (2003).
46. Fitzgerald, D.J. et al. Protein complex expression by using multigene baculoviral vectors. Nat Methods 3, 1021-32 (2006).

4

47. Studier, F.W. Protein production by auto-induction in high density shaking cultures. Protein Expr Purif 41, 207-34 (2005).
48. Leslie, A.G. The integration of macromolecular diffraction data. Acta Crystallogr D Biol Crystallogr 62, 48-57 (2006).
49. Evans, P. Scaling and assessment of data quality. Acta Crystallogr D Biol Crystallogr 62, 72-82 (2006).
50. Vonrhein, C., Blanc, E., Roversi, P. & Bricogne, G. Automated structure solution with autoSHARP. Methods Mol Biol 364, 215-30 (2007).
51. Langer, G., Cohen, S.X., Lamzin, V.S. & Perrakis, A. Automated macromolecular model building for X-ray crystallography using ARP/wARP version 7. Nat Protoc 3, 1171-9 (2008).
52. Emsley, P. & Cowtan, K. Coot: model-building tools for molecular graphics. Acta Crystallogr D Biol Crystallogr 60, 2126-32 (2004).
53. Adams, P.D. et al. PHENIX: a comprehensive Python-based system for macromolecular structure solution. Acta Crystallogr D Biol Crystallogr 66, 213-21 (2010).
54. Blanc, E. et al. Refinement of severely incomplete structures with maximum likelihood in BUSTER-TNT. Acta Crystallogr D Biol Crystallogr 60, 2210-21 (2004).
55. Potterton, L. et al. Developments in the CCP4 molecular-graphics project. Acta Crystallogr D Biol Crystallogr 60, 2288-94 (2004).
56. Gouet, P., Courcelle, E., Stuart, D.I. & Metoz, F. ESPript: analysis of multiple sequence alignments in PostScript. Bioinformatics 15, 305-8 (1999).
57. Krissinel, E. & Henrick, K. Inference of macromolecular assemblies from crystalline state. J Mol Biol 372, 774-97 (2007).
58. Kabsch, W. & Sander, C. Dictionary of protein secondary structure: pattern recognition of hydrogen-bonded and geometrical features. Biopolymers 22, 2577-637 (1983).
59. Svergun, D.I., Petoukhov, M.V. & Koch, M.H. Determination of domain structure of proteins from X-ray solution scattering. Biophys J 80, 2946-53 (2001).

4

Table of contents Supplementary information

4

Data collection statistics	HUBL (Native)	HUBL (SeMet)
Wavelength (Å)	0.873	0.979
Resolution (Å)	2.7	3.0
Space group	$P2_12_12_1$	$P2_12_12_1$
Cell dimensions: a, b, c (Å)	79.98, 82.31, 150.63	79.54, 81.38, 150.10
Resolution (Å)	39.7 – 2.7 (2.85 – 2.7)	45.33 – 2.99 (3.16 – 3.0)
R_{merge} (%)	7.2 (69.3)	6.2 (32.7)
I/σI	11.8 (2.0)	26.2 (7.0)
Completeness (%)	100.0 (99.9)	99.5 (97.0)
Redundancy	4.5 (4.6)	13.1 (12.8)
Refinement		
Number of unique reflections	27939	20203
Number of protein atoms	4340	
Number of waters	129	
Rwork / Rfree (%)	19.1/21.6	
RMSD from ideal geometry		
Bond lengths[a] (Å)	0.009	
Bond angles[a] (°)	1.07	
Ramachandran statistics[a]	514/15/0	
(preferred/allowed/outliers)		

Highest-resolution shell is shown in parentheses
[a] Calculated using Molprobity

Supplementary Table S1. Data collection and refinement statistics

	k_{cat} [s^{-1}]	K_m [μM]	k_{cat}/K_m [M^{-1} s^{-1}]	Ub K_d [μM]
USP7FL	1.42 ± 0.02	2.89 ± 0.10	4.92 *10^5	n.d.
USP7CD-HUBL	1.35 ± 0.06	3.62 ± 0.42	3.72 *10^5	1.5 ± 0.5
USP7CD	0.06 ± 0.02	15.13 ± 1.09	0.04 *10^5	>>35
USP7CD-45	1.32 ± 0.03	2.89 ± 0.20	4.57 *10^5	4.0 ± 0.6
USP7CD + HUBL	0.29 ± 0.03	14.67 ± 1.98	0.20 *10^5	12.9 ± 1.4
USP7CD-HUBL WE285DA	0.31 ± 0.05	9.80 ± 0.59	0.32 *10^5	65.0 ± 5.3
USP7CD-HUBL I1100S	0.07 ± 0.02	10.51 ± 0.58	0.07 *10^5	n.d.
USP7CD-HUBL / GMPS	7.69 ± 0.23	8.95 ± 0.53	8.60 *10^5	2.5 ± 0.2
USP7CD-HUBL WE285DA / GMPS	0.32 ± 0.05	10.78 ± 0.59	0.30 *10^5	n.d.
USP7CD-HUBL I1100S / GMPS	0.07 ± 0.001	13.05 ± 0.13	0.05 *10^5	n.d.

Supplementary Table S2. Summary of the kinetic data determined in Ub-AMC assays and ubiquitin binding, determined using SPR
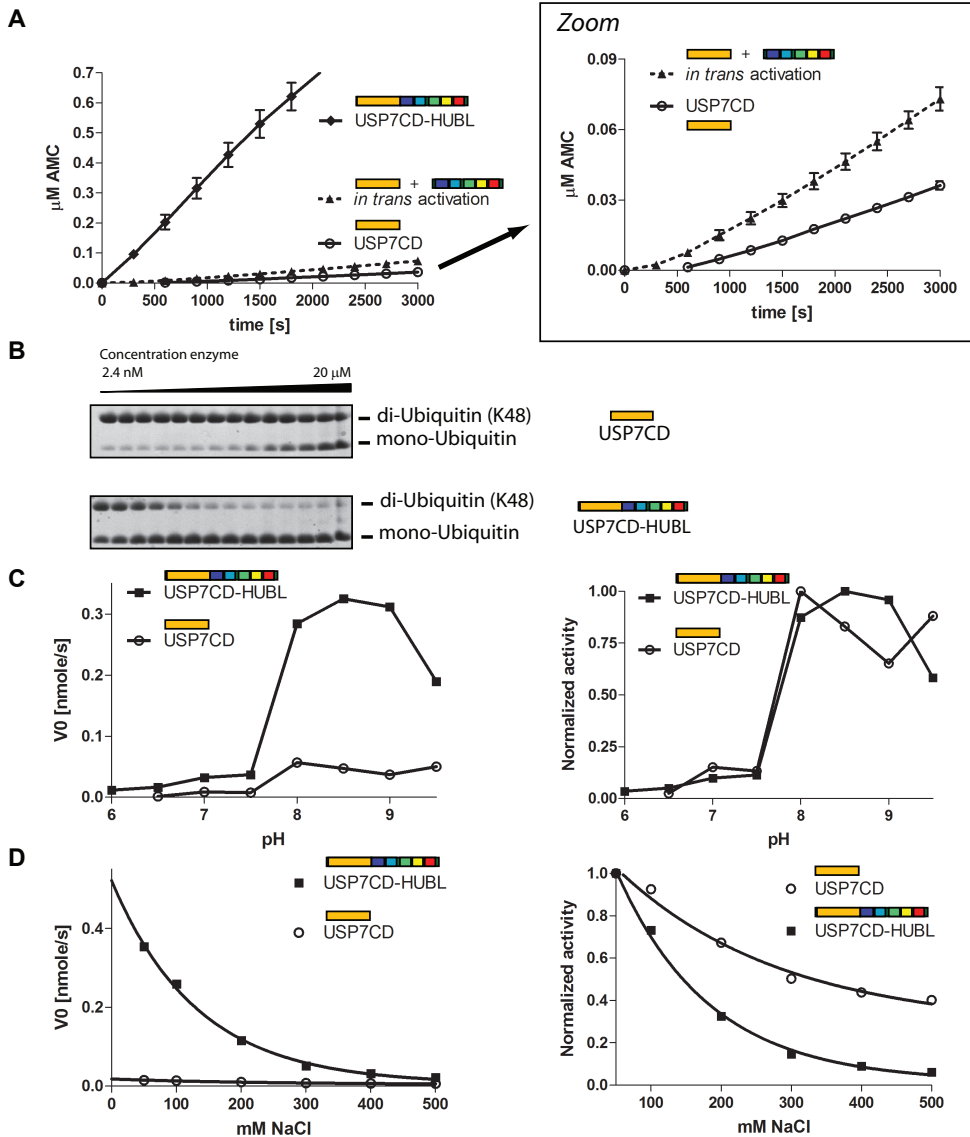
Supplementary Figure S1 related to Figure 1. Characterization of HUBL activation. A. USP7CD can be activated both in trans and in cis by the HUBL domain. Using 1 μM UbiAMC and 1 nM USP7, the activity decreases strongly in the absence of the HUBL domain. This loss can be partially recovered by adding 10 μM HUBL to USP7CD. **B.** USP7CD concentrations need to be 1000-fold increased to achieve the same catalytic turn-over as USP7CD-HUBL. **C.** The pH profile was determined of the USP7 activity was monitored using 1 μM UbiAMC. Both USP7CD and USP7CD-HUBL show a similar pH profile, but it is more pronounced with USP7CD-HUBL due to the higher catalytic rate. **D.** The activity of both USP7CD and USP7CD-HUBL decrease upon increasing NaCl concentration, with a limited strengthening effect of the HUBL domain.

A

Interface Area [Å²]	742.3
ΔiG [kcal/mole]	-7.1
# H-bonds	10
# Salt bridges	2

B

Cα rmsd [Å] →

HUBL	1	2	3	4	5	Ubiquitin
1		2.5	2.1	2.9	2.8	2.0
2	9.1		2.5	2.6	2.7	1.9
3	10.6	9.1		2.9	2.6	2.0
4	9.1	15.2	6.1		2.9	2.5
5	7.6	3.0	12.1	7.6		2.5
Ubiquitin	19.7	12.1	9.1	6.1	15.2	

→ Sequence identity [%]

C

				β1			β2	α1	η1 β3		β4	η2		β5
Ubiquitin	1													
HUBL-1	564													
HUBL-2	684													
HUBL-3	793													
HUBL-4	892													
HUBL-5	987													

Ile44

D

	1-2	2-3	3-4	4-5
Interface Area [Å²]	1199.4	171.1	0	738.7
ΔiG [kcal/mole]	-10.5	0.440		-8.3
# H-bonds	19	1	0	7
# Salt bridges	6	0	0	4

E

Degradation USP7CD-HUBL   *Expression deletion constructs*

USP7CD-HUBL
USP7CD-123
USP7CD-12
USP7CD

Supplementary Figure S2 related to Figure 2. Structural analysis HUBL crystal structure. A. The second helix in the linker region between HUBL-2 and -3 interacts with HUBL-2. Left: Cartoon representation, colours as in Figure 2, Right: Interface parameters, calculated with SSM 1. **B.** Despite the homologous fold, which is quantified by the low Cα rmsd, the primary sequence identity between the Ubl's and with ubiquitin is low. Numbers based on the alignment in C. **C.** Structure based sequence alignment using SSM shows that the Ubl's share the β-grasp fold with ubiquitin. **D.** Interface analysis by PISA 1 revealed extensive interactions between HUBL-1 and -2 and HUBL-4 and -5. **E.** The Ubl domains within HUBL group in a 2-1-2 configuration in solution. USP7CD-HUBL degrades during purification to stable intermediates with masses corresponding to USP7CD-123, USP7CD-12 and USP7CD.
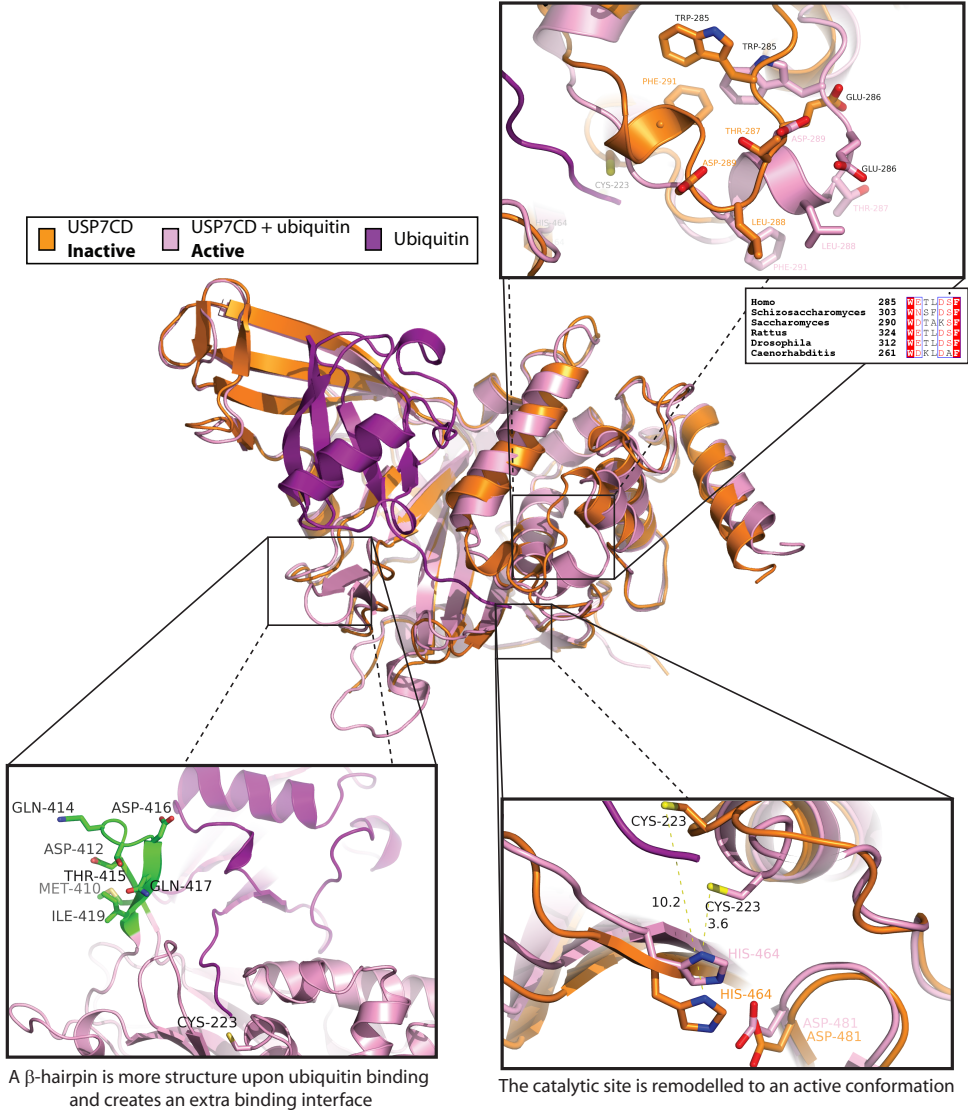
Supplementary Figure S3 related to Figure 4. The C-terminal peptide is essential, but not sufficient, for activation. A. Activity on Ub-AMC shows that upon removal of the C-terminal 19 residues in the flexible peptide loop (ΔC), the activation by the HUBL domain is greatly reduced. However, this peptide is not sufficient to achieve *in trans* activation, to similar levels as complete HUBL-45. **B.** Using SPR, no binding between USP7CD and the C-terminal peptide is observed. The responses are due to aspecific binding to the SPR chip and show no concentration dependence.
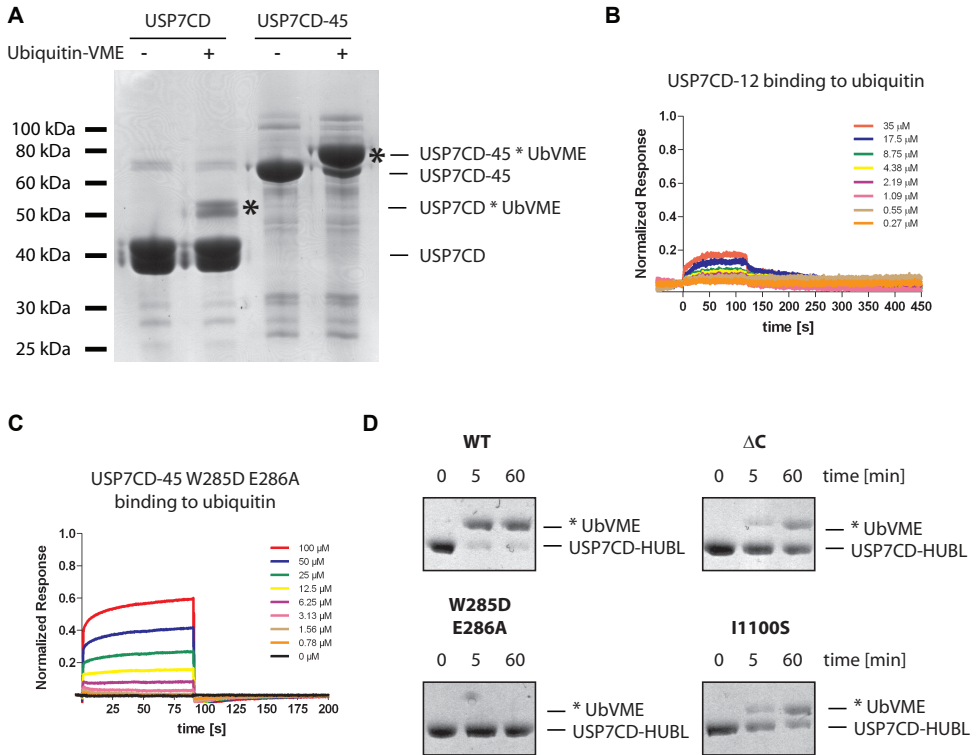
Supplementary Figure S4 related to Figure 5. Ubiquitin affinity is increased by the HUBL domain. A. When incubated with 20 μM suicide substrate ubiquitin-VME2, only USP7CD-45 and not USP7CD was robustly able to form covalent complexes with ubiquitin as shown in this Coomassie stained SDS PAGE gel. Asterisk shows the USP7-ubiquitin complex. **B.** Using SPR binding experiments, very weak binding to ubiquitin was observed for USP7CD-12. GST-ubiquitin was immobilized to the CM5 sensor chip. **C.** Mutations in the 'switching loop' lower affinity for ubiquitin. SPR Sensorgram of the ubiquitin binding of USP7CD-45 W285D E286A (K_d = 65 μM). **D.** When incubated with 5 μM suicide substrate ubiquitin-VME, only WT USP7 and not the mutants was robustly able to form covalent complexes with ubiquitin as shown in Coomassie stained SDS PAGE gel. Asterisk shows the USP7-ubiquitin complex

A

The switching loop changes conformation in the active state

| USP7CD **Inactive** | USP7CD + ubiquitin **Active** | Ubiquitin |

A β-hairpin is more structure upon ubiquitin binding and creates an extra binding interface

The catalytic site is remodelled to an active conformation

Supplementary Figure S5 related to Figure 6. Crystal structure of USP7CD shows conformational changes upon remodelling of the active site and ubiquitin binding. A. Comparison of the apo structure of USP7CD (1NB8), with the ubiquitin complex of USP7CD (1NBF) show movement of a β-hairpin (bottom left), organization of the active site (bottom right) and remodelling of a 'switching loop' (top right), for which the sequence conservation is indicated.

B

HUBL domain

Catalytic domain (PDB: 1NBF)

C
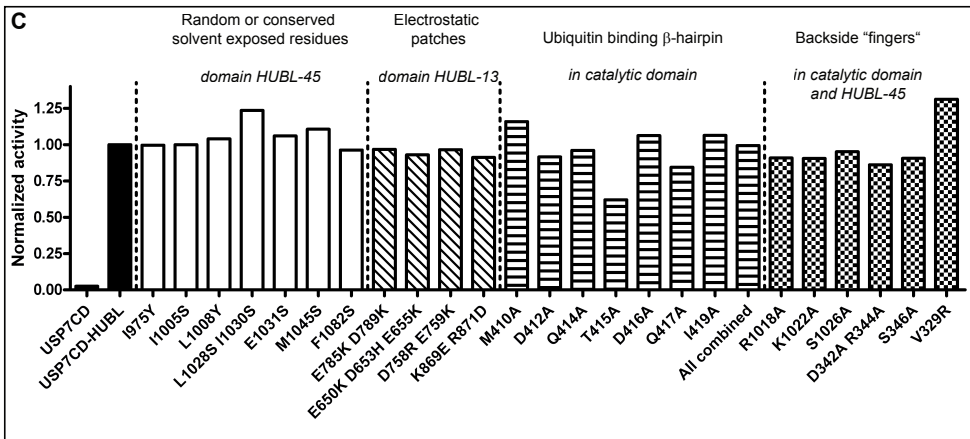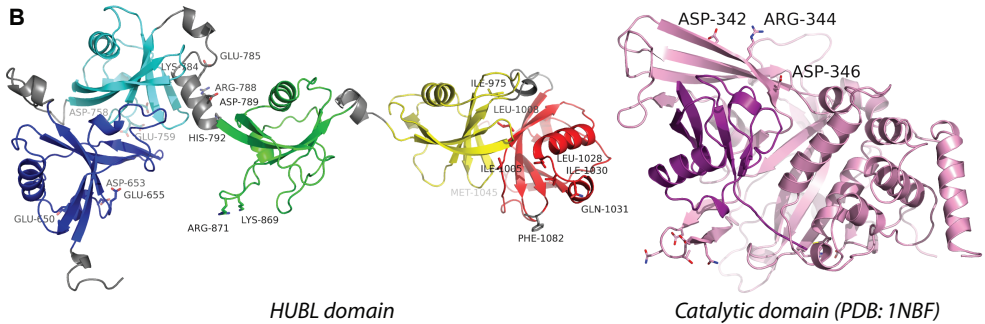
D *Electrostatics HUBL domain*
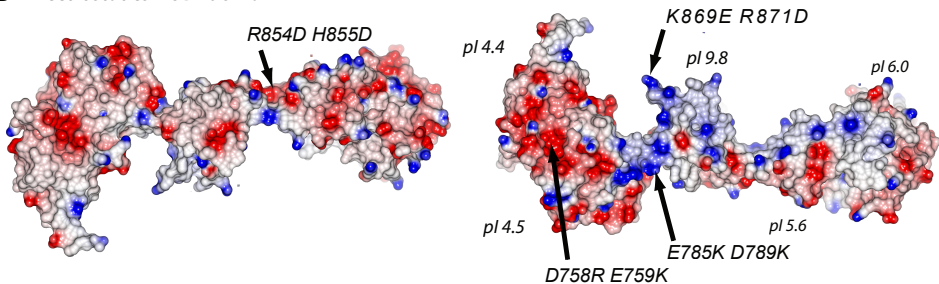
Continued from previous page

B-D. Overview mutations. A priori, three possible activation mechanisms could be envisaged, i) the stabilization of a β-hairpin in the catalytic domain (residues 410 to 420), which is more structured when co-crystallized with ubiquitin, making an extra interface with ubiquitin, ii) restricting the movement of the "finger region", as is achieved in other DUBs by the insertion of an extra helix that stabilizes the fingers domain, or iii) near the active site there is dynamic switching of a loop that dependents on ubiquitin binding. However, since mutations within the ubiquitin binding β-hairpin or the backside of the "finger region" did not have an effect on activation by the HUBL domain, we excluded the first two possibilities. Domains are depicted in cartoon respresentation and the mutants are show in sticks. The activity is normalized to full length USP7. The electrostatic potential is calculated using CCP4MG.
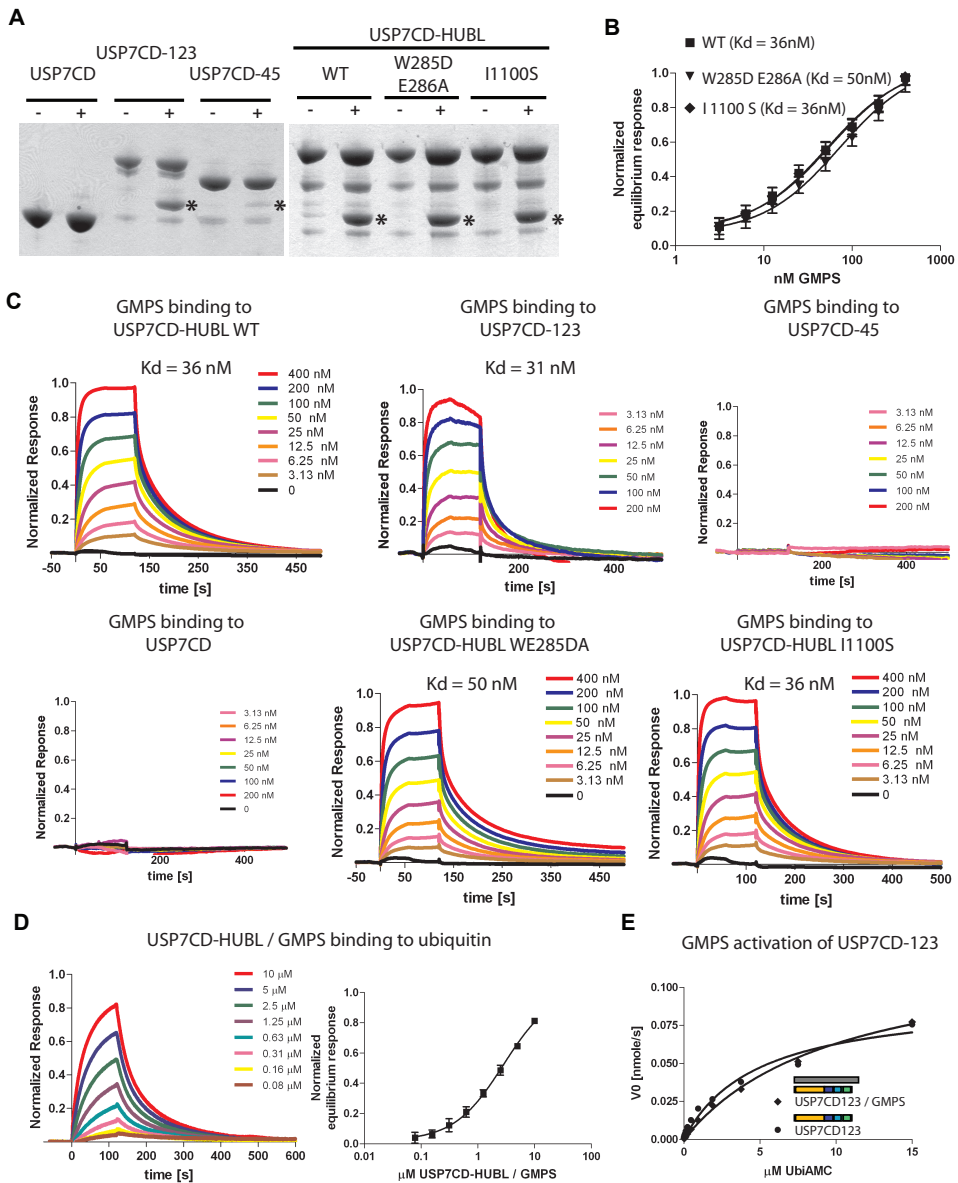
Supplementary Figure S6 related to Figure 7. GMPS activation and binding. A. GMPS can only robustly be pulled down by GST-tagged USP7 constructs containing HUBL-123. **B and C**. Equilibrium responses (B) and sensorgrams (C) of GMPS binding to USP7 constructs and mutants. Using SPR a K_d of 30-40 nM was determined between USP7CD-HUBL and GMPS. The mutants WE285DA and I1100S, and USP7CD-13 behaved similar as wild-type in GMPS binding. No binding was observed for USP7CD and USP7CD-45. **D.** SPR sensorgram of USP7CD-HUBL/GMPS binding ubiquitin ($K_d = 2.5\mu M$). **E.** USP7CD-123 can not be hyper-activated by GMPS in the Ub-AMC assay.

Chapter 5

General discussion

Both ubiquitination and deubiquitination play important roles in many cellular processes, and they often have a causal role in diseases. Over the last decade our knowledge on DUBs has increased significantly, however many questions regarding their biochemical behavior and structural features remain unanswered. Since DUBs are increasingly acknowledged as possible drug targets, it is imperative that we understand how they work. This will not only give better insights in the biology of the enzymes that will be inhibited, but will also aid in the drug development itself. To this end, we present in this thesis new biochemical, structural and mechanistic insights concerning the modulation of the activity of the largest DUB family; the USPs.

Enzyme kinetics

To understand the biochemical properties of the USP family, we determined the activity kinetics of twelve USPs, as described in chapter two. This revealed large variations in the two kinetic parameters: catalytic turnover (k_{cat}) and ubiquitin binding (approximated by K_M). This shows that the USPs apparently have evolved to play specific biological roles. It would be interesting to see how these numbers correlate with the biological function and context of the DUBs. For example, one could envision that the very active DUBs have a lot of substrates or are needed in very fast processes.

One of the major biochemical questions of the DUBs in general, concerns their differential activity towards the different ubiquitin topoisomers. Until now, most studies have focussed on the canonical K48- and K63-linked poly-ubiquitin. However, the other linkages have also been found *in vivo* and also have important functions[1]. Therefore, we for the first time analysed the activity of all our twelve USPs towards all seven lysine-linked di-ubiquitin topoisomers. We found that the small, but surprising differences are probably due to a steric hindrance by the proximal ubiquitin. A possible function for these preferences can be that DUBs remove the ubiquitination by a certain linkage, and therefore specifically change the function of that protein. Alternatively the DUBs can trim the ubiquitin chains of unwanted linkages. Whether these preferences are biologically relevant remains a question. This will depend on the ubiquitin linkages found on the substrates and biological complex the USPs are part of. Fact is that DUBs are often found in complex with E3 ligases, and therefore potentially change or fine-tune their biological activity.

We determined the ubiquitin topoisomers preference by using di-ubiquitin. However, ubiquitin chains can be much longer than di-ubiquitin, and these longer ubiquitin chains possibly have different properties. For example, K48-linked ubiquitin adopts a closed conformation when it is composed of at least four ubiquitin moieties[2]. Moreover, this closed tetra-ubiquitin represents the minimal signal for degradation[3]. This ability to form high-order structures is possibly not unique for K48-linked ubiquitin. The crystal packing of K11-linked di-ubiquitin shows the stacking of two ring-shaped tetramers, forming a barrel-shaped octamer[4]. This ubiquitin organization will have a profound effect on the hydrolysis by DUBs. Therefore future studies are required to determine the minimal length of all ubiquitin chain-types needed to invoke their biological function or a high-order structure. Only then we will obtain the full picture of the differential effects of ubiquitin linkages on the hydrolysis by DUBs.

Overall, the biological relevance of the enzyme properties will depend much on the protein complex they are part of[5]. DUBs are promiscuous enzymes by nature. They often have limited substrate specificity and deubiquitinate many proteins in the cell. Therefore, the activity of the DUBs is regulated by interacting proteins. So, we need to understand more of the larger protein complexes to fully understand the function of the preferences for ubiquitin topoisomers and the large variations in enzyme properties.

Activity modulation

Another way to regulate the activity of DUBs is by modulating its activity. The characterization of the enzymatic properties of the USPs, revealed that the activity of several USPs can

be modulated. In light of the promiscuous behavior of the USPs, it is not surprising that domains and interacting proteins can influence the activity. After all, this allows the adjustment of the activity to match the requirements within a larger protein complex. This modulation of the activity can happen at several levels, by small variations in the catalytic domain, by internal domains or by interacting proteins.

Some USPs have structural plasticity or small insertions in the catalytic domains that possibly influence their activity. For example, the two ubiquitin-binding surface loops in USP4 (chapter three) and USP14[6] block the active site, but relocate after ubiquitin binding. Another example is the catalytic domain of USP8[7]. Due to an inserted α-helix at the backside of the finger region it is in a closed conformation. This suggests a perturbed ubiquitin binding, which nicely correlates in the weak K_M value observed in the kinetic analysis.

In USP4, USP7 and USP16 the activity is modulated by internal domains. The mechanisms of USP4 (UBL inserted in the catalytic domain) and USP7 (HUBL domain) are discussed in chapters three and four. To date, the activation mechanism of USP16 by the ZnF-UBP domain is unclear. This domain is also present in USP5 where it is involved in ubiquitin binding and is responsible for activating USP5 by increasing the affinity for poly-ubiquitin[8]. But since the domain in USP16 increases k_{cat} rather than K_M, the activation mechanism in USP16 is probably different.

The activity of DUBs can also be modulated by interacting proteins. In this thesis we discuss the activation of USP7 by GMPS (chapter four). We also characterized the UAF1 activation of USP1, USP12 and USP46. Both these modulators increase the k_{cat} of their associated USP. However GMPS and UAF1 probably use a different activation mechanism. GMPS hyper-activates USP7, which on its own already is active. On the other hand, USP1, USP12 and USP46 show only very limited activity without UAF1. Modulators have also been found in other DUB families. For example in *drosophila* the UCH DUB Calypso (BAP1 is the closest homologue in

humans) needs to interact to the Asx protein to be active[9]. Also, the Ubp8 (yeast homologue of USP22) is only active when it is embedded in the SAGA complex[10,11]. Unfortunately, we do not yet understand all the mechanisms underlying the activation.

It is clear that (often small) details do seem to add up to large difference in the overall activity of the USPs. Crystal structures will reveal many of these details and will be valuable for (structure-based) drug design. Therefore, what is missing are (more) structures of catalytic domains with large insertions, full-length multi-domain enzymes or even complex structures to fully explain the function and activity of the DUBs.

Ubiquitin-like domains in Ubiquitin-Specific Proteases

The presence of ubiquitin-like domains within the context of ubiquitin-specific proteases is surprising, and their incorporation in at least 17 USPs makes them abundant as well. This thesis shows that UBL domains have diverse functions in USPs. Judging by their low sequence identity with each other and with ubiquitin, they have been incorporated in the USPs early in the evolution (Figure 1). Still, in USP4 the UBL domain sufficiently mimics ubiquitin to allow competition for ubiquitin binding.

When looking at the sequence similarity of the USP family members, one can identify two distinct clusters of UBL integrations. The first contains almost all the USPs with insertions in the catalytic domain. The second group has a relatively large sequence divergence compared to the first, and contains the USPs with N-terminal and C-terminal UBL domains. The N-terminal and C-terminal UBL containing USPs in turn cluster in two subgroups, with USP47 in between, which contains UBL at both sides of the catalytic domain.

The UBL domains are capable to modulate the activity of the USPs. Chapter three describes the mechanistic characterization of the competition for binding between a UBL and ubiquitin to the catalytic domain in USP4. This competition is intriguing, since the UBL in solution is such a
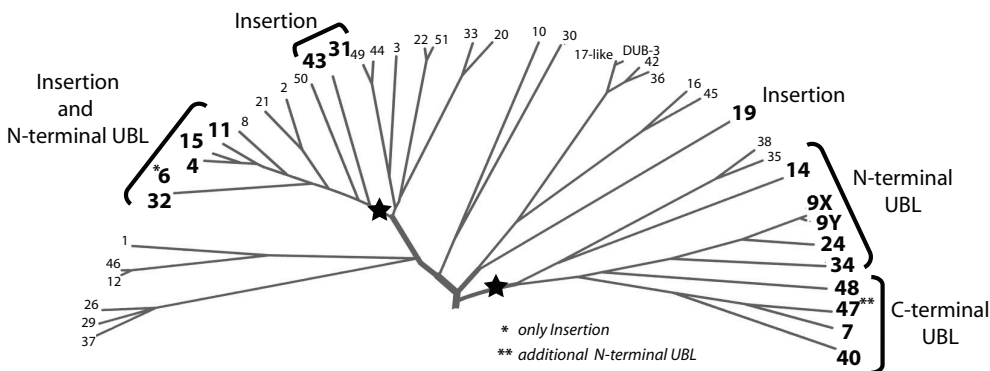
Figure 1. Dendogram showing the phylogenetic relationship of part of the USPs. This revealed two likely evolutionary UBL integration points (stars). Diagram adapted from *Nijman et al. Cell (2005)*.

good ubiquitin mimic that the binding behavior to the catalytic domain is very similar. In fact, both binding constants to the catalytic domain are identical. This poses a problem that is not fully understood yet. The local concentration of the UBL is very high (after all it is in the same chain) and is always (much) higher than the concentration of ubiquitin. Therefore, one would suspect that only in a very limited number of conditions, the ubiquitin would be able to successfully compete for binding to the catalytic domain. However, this does not seem to be the case, since the enzyme with the UBL still shows robust activity. Apparently the ability of the UBL to bind to the catalytic domain is impaired when it is within the same chain as the catalytic domain. It is unclear what causes this impaired binding. Possibly, the ability of the UBL to bind to the catalytic domain changes during the reaction cycle. Alternatively, there could be structural elements in the rest of the insert modulate the binding of the UBL. What these conditions and features are is still unknown.

In some cases, the UBLs have evolved beyond ubiquitin mimics and have taken up different functions. Chapter four describes how USP7 has UBL domains that can function as protein-protein interaction domains with interesting functional consequences. In contrast to the two UBLs in USP4, there are five consecutive UBLs in the HUBL domain, making it a unique domain amongst USPs. Based on our SAXS experiments, the HUBL domain can be divided into two different regions, HUBL-123 and HUBL-45, connected through a flexible linker. Both HUBL subdomains are protein-protein interaction sites, capable of binding to different proteins. We show that HUBL-123 is dispensable for USP7 activity, but rather it serves as a binding platform and interacts with GMPS. This interaction allosterically activates USP7. From the literature we know that HUBL-123 also binds to the E3 ligases ICP0 and HDM2. ICP0 and HDM2 seem to have no activating role, but interact to prevent their auto-ubiquitination[12,13].

In contrast to HUBL-123, HUBL-45 is the active unit within the HUBL domain and is sufficient for the activation of USP7. It makes a (weak) intra-molecular interaction with the catalytic domain of USP7. This interaction remodels a switching loop, which in turn re-aligns the catalytic residues to form an active enzyme. This "switch" results in the increase of ubiquitin affinity and catalytic turnover. The binding of GMPS to HUBL-123 promotes the binding of HUBL-45 to the catalytic domain. This shifts the equilibrium between "active" and "inactive" conformations towards the active state, and therefore results in more active molecules. The fact that GMPS can enhance the interaction between HUBL-45 and the catalytic domain, suggests that this interaction is dynamic. Therefore GMPS probably acts as a molecular lock, preventing the flexibility within the HUBL domain. The crystal structure of the complex of USP7 and GMPS complex would explain the molecular details of this interaction and activation.

However, HUBL-45 also serves as a binding platform and interacts with two different USP7 substrates: p53 and FOXO4. It is unknown whether these interactions affect USP7 activity. A large proteomics effort has identified a list of additional interactors of USP7, for which most neither interaction site nor function are known[5]. Since the HUBL domain is flexible, potentially different proteins can interact with different conformations of the HUBL domain. GMPS binds to a conformation that promotes activity, but it could be possible that one of those interactors binds to a conformation that does not allow HUBL activation. This protein would be able to negatively regulate USP7 activity. Future research is needed to see whether the uncharacterized interactors have implications for the USP7 function, and whether the dynamic switching between different conformations of the HUBL domain induces different binding profiles of interacting proteins.

So, in contrast to the inhibition by a UBL in USP4, there is an activation of USP7. Moreover, the UBL domain in USP14 is needed for the recruitment to the proteasome[14]. Therefore, to date three UBL domains in the USP family have been functionally characterized and all have a different function. The phylogenetics show that the three USPs are relatively distant family members (Figure 1). Probably the inserted UBL domains in USP11 and USP15 apply a similar auto-inhibiting as we have seen in USP4. However, the large sequence divergence of the UBL domains allows for large variations in function. So for now, it is difficult to extrapolate our results and predict the functions of the other UBL domains. Also, to date it remains unclear why the USPs have evolved to use ubiquitin-like β-grasp for their function.

Regulation of the modulation
The intriguing consequence of activity modulation is that it creates possibilities for regulation. In chapter three we describe that USP4 can be relieved of its auto-inhibition by the sequestering of the UBL by at least two other USPs. Since this UBL seems to be a good ubiquitin mimic, it is therefore possible that more USPs can bind and have functional consequences. It is also possible that this UBL can bind to ubiquitin-binding domains, which would mean that many more proteins are able to regulate USP4 activity.

USP7 plays a pivotal role in directly regulating many important cellular processes. Therefore, the regulation of the HUBL activation could provide a fast response to external stimuli. As seen in chapter four, the HUBL domain activation is also essential for the activity of USP7 in cells. From literature we know that the GMPS interaction activates USP7 towards p53 and is essential for H2B deubiquitination *in vivo*[15-17]. However, *in vivo* not all USP7 is bound to GMPS and vice versa, which suggests that there are distinct conditions in which USP7 needs to be modulated by GMPS. In other words, the USP7 activity modulation is regulated. This is possibly regulated by post-translational modifications on USP7 itself[18].

It is tempting and exciting to speculate that the dynamic regulation of USP7 activity by its internal HUBL domain also exists in cells. Hopefully in the near future, we will be able to study this switching of states insides cells. This will enable the analysis of USP7 regulation under diverse cellular conditions and with the many known USP7 interacting proteins. This might identify the situations where targeting USP7 with drugs is most beneficial.

Overall, this thesis presents new insights in the activity characteristics of the USP family. DUBs are involved in several diseases[19-24], and have been acknowledged as promising drug targets[25]. The unique features of the USPs in both enzyme kinetics and activity mechanisms that we present in this thesis, create new possibilities in designing specific drugs.

5

References

1.   Komander, D. The emerging complexity of protein ubiquitination. Biochem Soc Trans 37, 937-53 (2009).
2.   Cook, W.J., Jeffrey, L.C., Kasperek, E. & Pickart, C.M. Structure of tetraubiquitin shows how multiubiquitin chains can be formed. J Mol Biol 236, 601-9 (1994).
3.   Thrower, J.S., Hoffman, L., Rechsteiner, M. & Pickart, C.M. Recognition of the polyubiquitin proteolytic signal. Embo J 19, 94-102 (2000).
4.   Bremm, A. & Komander, D. Emerging roles for Lys11-linked polyubiquitin in cellular regulation. Trends Biochem Sci 36, 355-63 (2011).
5.   Sowa, M.E., Bennett, E.J., Gygi, S.P. & Harper, J.W. Defining the human deubiquitinating enzyme interaction landscape. Cell 138, 389-403 (2009).
6.   Hu, M. et al. Structure and mechanisms of the proteasome-associated deubiquitinating enzyme USP14. Embo J 24, 3747-56 (2005).
7.   Avvakumov, G.V. et al. Amino-terminal dimerization, NRDP1-rhodanese interaction, and inhibited catalytic domain conformation of the ubiquitin-specific protease 8 (USP8). J Biol Chem 281, 38061-70 (2006).
8.   Reyes-Turcu, F.E. et al. The ubiquitin binding domain ZnF UBP recognizes the C-terminal diglycine motif of unanchored ubiquitin. Cell 124, 1197-208 (2006).
9.   Scheuermann, J.C. et al. Histone H2A deubiquitinase activity of the Polycomb repressive complex PR-DUB. Nature 465, 243-7 (2010).
10.   Kohler, A., Zimmerman, E., Schneider, M., Hurt, E. & Zheng, N. Structural basis for assembly and activation of the heterotetrameric SAGA histone H2B deubiquitinase module. Cell 141, 606-17 (2010).
11.   Samara, N.L. et al. Structural insights into the assembly and function of the SAGA deubiquitinating module. Science 328, 1025-9 (2010).
12.   Boutell, C., Canning, M., Orr, A. & Everett, R.D. Reciprocal activities between herpes simplex virus type 1 regulatory protein ICP0, a ubiquitin E3 ligase, and ubiquitin-specific protease USP7. J Virol 79, 12342-54 (2005).
13.   Meulmeester, E. et al. Loss of HAUSP-mediated deubiquitination contributes to DNA damage-induced destabilization of Hdmx and Hdm2. Mol Cell 18, 565-76 (2005).
14.   Borodovsky, A. et al. A novel active site-directed probe specific for deubiquitylating enzymes reveals proteasome association of USP14. Embo J 20, 5187-96 (2001).
15.   Sarkari, F. et al. EBNA1-mediated recruitment of a histone H2B deubiquitylating complex to the Epstein-Barr virus latent origin of DNA replication. PLoS Pathog 5, e1000624 (2009).
16.   van der Knaap, J.A., Kozhevnikova, E., Langenberg, K., Moshkin, Y.M. & Verrijzer, C.P. Biosynthetic enzyme GMP synthetase cooperates with ubiquitin-specific protease 7 in transcriptional regulation of ecdysteroid target genes. Mol Cell Biol 30, 736-44 (2010).
17.   van der Knaap, J.A. et al. GMP synthetase stimulates histone H2B deubiquitylation by the epigenetic silencer USP7. Mol Cell 17, 695-707 (2005).
18.   Fernandez-Montalvan, A. et al. Biochemical characterization of USP7 reveals post-translational modification sites and structural requirements for substrate processing and subcellular localization. Febs J 274, 4256-70 (2007).
19.   Nijman, S.M. et al. The deubiquitinating enzyme USP1 regulates the Fanconi anemia pathway. Mol Cell 17, 331-9 (2005).
20.   Singhal, S., Taylor, M.C. & Baker, R.T. Deubiquitylating enzymes and disease. BMC Biochem 9 Suppl 1, S3 (2008).
21.   Brummelkamp, T.R., Nijman, S.M., Dirac, A.M. & Bernards, R. Loss of the cylindromatosis tumour suppressor inhibits apoptosis by activating NF-kappaB. Nature 424, 797-801 (2003).

22.   Bignell, G.R. et al. Identification of the familial cylindromatosis tumour-suppressor gene. Nat Genet 25, 160-5 (2000).
23.   Papa, F.R. & Hochstrasser, M. The yeast DOA4 gene encodes a deubiquitinating enzyme related to a product of the human tre-2 oncogene. Nature 366, 313-9 (1993).
24.   Sacco, J.J., Coulson, J.M., Clague, M.J. & Urbe, S. Emerging roles of deubiquitinases in cancer-associated pathways. IUBMB Life 62, 140-57.
25.   Colland, F. The therapeutic potential of deubiquitinating enzyme inhibitors. Biochem Soc Trans 38, 137-43 (2010).

5

$\leftrightarrow$

Addendum

Summary
Samenvatting
List of abbreviations
Curriculum Vitae
PhD portfolio
List of publications
Dankwoord

$\leftrightarrow$

Summary

In concert with DNA, proteins form the hart of all cellular processes. They are therefore essential for the cell to perform its task. To ensure optimal control of these processes, tight regulating of these proteins is required. To achieve this, the cell controls the levels of protein synthesis, degradation or modification. Posttranslational modifications are both a powerful and rapid way to dramatically change the fate of the protein, its function or subcellular localization. Especially in signaling cascades, they provide a fast and accurate way to ensure control over protein function, sometimes in very complex networks.

Several chemical modifications exist in cells, ranging from small chemical groups, like phosphorylation, methylation or acetylation, to even small proteins. The most famous protein modification is the covalent attachment of the small protein ubiquitin to lysine residues of the target protein. This essential, common and widespread modification is involved in virtually all cellular processes. Like other modifications, ubiquitination is a dynamic process. The ubiquitin moieties can be removed from target proteins by Deubiquitinating enzymes (DUBs). They provide negative feedback, and therefore are an important and integral part of the ubiquitin conjugation system.

The work described in this thesis provides mechanistic insight in de-ubiquitination by describing biochemical and structural aspects of the largest DUB family, the Ubiquitin Specific proteases (USPs). USP family members share a homologous catalytic domain, which would suggest they share biochemical properties. However, protein sequence analysis and crystal structures identified several distinct variations that affect their properties. Since we lack the tools to predict the effect of these variations on the activity, we performed a large-scale kinetic analysis of twelve USP family members, as described in **chapter two**. The very large differences in both in the catalytic turnover and ubiquitin binding that we observed, result in a unique kinetic behaviour of each USP. On top of this great diversity in kinetic properties, an extra layer of regulation exists by means of activity modulation. This way a domain or interacting protein can change the activity characteristics. We characterized the activation or inhibition of the catalytic domain of three USPs by internal domains. In addition, four USPs can bind to a non-DUB protein which results in an increase of the catalytic turnover.

One of the major questions of the DUBs in general, concerns their differential activity towards the different poly-ubiquitin linkages. So far, most studies have focussed on the canonical K48- and K63-linked poly-ubiquitin. Although we do not fully understand the functions and biological roles of the other five linkages, they serve equally important functions in the cell. Therefore, we also describe for the first time the activity of all our twelve USPs towards all seven lysine-linked di-ubiquitin topoisoforms. We found that the small, but surprising differences are most likely due to a steric hindrance of one of the ubiquitin moieties. Future research is required to determine the biological relevance of these differences.

Some USPs contain surprising additional domains. One of the most striking is the Ubiquitin-like (UBL) domain. Fold recognition algorithms show that at least 17 USPs contain such a UBL domain in their context. **Chapter three** describes the function of a UBL inserted in the catalytic domain of USP4. We determined the crystal structure of the USP4 catalytic domain without the UBL. This UBL was able to compete for ubiquitin binding to this catalytic domain, and was therefore able to inhibit its activity. Additionally, other USPs can bind to this UBL insert, which in turn relieves USP4 from its auto-inhibition.

However, not all UBL domains behave as competitive inhibitors. In USP7, also known as Hausp, UBL domains just outside its catalytic domain are essential for the activity. USP7 is one of the most famous and best studied DUBs, since it directly regulates many important proteins in oncogenic pathways, like p53, MDM2 and PTEN. This makes it an interesting drug target that is actively pursued by both academia and the pharmaceutical industry. **Chapter four**

&

describes the activation mechanism of USP7 by this Hausp UBL (HUBL) domain. We solved the crystal structure of HUBL domain, which showed us that it contains five consecutive UBL domains with two novel di-UBL units (2-1-2). The last two UBLs (HUBL-45) were sufficient to achieve full activity and ubiquitin binding. This di-UBL unit interacted directly with the catalytic domain, which caused the remodeling of the active site to an active conformation. Therefore, binding of HUBL-45 resulted in the switching from an 'inactive' to an 'active' state. This switching is dynamic, because the metabolic enzyme GMP sythetase (GMPS) can bind to HUBL-123, which promotes the 'active' state by increasing the affinity of HUBL-45 to the catalytic domain. Therefore the HUBL activation is allosterically regulated by GMPS binding, resulting in more active enzymes.

Overall, USPs play important role in many cellular processes, and often have a causal role in diseases. They have been acknowledged as promising drug targets. However, to aid the (structure-based) drug design, it is also important to understand the biochemical and biophysical properties and activity mechanisms. Together this will give us a complete picture of how the enzymes work. Therefore we performed a general biochemical characterization, which provided new insights in the linkage specificity and variability within the USP family. In this thesis we also show that the activity of individual USPs can be modulated by both intra- and intermolecular domains or proteins, and we elucidated the modulation mechansism of USP4 and USP7. The fact that USPs have unique characteristics and activity mechansisms, presents opportunities in the development of new and specific drugs.

&

Samenvatting

Samen met DNA, vormen eiwitten het hart van alle cellulaire processen. Zonder eiwitten zou een cel zijn taken niet kunnen uitvoeren. Echter om te zorgen dat de eiwitten hun taken goed uitvoeren, moet de cel wel strikte controle over ze houden. Dit kan op verschillende manieren. De cel kan bijvoorbeeld reguleren hoeveel er van een bepaald eiwit aanwezig is. Maar hij kan ook besluiten een eiwit te inactiveren door het te laten afbreken. In dit proefschrift hebben we het vooral over de mogelijkheid om chemische veranderingen aan te brengen aan bestaande eiwitten. De chemische verandering van een eiwit zorgt ervoor dat het nieuwe eigenschappen krijgt. Hierdoor kan de activiteit van een eiwit veranderd worden, maar ook bijvoorbeeld de functie of locatie in de cel.

Er zijn verschillende soorten chemische modificaties mogelijk. Zo kan een eiwit gemodificeerd worden door kleine chemische groepen, zoals fosfor, methyl-groepen of acetaat. Maar er worden ook kleine eiwitten gebruikt en de meest bekende is met een eiwit genaamd ubiquitine. Door middel van een cascade van drie enzymen (E1, E2 en E3) kan heel specifiek een covalente koppeling gemaakt worden tussen het substraateiwit en de ubiquitine. Dit ubiquitine conjugatie systeem is essentieel en wordt veel gebruikt en is betrokken in bijna alle processen in een cel. Echter, de ubiquitine kan ook weer verwijderd worden van het substraateiwit waardoor het weer in de oude toestand terugkeert. Dit wordt gedaan door Deubiquitinerende Enzymen (DUBs in het Engels). Deze enzymen spelen dus ook een belangrijke rol in de dynamische regulatie van eiwitten. Het is dus ook geen verassing dat meerdere DUBs betrokken zijn in verschillende ziektes. Mede daarom worden DUBs ook gezien als interessante enzymen voor de ontwikkeling van medicijnen. Onze kennis over de DUBs is groeiende, maar er zijn nog veel open vragen. En om het medicijnonderzoek te vergemakkelijken is het belangrijk dat we beter begrijpen hoe deze enzymen werken.

In dit proefschrift beschrijven we een karakterisatie van de grootste familie van deubiquitinerende enzymen: de Ubiquitine Specifieke Proteasen (USPs). Alle USPs hebben een homoloog katalytisch domein, wat suggereert dat ook de biochemische eigenschappen vergelijkbaar zijn. Echter, de eiwitsequentie en de drie dimensionale eiwitstructuren brachten specifieke verschillen aan het licht die invloed kunnen hebben op de biochemische eigenschappen. Bovendien is er veel variatie in de domeinen die de USPs hebben naast hun katalytisch domein. Aangezien we niet kunnen voorspellen hoe die verschillen zich precies laten vertalen, hebben we op grote schaal een analyse gedaan naar de kinetische eigenschappen van twaalf USPs. Het resultaat hiervan staat beschreven in **hoofdstuk twee**. Dit laat zeer grote verschillen zien in zowel de reactie snelheid als de ubiquitine binding. Dit betekent dat elke USP unieke kinetische eigenschappen heeft ontwikkeld.

Ubiquitine kan in verschillende vormen in de cel voorkomen. Het kan namelijk ook ketens vormen door gekoppeld te worden aan andere ubiquitine moleculen. Deze ketens worden gevormd door gebruik te maken van de zeven lysine aminozuren van ubiquitine. Welke lysine wordt gebruikt bepaald bovendien wat de functie van de keten is. Verschillende soorten ketens hebben namelijk een andere uitwerking op het substraateiwit. DUBs kunnen deze keten afbreken door de verbindingen tussen de ubiquitines te hydrolyseren. Maar een belangrijke vraag is of ze misschien een voorkeur het voor een bepaald type keten. Tot nu toe werd er voornamelijk gekeken naar twee van de zeven mogelijke ubiquitine ketens (gekoppeld via lysine 48 en 63). Onze kennis van de andere vijf soorten ketens is nog relatief beperkt, maar het is wel duidelijk dat ze belangrijke functies hebben in de cel.

Om te zien of onze twaalf USPs een voorkeur hebben voor een bepaald type ubiquitine keten, hebben wij voor de eerste keer systematisch gekeken naar alle zeven verschillende (lysine) koppelingen. We vonden inderdaad variaties en we kunnen die waarschijnlijk verklaren doordat bij sommige ubiquitine koppelingen de onderlinge oriëntatie van twee ubiquitines de binding aan het katalytisch domein

&

verstoort. Wat de biologische relevantie van deze verschillen is, moet nog verder onderzocht worden.

Buiten het katalytisch domein hebben USPs extra domeinen. Een van de meeste verassende domeinen is het Ubiquitine Achtige domein (UBL in het Engels). Eiwit vouwing herkenning algoritmes voorspellen op basis van eiwit sequentie dat minstens 17 USPs een UBL domein in hun context hebben. In hoofdstuk twee zagen we al dat de UBL domeinen van USP4 en USP7 de activiteit van hun USP kunnen beïnvloeden. In **hoofdstuk drie** beschrijven we de functie van een UBL domein dat midden in het katalytische domein van USP4 zit. We hebben de structuur van het katalytisch domein zonder het UBL domein opgelost. We vonden dat de activiteit van USP4 werd verlaagd door het UBL domein, omdat het concurreert met ubiquitine voor het binden aan het katalytische domein. Bovendien kunnen ook andere USPs aan het UBL domein van USP4 binden. Hierdoor wordt het UBL domein dan weggevangen, waardoor de zelfremmende functie van de UBL wordt tegengaan.

Niet alle UBL domeinen hebben een remmende werking. In USP7, ook wel bekend onder de naam Hausp, wordt de activiteit verassend genoeg juist verhoogd door de UBL domeinen die net buiten het katalytische domein liggen. De activiteit van USP7 is zelfs bijna helemaal afhankelijk van deze UBL domeinen. USP7 reguleert de functie van de eiwitten p53, HDM2 en PTEN. Omdat dit eiwitten zijn die een belangrijke rol spelen in het ontstaan van kanker, is USP7 een van de meest bestudeerde DUBs. Daarom is het een interessant eiwit voor medicijnonderzoek en zijn zowel de farmaceutische industrie als academische onderzoeksgroepen actief op zoek naar een specifieke remmer. In **hoofdstuk vier** beschrijven we het mechanisme waarmee het Hausp UBL (HUBL) domein de activiteit van USP7 verhoogd. We hebben de structuur van het HUBL domein opgelost, en deze bleek te bestaan uit vijf opeenvolgende UBL domeinen met twee nog nooit vertoonde di-UBL eenheden (2-1-2). De laatste twee UBL domeinen (HUBL-45) bleken voldoende om

het activerende effect van het HUBL domein tot stand te brengen. Dit di-UBL eenheid bleek direct te binden aan het katalytische domein, en deze interactie bepaalt of het eiwit zich in een 'actieve' of een 'inactieve' toestand bevindt. Deze omschakeling tussen de twee toestanden is dynamisch. Immers, het binden van het metabolisch enzym GMP synthetase (GMPS) aan HUBL-123, promoot de actieve toestand door de bindingsterkte tussen HUBL-45 en het katalytische domein te verhogen. Het binden van GMPS aan USP7 resulteert daarom in een toename van de hoeveelheid actieve enzym moleculen.

Kortom, DUBs zijn belangrijk zijn in tal van cellulaire processen, en zijn dus ook vaak betrokken bij de ontwikkeling van ziektes. DUBs zijn daarom interessant voor de medicijnontwikkeling. Om daarmee te helpen is het belangrijk dat we de biochemische en biofysische eigenschappen en werkingsmechanismen begrijpen. Dit proefschrift laat zien dat er grote variatie bestaat in de USP familie en dat er een voorkeur bestaat voor bepaalde types ubiquitine ketens. We laten ook zien dat de activiteit van sommige USPs gemoduleerd wordt door zowel de intramoleculaire domeinen of interacterende eiwitten. Dit laat zien dat ondanks dat de USPs een homoloog katalytische domein hebben, zij toch persoonlijke werkingsmechanismen hanteren. Het feit dat de USPs unieke eigenschappen en mechanismen hebben, biedt mogelijkheden tot de ontwikkeling van nieuwe en specifieke medicijnen.

List of abbreviations

Å	Ångstrom (1 Ångstrom = 0.1 nm)
APC	Anaphase promoting complex
ATM	Ataxia telangiectasia mutated
ATR	Ataxia telangiectasia and Rad3-related
CD	Catalytic domain
Da	Dalton
DNA	Deoxyribonucleic acid
DUB	Deubiquitinating enzyme
E1	Ubiquitin-activating enzyme
E2	Ubiquitin-conjugating enzyme
E3	Ubiquitin ligase
EBNA-1	Epstein Barr Virus Nuclear Antigen –1
FL	Full-length
FOXO	Forkhead box protein O
FP	Fluorescence Polarization
GFP	Green fluorescence protein
GMPS	GMP-synthetase
GST	Glutathione S-transferase
H2B	Histone 2B
HDM2	Human Double Minute 2
HUBL	Hausp Ubiquitin-like
hDaxx	Death domain-associated protein 6
HDM2	Human orthologue of Murine Double Minute 2 (MDM2)
ICP0	Infected Cell Protein 0
ITC	Isothermal Titration Calorimetry
K48	Lysine on position 48
k_{cat}	Catalytic turnover
Kd	Dissociation constant
Ki	dissociation constant for inhibitor binding
K_M	Michaelis-Menten constant
MJD	Machodo-Josephin Disease protease
OTU	Ovarian Tumour protease
p53	Tumour antigen p53
PML	Promyelocytic leukaemia protein
PRC	Polycomb repressive complex
PTEN	Phosphatase and tensin homolog
RMSD	Root Mean Square Deviation
SAXS	Small Angle X-ray Scattering
SPR	Surface Plasmon Resonance
TRAF	Tumour necrosis factor receptor associated factor
UAF1	USP1 associated factor 1
UCH	Ubiquitin C-terminal Hydrolase
Ub	Ubiquitin
UBA	Ubiquitin-associated
UBD	Ubiquitin binding domain
UBL	Ubiquitin-like
UIM	Ubiquitin interacting motif
USP	Ubiquitin Specific Protease
Znf UBP	Zinc-finger ubiquitin specific protease

&

$\leftrightarrow$

Curriculum Vitae

Alex Faesen werd geboren op 7 maart 1982 te Amsterdam. Hij behaalde zijn VWO-gymnasium diploma in 2000 aan het Valuascollege in Venlo. Aansluitend begon hij met de studie BioMedische Technologie aan de Technische Universiteit Eindhoven. Zijn eerste afstudeerstage vond plaats in Eindhoven in de vakgroep "BioModeling and BioInformatics" onder supervisie van dr. Koen Pieterse. Zijn tweede afstudeerstage deed hij in de vakgroep "Protein Engineering" in Eindhoven in de groep van dr. Maarten Merkx en prof. dr. ir. Bert Meijer. Met een Erasmus beurs kon hij een derde afstudeerstage doen in de groep van prof. dr. Daan van Aalten in de "School of Life Sciences" in Dundee (UK). Zijn afstudeerwerk werd beoordeeld met het judicium cum laude en hij won in 2005 de "Young KNCV prize". Ook werd zijn afstudeerwerk uitgeroepen tot het beste van de faculteit van dat jaar, en dat resulteerde in de nominatie voor de Mignot prijs. Sinds september 2005 is hij werkzaam geweest als onderzoeker in opleiding in de groep van prof. dr. Titia Sixma op de afdelingen moleculaire carcinogenese en biochemie aan het Nederlands Kanker Instituut te Amsterdam. Met zijn promotieonderzoek won hij de CGC/CBG poster prijs met bijbehorende reisbeurs en won hij bovendien de NWO-CW "Beste Lecture Award" in 2010.

&

$\rightarrow$

PhD portfolio

Summary of PhD training and teaching

Name PhD student   Alexis Caspar Faesen
Erasmus MC Department   Genetics
Research School   Onderzoekschool Oncologie Amsterdam
PhD period   2005-2011
Promotor/Supervisor   prof. dr. Titia K. Sixma

1. PhD training

General courses

2009   Writing and presenting in Biomedicine
2006   Stralinghygiene

Specific courses

2007 and 2009   Basics of crystallography, Amsterdam (the Netherlands)
2006   OOA Course 'Protein structure and Function', Amsterdam (the Netherlands)
2006   'Protein-protein Interaction Caput course', Leiden University (the Netherlands)
2005   PhD student Experimental Oncology course, Netherlands Cancer Institute
                Amsterdam (the Netherlands)

Seminars and workshops

2011   Seminar at the Staff-Meeting Netherlands Cancer Institute, Amsterdam (the
                Netherlands)
2007   BaculoVirus Expression System Workshop, Strasbourg (France)
2007   SPINE2 Workshop Mammalian Expression Systems, Oxford (UK)

Presentations

2011   Annual Rubicon plenary meeting (Malta)
2010   Annual meeting "studiegroep eiwitonderzoek", Veldhoven (the Netherlands)
2006 - 2007   PhD student retreat, Texel (the Netherlands)

(Inter-)national conferences

2011   Annual Rubicon plenary meeting, Malta (poster contribution and lecture)
2010   CGC/CBG meeting 'Molecular Mechanisms in Cancer', Amsterdam,
                the Netherlands (poster contribution)
2010   'A role of ubiquitin-like protein modifications in cancer', Glasgow, UK (poster
                contribution)
2009   The Ubiquitin Family, Cold Spring Harbor, New York, USA (poster contribution)
2005 - 2010   Annual meeting "studiegroep eiwitonderzoek", Lunteren/Veldhoven,
                the Netherlands (poster contribution in 2004 – 2009 and lecture in 2010)
2008   Annual Meeting 3D-Repertoire EU consortium, Milan, Italy
                (poster contribution)
2007   Annual Meeting 3D-Repertoire EU consortium, Barcelona, Spain
                (poster contribution)
2006   Annual Rubicon plenary meeting, Florence, Italy
                (poster contribution)
2006   Annual meeting studiegroep crystallography, Lunteren, the Netherlands
                (poster contribution)
2006   Annual Meeting 3D-Repertoire EU consortium annual meeting, Grenoble,
                France (poster contribution)

2. Teaching

2007   Speaker at BaculoVirus Expression Workshop, Strasbourg, France
2006   Supervising Student

&

List of publications

Faesen AC, Luna-Vargas MPA, Sixma TK.
"Ubiquitin-like domains in Ubiquitin Specific Proteases"
Manuscript in preparation

Faesen AC*, Luna-Vargas MPA*, Geurink PP, El Oualid F, Clerici M, Ovaa H, Sixma TK.
"The differential modulation of USP activity by internal regulatory domains, interactors and seven Ub-chain types"
Manuscript submitted

Faesen AC, Dirac MG, Shanmugham A, Ovaa H, Perrakis A, Sixma TK.
"Mechanism of USP7/HAUSP activation by its C-terminal ubiquitin-like domain (HUBL) and allosteric regulation by GMP-synthetase"
Mol Cell (2011) Oct 7; 44:1-14

Faesen AC, Sixma TK, Everett RD.
"Ubiquitin Specific Protease 7"
Handbook of Proteolytic Enzymes edited by Neil Rawlings and Guy Salvesen, volume 3 (2011)

Luna-Vargas MPA, **Faesen AC**, Dijk WJ van, Rape M, Fish A, Sixma TK.
"Ubiquitin-specific protease 4 is inhibited by its ubiquitin-like domain"
EMBO reports (2011) Apr 1;12(4):365-72.

Shanmugham A, Fish A, Luna-Vargas MPA, **Faesen AC**, El Oualid F, Sixma T.K., Ovaa H
"Non-hydrolyzable Ubiquitin-Isopeptide isosteres as Deubiquitinating enzymes probes"
J. Am. Chem. Soc. (2010) Jul 7 ;132(26) :8834-5

Evers TH, Dongen van EMWM, **Faesen AC**, Meijer EW, Merkx M.
"Quantitative Understanding of Energy Transfer between Fluorescent Protein Domains Connected via Flexible Peptide Linkers Using the Worm-Like Chain Model"
Biochemistry. (2006) Nov 7;45 (44): 13183-92

* These authors contributed equally to this work.

&

Dankwoord

A long journey trough rough terrain. Trying to reach the top of the mountain that is visible from the start, yet seemingly out of reach. The road winding downhill, it seems, more often than uphill. Shortcuts can't be taken for lack of the right climbing gear. And there is no roadmap. Faced with such a challenge, it has been comforting to know there were always people ready to give directions when I needed them. Even if sometimes unwillingly pointing me the wrong way. This is how I made it to the top: independently, but not alone.

Het was een heel avontuur. Onderweg ben ik verbaasd, soms teleurgesteld, maar heb ik vooral ook gelachen en gejuicht. Een van de mooiste dingen in de wetenschap is het ontmoeten van mensen die echt geven om wat ze doen. Daarom wilde ik graag een aantal van de mensen bedanken die onderweg een grote rol hebben gespeeld in het tot stand brengen van dit boekje.

Laten we uiteraard beginnen met Titia. Mijn sollicitatie staat me nog vers in mijn geheugen. Ik was erg onder de indruk en misschien zelfs wel geïntimideerd. Ik had duidelijk een gebrek aan kennis en ervaring. Dank je wel dat je me deze kans hebt gegeven en voor het geduld dat je hebt gehad om me mijn lessen te laten leren. De vele levendige discussies en individuele werkbesprekingen hebben eraan bijgedragen dat ik enorm veel van je heb geleerd en ik hoop dat ik je dat enigszins terug heb kunnen betalen.

Mark, ik kan me nog goed herinneren dat we naar je project zaten te kijken tijdens mijn sollicitatie. Als we toch eens wisten wat er nog allemaal op ons pad zou komen. Ik zie ons ook nog zo zitten op het terras op Texel. Ik was net de week ervoor begonnen en we hadden allebei grootse plannen! Ik vond het erg leuk om het laatste stuk intensief met je samen te werken. Ik denk dat we elkaar heel mooi aanvullen en dat blijkt ook uit de enorme hoeveelheid werk die we verzet hebben. Vandaag gaat de kroon op het werk, en gaan we samen (en als elkaars paranimfen) die bul ophalen! Dank je wel voor al je hulp en het gezamenlijke USP avontuur. Veel succes in New York.

Tassos, first thing that comes to my mind is your seemingly endless knowledge of crystallography. But equally impressive is your attitude and approach towards life and science. The interplay with Titia was very interesting to watch ;-). During our synchrotron trips you were an excellent teacher, and I was always welcome for discussions on SAXS, enzyme kinetics and even career advice. Hopefully at some point we will understand the Russian-English manuals. Thanks for all your help!

Pim, altijd sta je klaar om te helpen. Zonder jou zou dit lab een heel stuk minder soepel lopen. Herrie, sorry dat we je elke dag kwamen lastig vallen tijdens je lunch. Tati, thanks for all your help, you are a star! Always ready to help and always you do just a little bit extra. When my mutagenesis fails again, I'll know where to find you!

Annette, we moesten gescheiden worden van H2 om eindelijk samen te werken en publiceren. Dank je wel en veel succes in je carrière.

De vele discussies op de gang, in het lab, tijdens lunch of gewoon tijdens de werkbesprekingen hebben veel bijgedragen aan mijn projecten, maar ook zeker aan de lol. Rick, altijd kritisch en moeilijk te overtuigen, maar juist daarom al heel snel een zeer gewaardeerde collega. Judith, eindelijk begint het voor jou te werken! Hopelijk het wordt een mooi verhaal en een mooi (en snel) einde. Prakash, you are still my favourite grumpy post-doc. All the best in Lille! Sasha, thanks for your help when the Biacore when it misbehaved again. Francesca, you were a lovely office and bench mate. Of course you can steal my buffers. Fingers crossed for your paper! Flora, het gaat je lukken met het grote complex! Also I would like to thank all the other (former) B8 members for all your help,

advice and fun over the last years. Succes gewenst voor allemaal!

Natuurlijk ook een bedankje voor de Ovaa-clan. Huib, Farid, Paul, Remco, Reggy en Anitha, we wisten elkaar steeds beter te vinden en uiteindelijk hadden we samen een mooie symbiose met meerdere papers. Ik weet zeker dat jullie nog vele mooie chemical tools gaan maken. Succes en dank jullie wel!

En dan hebben we natuurlijk ook Marlieke nog. Ik zal de vele autoritten naar trainingen, lessen, lectures, wedstrijden en demonstraties niet snel vergeten. Je lijkt zo stil maar je kan heel veel praten! Veel over dansen, maar we lossen net zo gemakkelijk alle wetenschappelijke problemen op tijdens een autoritje. Ondanks onze gezamenlijke publicatie (!), hebben we allebei onze danscarrière redelijk stil gehouden op het NKI. Bijna niemand weet hoe hard we samen gewerkt hebben, maar daar ging het ook niet om. We kregen helaas zelden loon naar werken, maar ik ben heel trots op wat we bereikt hebben. We hebben samen wel heel veel mee gemaakt, veel geleerd en iets moois opgebouwd. Dank je wel voor je energieke en enthousiaste aanwezigheid. Ik wens je al het beste met het afronden van de promotie!

Pap, Mam en Marloes, waarschijnlijk is het nooit helemaal duidelijk geworden wat ik nou precies deed daar in Amsterdam. Ondanks dat, was er onophoudelijke steun en interesse voor mijn gegoochel met eiwitjes. Mam, ondanks al je eigen tegenslag bleef je onuitputtelijk geïnteresseerd in wat ik doe. Pap, ik weet dat je heel trots bent, dank je wel dat je mijn paranimf wilde zijn. Die steun in mijn rug van jullie heb ik altijd al gevoeld, ik ben blij dat je straks naast me staat.

Casper en Romy, jullie zijn het mooiste relativeringmiddel dat je je kunt voorstellen. Casper, vaak als ik je naar bed breng, zeg je dat ik niet mag gaan werken. Ik ben bang dat ik af en toe gelogen heb. Romy, je begroeting als ik thuis kom is heerlijk. Hopelijk kan ik een goed voorbeeld voor jullie zijn.

Suzan, ik vroeg om zilver, ik kreeg goud.

Het gaat jullie allen goed,
Alex